ATM-dependent RHEB phosphorylation couples DNA damage to lysosomal mTORC1 signaling to orchestrate the cellular response to genotoxic stress

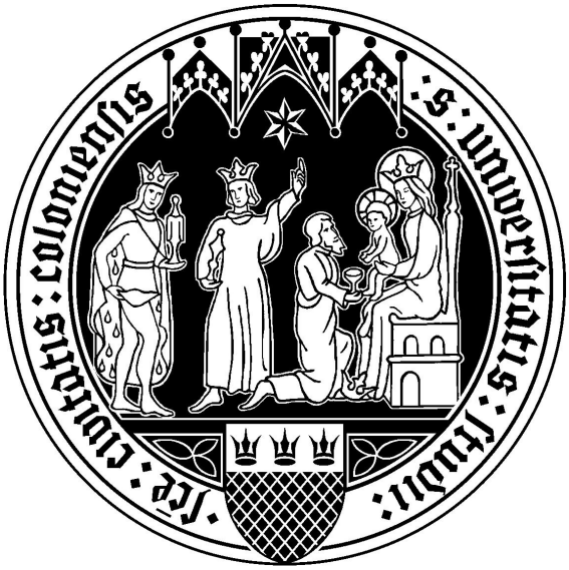

Doctoral thesis

for

the award of the doctoral degree

of the Faculty of Mathematics and Natural Sciences

of the University of Cologne

submitted by

Jiyoung Pan

accepted in the year 2025

The work presented in this thesis was carried out at the Max Planck Institute for Biology of Ageing in Cologne, Germany from October 2019 to September 2025.

Date of defense: November 25, 2025

“Ever tried. Ever failed. No matter. Try again. Fail again. Fail better.”

Samuel Beckett, Worstward Ho (1983)

“Cells model resilience: detect damage, marshal repair, and grow”

JPfSK (Jiyoung Pan from South Korea, 2025)

Table of Contents

Zusammenfassung

Zellen können sich dynamisch an veränderte Umweltbedingungen anpassen, indem sie Signalkaskaden regulieren um das Zellwachstum, ihren Stoffwechsel und die Genomintegrität zu kontrollieren. Die DNA-Schadensantwort (DDR) und die mTORC1-Signalwege steuern jeweils die DNA-Reparatur und das Zellwachstum, aber wie sich diese Signalwege miteinander verknüpft sind, ist bis heute nicht vollständig geklärt. In dieser Arbeit identifizieren wir RHEB, einen direkten mTORC1-Aktivator, als Substrat der DDR-Kinase ATM. Interessanterweise stellen wir fest, dass, genotoxischer Stress die mTORC1-Aktivität unterschiedlich reguliert. Zum einem wird die Phosphorylierung des lysosomalen mTORC1 Substrats TFEB reduziert und gleichzeitig die Phosphorylierung des zytoplasmatischen Substrats S6K verstärkt. Die DDR-induzierte Phosphorylierung von RHEB steuert jedoch speziell den lysosomalen mTORC1-Signalweg. Die Verhinderung der RHEB-Phosphorylierung beeinträchtigt die nukleäre Translokation von TFEB und die Lysosomenbiogenese bei DNA-Schäden. Funktionell ist die RHEB-Phosphorylierungs-abhängige TFEB-Regulation für die proliferative Erholung nach genotoxischem Stress erforderlich. Diese Ergebnisse decken erstmals eine ATM-RHEB-mTORC1-TFEB-Signalachse auf, die DNA-Schäden mit selektiven mTORC1-Ausgaben verbindet und einen Mechanismus offenbart, der es Zellen ermöglicht, sich an genotoxische Signale anzupassen.

Abstract

Cells dynamically adapt to environmental stressors by rewiring signaling networks that coordinate growth, metabolism, and genome maintenance. The DNA damage response (DDR) and mTORC1 signaling pathways govern DNA repair and cell growth, respectively, but how these pathways intersect remains incompletely understood. Here, we identify RHEB, the most direct mTORC1 activator, as a substrate of the DDR kinase ATM. Strikingly, we find that, although genotoxic stress differentially regulates mTORC1 activity—reducing the phosphorylation of its lysosomal target TFEB, while enhancing phosphorylation of its cytoplasmic target S6K—the DDR-induced phosphorylation of RHEB specifically controls the lysosomal mTORC1 signaling branch. Preventing RHEB phosphorylation impairs TFEB nuclear translocation and lysosome biogenesis upon DNA damage. Functionally, the RHEB phosphorylation-dependent TFEB response is required for proliferative recovery following genotoxic stress. These findings uncover an ATM-RHEB-mTORC1-TFEB signaling axis that links DNA damage to selective mTORC1 outputs, revealing a mechanism that enables cells to adapt to genotoxic cues.

List of figures

List of tables

Chapter 1. Introduction

1.1 Signal transduction in cellular physiology

Cells continuously experience fluctuating environmental and intrinsic conditions, including variations in nutrient and oxygen availability, oxidative and replication stress, and diverse genotoxic insults. Survival and adaptation under these challenges rely on signal transduction, a multilayered regulatory system that translates extracellular and intracellular cues into coordinated cellular responses[1,2]. This regulation is largely mediated through post-translational modifications (PTMs), most prominently phosphorylation, which enable rapid, reversible, and spatially controlled modulation of protein activity, localization and interactions.

Among the PTM-driven signaling systems, two pathways play particularly important roles in cellular stress adaptation: the DNA damage response (DDR) and the mechanistic target of rapamycin complex 1 (mTORC1) pathway. The DDR safeguards genome integrity by detecting DNA lesions and coordinating cell-cycle arrest, repair, or, when damage is irreparable, senescence and apoptosis[3,4]. In parallel, mTORC1 integrates nutrient, energy, and growth factor signals to balance anabolic and catabolic processes, aligning biosynthetic capacity with metabolic demands[5,6]. Together, these signaling axes exemplify how cells couple stress sensing with adaptive physiological outcomes.

Although traditionally studied as distinct modules–one maintaining genome stability and the other controlling metabolic homeostasis–emerging evidence reveals functional crosstalk between the DDR and mTORC1 pathway[7,8]. The DDR constitutes one of the most energy-intensive cellular responses, requiring substantial metabolic input to support checkpoint activation, repair and downstream cell-fate decisions[9]. Conversely, mTORC1 functions as a central regulator of cellular resource allocation, modulating energy expenditure and biosynthetic and recycling processes in response to nutrient and stress

cues. This convergence suggests that coordinated regulation between DDR and mTORC1 may be crucial for maintaining cellular homeostasis while balancing the energetic demands of genome maintenance.

1.2 DNA damage response (DDR)

Preserving genomic stability is fundamental to cell viability and organismal health. As DNA is continuously exposed to both endogenous and exogenous sources of damage, cells have evolved a comprehensive surveillance network known as the DNA damage response (DDR)[10]. This system detects lesions, transmits damage signals, and activates appropriate repair or checkpoint control to maintain genome integrity. The following sections outline the principal components and signaling mechanisms of the DDR, with particular emphasis on ataxia–telangiectasia mutated (ATM) as a central regulatory kinase.

1.2.1 DDR overview

The genetic material of eukaryotic cells is continuously challenged by diverse sources of DNA damage originating from both environmental and endogenous factors. Exogenous sources include ultraviolet (UV) light, ionizing radiation (IR), and genotoxic chemicals such as alkylating agents and topoisomerase inhibitors, while endogenous challenges arise from replication errors, spontaneous base modifications, and reactive oxygen species (ROS) generated during metabolism (Figure 1.1)[10,11]. These factors generate a spectrum of lesions—from base modifications, single-strand breaks (SSBs), and bulky adducts to inter- and intra-strand crosslinks and the highly cytotoxic double-strand breaks (DSBs). Unrepaired or misrepaired lesions can lead to mutagenesis, chromosomal rearrangements, and loss of genetic material, threatening genome stability and cellular survival. To counteract these challenges, cells deploy the DDR—a hierarchical signaling network that detects damage, amplifies and integrates the signal, coordinates repair, and ultimately determines whether cells resume proliferation, enter senescence, or undergo apoptosis.

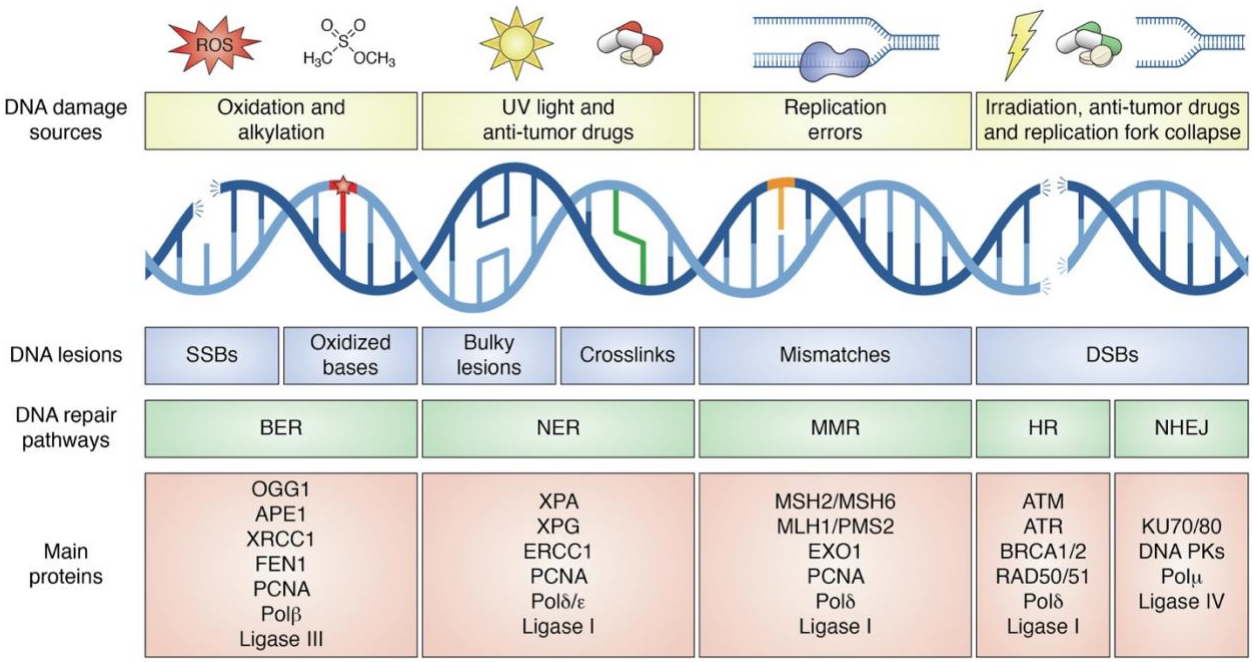

Figure 1.1 Overview of DNA damage sources, lesions, and repair pathways.

Schematic representation of how genotoxic inputs–oxidation/alkylation, UV light and chemotherapeutics, replication errors, and irradiation/replication-fork collapse–give rise to distinct DNA lesions (single-strand breaks, oxidized bases, bulky adduct/crosslinks, mismatches, and double-strand breaks) and the principal repair routes they engage: base excision repair (BER), nucleotide excision repair (NER), mismatch repair (MMR), homologous recombination (HR), and non-homologous end joining (NHEJ). Figure obtained from Dall'Agnese *et al.*[12]

1.2.1.1 Damage sensing

The initiation of the DDR depends on lesion recognition by specialized sensor complexes that define the nature of the damage. DSBs are detected by the MRE11-RAD50-NBS1 (MRN) complex, which binds DNA ends, stabilizes the break, and recruits the apical kinase ATM to initiate signaling[13-15]. Single-stranded DNA (ssDNA) generated at stalled replication forks or during DSB resection is coated by replication protein A (RPA), which subsequently recruits ATR-interacting protein (ATRIP) and facilitates loading and activation of ataxia–telangiectasia and Rad3-related (ATR)[16,17]. DNA-dependent protein kinase (DNA-PK), consisting of the Ku70-Ku80 heterodimer and the catalytic subunit DNA-PKcs, directly binds DNA ends to mediate end-joining repair through non-homologous end joining (NHEJ)[18-20].

Together, these sensor proteins constitute the primary lesion-recognition module of the DDR, initiating the assembly of downstream signaling and repair machinery.

1.2.1.2 Signal transduction

Once DNA damage is detected, the signal must be amplified and transmitted to coordinate cellular response. This is mediated by the phosphoinositide 3-kinase–related kinase (PIKK) family members: ATM, ATR and DNA-PK. Together, these kinases form the apical core of the DDR signaling network, acting in distinct but overlapping contexts. ATM responds primarily to DSBs, ATR to RPA-coated ssDNA that arises during replication stress or DSB resection, and DNA-PK to blunt or processed DSBs during NHEJ[10,11]. Once activated, these kinases phosphorylate numerous substrates involved in chromatin remodeling, checkpoint activation, repair, and cell-fate regulation

Chromatin-based signal amplification

A defining feature of the DDR is the conversion of local DNA lesions into a broad chromatin response. One of the earliest events is phosphorylation of histone H2A variant H2AX at Ser139 (γH2AX), which spreads over megabase regions surrounding a DSB[21]. While forming a microscopically visible DNA focus, γH2AX recruits mediator of DNA damage checkpoint protein (MDC1) via its BRCT domains[22], which in turn recruits E3 ubiquitin ligase RING finger protein 8 (RNF8). RNF8 ubiquitylates the linker histone H1 and the chromatin-associated protein L3MBTL2 (lethal(3) malignant brain tumor-like protein 2), thereby facilitating the recruitment of RING finger protein 168 (RNF168), which modifies histones H2A and H2AX at Lys13 and Lys15[23-25]. These ubiquitin marks recruit tumor suppressor p53-binding protein 1 (53BP1) and the BRCA1 (breast cancer type 1 susceptibility protein)–RAP80 (receptor-associated protein 80)–ABRAXAS complex to sites of damage, promoting the formation of DNA repair foci. RNF169, by competing for ubiquitin binding, and deubiquitylating enzymes such as BRCC36, USP3 (ubiquitin-specific protease 3), and USP16 counteract this process to prevent excessive signal amplification[26-28].

Propagation through effector kinases

ATM, ATR, and DNA-PK also signal through downstream effector kinases. ATR is recruited to RPA-coated ssDNA via ATR-interacting protein (ATRIP), while the RAD9–HUS1–RAD1 (9–1–1) complex, loaded via RAD17, recruits DNA topoisomerase II-binding protein 1 (TOPBP1), whose ATR-activating domain stimulates ATR kinase activity[16]. Claspin acts as an adaptor that bridges ATR and CHK1, enabling efficient ATR-dependent phosphorylation and activation of CHK1[29]. Similarly, ATM phosphorylates checkpoint kinase 2 (CHK2), triggering its dimerization, autophosphorylation, and amplification of the damage signal[30]. ATM also targets additional substrates such as structural maintenance of chromosomes protein 1 (SMC1) and Nijmegen breakage syndrome protein 1 (NBS1), linking ATM signaling to sister chromatid cohesion and DNA end processing[31]. Together, these signaling cascades amplify the initial DNA damage signal and enforce checkpoint arrest, stabilizing replication forks and coordinating repair before cell-cycle progression resumes.

Coordination among apical kinases

Although activated by distinct DNA structures, these kinases act cooperatively. DNA-PK mediates rapid ligation at blunted DSBs, while ATM promotes end resection, generating RPA-coated ssDNA that activates ATR, thereby shifting signaling as repair progresses. They also share substrates such as H2AX (phosphorylated by all three) and the RPA2 (also known as RPA32) subunit of RPA, whose ATR- and DNA-PK-dependent phosphorylation stabilizes ssDNA intermediates and promotes recruitment of downstream repair factors[32-34].

Signal attenuation and recovery

To terminate checkpoint signaling after repair, protein phosphatase 2A (PP2A), protein phosphatase 4 (PP4), and wild-type p53-induced phosphatase 1 (WIP1/PPM1D) dephosphorylate γH2AX, CHK1, CHK2, and RPA2[35-40]. Concurrently, deubiquitylating enzymes such as BRCC36, USP3, and USP16 remove RNF8/RNF168-dependent ubiquitin

conjugates to restore chromatin integrity[26,27]. These mechanisms ensure that checkpoint arrest is reversible once genome stability is re-established.

This phosphorylation- and ubiquitin-driven amplification propagates local DNA damage signals into a coordinated nuclear response that preserves genome integrity. ATM serves as the canonical DDR kinase, and its activation and downstream networks are discussed in Section 1.2.2.

1.2.1.3 Checkpoint activation and cell-cycle arrest

A central outcome of DDR signaling is the activation of cell-cycle checkpoints that delay progression to allow repair. The ATM–CHK2 axis primarily enforces the G1/S and G2/M checkpoints, whereas ATR–CHK1 signaling regulates the intra-S and G2/M checkpoints during replication stress[41,42]. Checkpoint activation converges on the inhibition of cyclin-dependent kinases (CDKs), which drive cell-cycle transitions. CHK1 and CHK2 phosphorylate cell division cycle 25 (CDC25) phosphatases, promoting degradation of CDC25A and cytoplasmic sequestration of CDC25C, thereby preventing removal of inhibitory phosphates from CDKs[43,44]. This ensures that CDK1 and CDK2 remain inactive, halting S-phase entry and mitotic initiation. In parallel, ATM–CHK2 signaling stabilizes the tumor suppressor p53, inducing transcription of the CDK inhibitor $p21^{WAF1/Cip1}$ and reinforcing G1/S arrest[45,46]. At the G2/M transition, Wee1-like protein kinase (WEE1) further inhibits CDK1 by phosphorylation on Tyr15, strengthening mitotic blockade[47,48].

1.2.1.4 DNA repair pathways

Checkpoint activation provides a temporal window for repair, which is executed by specialized DNA repair pathways operating in a lesion-specific manner. These mechanisms range from the correction of small base modifications to the removal of bulky adducts and the repair of DNA strand breaks (Figure 1.2). Together, they form the effector arm of the DDR, preventing mutagenesis and chromosomal aberrations[11].

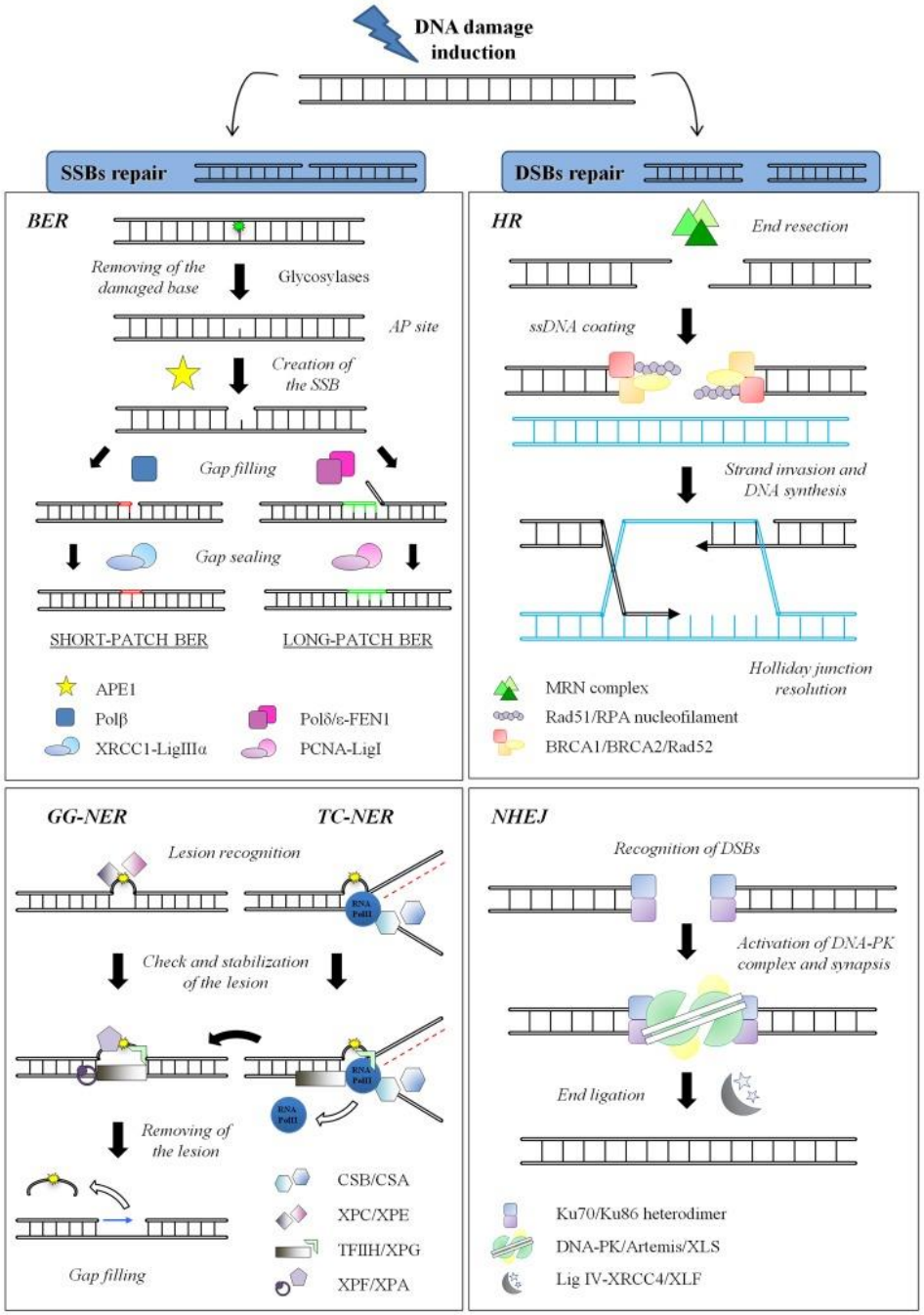

Figure 1.2 DNA repair pathways.

Schematic summary of the four principal DNA repair pathways: base excision repair (BER) for small base lesions and single-strand breaks; nucleotide excision repair (NER) shown as global-genome (GG-NER) and transcription-coupled (TC-NER) for bulky, helix-distorting damage; homologous recombination (HR) for resected double-strand breaks using a sister chromatid; and non-homologous end joining (NHEJ) for direct ligation of double-strand breaks. See main text for detailed mechanisms. Figure obtained from Nicolai *et al.*[49]

Non-homologous end joining (NHEJ) and homologous recombination (HR)

Double-strand breaks (DSBs) are among the most cytotoxic lesions, and their repair is mediated primarily by non-homologous end joining (NHEJ) and homologous recombination (HR)[50]. NHEJ is the predominant and rapid DSB repair pathway, operating throughout the cell cycle. The DNA ends are first recognized by the Ku70–Ku80 heterodimer, which recruits the catalytic subunit of DNA-dependent protein kinase (DNA-PKcs) to form the DNA-PK holoenzyme[18,19,51]. DNA ends that are incompatible for direct ligation are processed by the nuclease Artemis[52] and gap-filling DNA polymerases μ or λ[53,54]. Ligation is then catalyzed by DNA ligase IV, in complex with XRCC4 (X-ray repair cross-complementing protein 4) and XLF (XRCC4-like factor)[55]. Although highly efficient, end processing can introduce small insertions or deletions, making NHEJ potentially mutagenic.

In contrast, HR is largely restricted to S and G2 phases, when a sister chromatid provides a template, thereby enabling high-fidelity repair[56]. DSB resection is initiated by the MRE11–RAD50–NBS1 (MRN) complex together with CtBP-interacting protein (CtIP)[57], producing short 3’ single-stranded overhangs. Processive resection is then extended by exonuclease 1 (EXO1) or DNA2, in conjunction with the Bloom syndrome helicase (BLM)[58-60]. The resulting single-stranded DNA (ssDNA) is coated by RPA, which stabilizes it and prevents secondary structure formation. BRCA1, BRCA2 and partner and localizer of BRCA2 (PALB2) then facilitate the replacement of RPA by RAD51, which forms nucleoprotein filaments capable of homology search and strand invasion[61-63]. DNA synthesis across the invaded strand generates joint DNA intermediates (Holliday junctions), which are resolved through two distinct mechanisms. Dissolution is catalyzed by the Bloom syndrome helicase (BLM)–DNA topoisomerase III alpha (TOP3A)–RecQ-mediated genome instability protein 1/2 (RMI1/2) complex known as the dissolvasome, and produces exclusively non-crossover products that preserve sister chromatid alignment. In contrast, resolution is mediated by structure-selective nucleases such as Holliday junction resolvase GEN1, methyl methanesulfonate and ultraviolet-sensitive protein 81 (MUS81)–essential meiotic endonuclease 1 (EME1), and the SLX1–SLX4 endonuclease complex, which cleave junction intermediates to yield either

crossover or non-crossover outcomes, depending on the cleavage orientation and context[64-66]. Together, these coordinated mechanisms ensure faithful restoration of DNA sequence and chromosomal integrity.

Base excision repair (BER)

Base excision repair (BER) corrects small, non-bulky base lesions arising from oxidation, alkylation, or deamination. The pathway is initiated by lesion-specific DNA glycosylases, which excise the damaged base to generate abasic (AP) site[67,68]. AP endonuclease 1 (APE1) cleaves the DNA backbone at the AP site[69], creating a single-strand break that is repaired via short-patch or long-patch BER. In short-patch BER, DNA polymerase β inserts a single nucleotide, and DNA ligase III–XRCC1 seals the nick[70,71]. In long-patch BER, DNA polymerase δ or ε, aided by proliferating cell nuclear antigen (PCNA) and flap endonuclease 1 (FEN1), extends the repair patch by several nucleotides, followed by ligation by DNA ligase I[72-75]. These subpathways ensure continuous surveillance against oxidative and alkylation-induced base damage.

Nucleotide excision repair (NER)

Nucleotide excision repair (NER) removes bulky, helix-distorting lesions such as UV-induced cyclobutene pyrimidine dimers (CPDs) and (6-4) photoproducts[76,77]. Repair proceeds through two subpathways: global-genome NER (GG-NER) and transcription-coupled NER (TC-NER). In GG-NER, DNA helix distortions are continuously surveyed by the xeroderma pigmentosum group C (XPC)—RAD23B–centrin-2 (CETN2) complex, which detects lesions, induces local DNA unwinding and facilitates recruitment of the transcription factor IIH (TFIIH) complex to initiate repair[78]. In TC-NER, stalling of RNA polymerase II at a lesion triggers recruitment of the cockayne syndrome proteins A (CSA/ERCC8) and B (CSB/ERCC6), which displace the stalled polymerase and remodel the chromatin environment to allow access of the repair machinery[79].

Both pathways then converge on the core NER factors, beginning with xeroderma pigmentosum group A protein (XPA), which verifies the lesion and coordinates assembly of the repair machinery[80]. The TFIIH complex, containing helicases XPB (ERCC3) and XPD (ERCC2), unwinds the DNA around the damage site[81]. Dual incisions remove the damaged oligonucleotide: the ERCC1 (excision repair cross-complementation group 1)–XPF (xeroderma pigmentosum group F) endonuclease cuts 5' to the lesion, while xeroderma pigmentosum group G protein (XPG) cleaves on the 3' side[82-84]. The resulting gap is filled by DNA polymerase δ, ε, or κ, aided by replication factor C (RFC) and proliferating cell nuclear antigen (PCNA), and finally sealed by DNA ligase I or III[85,86]. Through this multistep repair reaction, NER restores native DNA structure and preserves transcriptional and replicative fidelity.

Mismatch repair (MMR)

MMR maintains replication fidelity by correcting mismatches and insertion–deletion loops that escape the proofreading activity of replicative DNA polymerases[87]. Mismatch recognition is initiated by MutS homolog (MSH) complexes: MutSα complex, composed of MutS homolog 2 (MSH2) and MutS homolog 6 (MSH6), detects single-base mismatches and small insertion–deletion loops[88], whereas the MutSβ complex, formed by MSH2 and MutS homolog 3 (MSH3), recognizes larger insertion–deletion loops[89,90]. These recognition complexes subsequently recruit the MutLα complex, consisting of MutL homolog 1 (MLH1) and post-meiotic segregation increased 2 (PMS2), which harbors endonuclease activity and coordinates excision of the error-containing strand[91]. Excision is carried out by exonuclease 1 (EXO1), guided by strand discrimination signals such as replication directionality and PCNA[92]. The resulting gap is resynthesized by DNA polymerase δ in a PCNA-dependent manner and sealed by DNA ligase I, restoring sequence accuracy. Through this continuous correction of replication errors, MMR acts as a crucial barrier against spontaneous mutagenesis and genomic instability.

1.2.1.5 Cell fate outcomes: senescence and apoptosis

When DNA damage is successfully repaired, checkpoint signaling is attenuated and cell-cycle progression resumes. However, when the extent of DNA damage exceeds the repair capacity of the cell, terminal outcomes are engaged to prevent propagation of compromised genomes. Senescence represents a typically stable form of cell-cycle arrest, primarily driven by the tumor suppressor p53, which transcriptionally induces the cyclin-dependent kinase (CDK) inhibitor $p21^{WAF1/Cip1}$ [93-95]. This sustained arrest is reinforced by $p16^{INK4a}$, which inhibits CDK4 and CDK6, thereby maintaining the retinoblastoma protein (RB1) in its hypo-phosphorylated, active state. Active RB1 sequesters E2F transcription factors and prevents G1/S transition[96-98]. The combined action of p21 and p16 stabilizes growth arrest and establishes the senescent phenotype, often accompanied by widespread chromatin remodeling and expression of senescence-associated secretory phenotype (SASP) genes[99]. While senescence is generally long-lasting and contributes to tumor suppression and tissue homeostasis, recent evidence suggests that under certain conditions, it may be partially reversible, particularly before stable chromatin remodeling is established.

Apoptosis, in contrast, eliminates cells harboring irreparable DNA damage. This process is initiated primarily through p53-dependent transcriptional induction of pro-apoptotic BCL-2 family proteins such as BAX, PUMA (p53 upregulated modulator of apoptosis), and NOXA, which antagonize anti-apoptotic BCL-2 members[100-105]. These events trigger mitochondrial outer membrane permeabilization (MOMP), followed by cytochrome c release, apoptosome formation, and caspase activation, resulting in ordered cell death. The decision between senescence and apoptosis is not dictated by a single determinant but reflects an integrated assessment of damage extent, repair capacity, and DDR signaling intensity[106,107]. Through these terminal responses, the DDR eliminates or permanently suppresses damaged cells, thereby preserving tissue integrity and organismal homeostasis.

1.2.2 ATM signaling

Physiological relevance of ATM is exemplified by the human disorder ataxia–telangiectasia, caused by loss-of-function mutations in the ATM gene, which lead to neurodegeneration, immunodeficiency, cancer predisposition, and radiosensitivity[108]. ATM is specifically activated by DSBs and orchestrates a coordinated response encompassing checkpoint activation, repair pathway selection, and chromatin remodeling through phosphorylation of diverse substrates. Building on Section 1.2.1, this section focuses on ATM-specific functions and regulation without reintroducing general concepts.

1.2.2.1 ATM recruitment and activation

In the absence of damage, ATM predominantly exists as inactive dimers or higher-order oligomers. Upon DSB formation, it is recruited to chromatin by the MRN (MRE11–RAD50–NBS1) complex, which bridges and stabilizes DNA ends through the DNA-binding and nuclease domains of MRE11 and the coiled-coil arms of RAD50[109,110]. The C-terminal region of NBS1 engages HEAT-repeat domains within ATM, anchoring it to the MRN complex at the break[111]. Once localized, ATM is activated by autophosphorylation at Ser1981 and acetylation by the histone acetyltransferase TIP60 (also known as KAT5), which promote dimer dissociation and formation of catalytically active monomers[112-114]. Although this MRN-dependent mechanism represents the canonical mode of ATM activation, alternative pathways can also stimulate ATM under non-DNA-damage conditions (see Section 1.2.2.3).

1.2.2.2 Downstream signaling and functions of ATM

Once activated, ATM coordinates the DDR through phosphorylation of numerous downstream effectors involved in chromatin remodeling, checkpoint signaling, DNA repair, and cell-fate regulation. As many of these signaling principles were outlined in Section 1.2.1, the following focuses specifically on ATM-dependent substrates and their mechanistic roles.

Chromatin remodeling and signaling

ATM rapidly modifies chromatin surrounding DSBs to enable efficient recruitment of repair complexes. The most prominent substrate is H2AX, which ATM phosphorylates on Ser139 to generate γH2AX, a chromatin mark that serves as a platform for the accumulation of DNA repair factors[21]. ATM further reinforces this chromatin response by phosphorylating mediator of DNA damage checkpoint 1 (MDC1), thereby strengthening its interaction with γH2AX and promoting the recruitment of downstream E3 ligases RNF8 and RNF168[115]. The resulting ubiquitin-dependent chromatin modifications promote recruitment of 53BP1 and BRCA1, thereby orchestrating the assembly of DSB repair machinery. In addition, ATM phosphorylates KRAB-associated protein 1 (KAP1; also known as TRIM28), inducing local heterochromatin relaxation and thereby improving repair factor accessibility to DNA lesions[116,117]. Through these coordinated chromatin-associated events, ATM integrates signaling with structural remodeling to ensure efficient repair at damaged sites.

Checkpoint activation

ATM serves as the principal activator of checkpoint signaling following DSBs. Its central substrate is checkpoint kinase 2 (CHK2), which it phosphorylates at Thr68, promoting CHK2 dimerization and full activation[118]. Activated CHK2 targets CDC25 phosphatases, leading to CDK inhibition and transient cell-cycle arrest. In parallel, ATM phosphorylates structural maintenance of chromosomes protein 1 (SMC1)–a subunit of the cohesion complex–at Ser957 and Ser966, thereby slowing DNA replication and activating S-phase checkpoint[31]. Through these integrated phosphorylation events, ATM temporarily halts cell-cycle progression, creating a permissive window for DNA repair.

DNA repair and pathway choice

Beyond checkpoint regulation, ATM directly influences repair pathway selection at DSBs. Phosphorylation of 53BP1 by ATM enables recruitment of replication timing regulatory factor (RIF1) and the shieldin complex, which protect DNA ends from resection and promote NHEJ[119]. In contrast, ATM-dependent phosphorylation of BRCA1 enhances its recruitment to damaged chromatin and stimulates DNA end resection and RAD51 loading, driving

homologous recombination (HR)[120]. By balancing these opposing activities, ATM ensures that pathway choice is governed by cell-cycle phase and the availability of a homologous template.

Cell fate regulation

ATM also determines longer-term cell-fate outcomes through its regulation of p53. Following DSBs, ATM phosphorylates p53 at several sites, including Ser15, stabilizing it and enhancing its transcriptional activity[121,122]. Activated p53 transcriptionally induces $p21^{WAF1/Cip1}$ to sustain cell-cycle arrest and facilitate repair[93]. If DNA damage persists, p53 promotes either senescence through prolonged p21 signaling or apoptosis via induction of pro-apoptotic targets such as BAX and PUMA/BBC3[100,101]. ATM further enhances p53 stability by phosphorylating and inhibiting its negative regulator, the E3 ubiquitin ligase mouse double-minute 2 homolog (MDM2)[123,124]. Through these interconnected mechanisms, ATM ensures that cells with repairable lesions resume proliferation, whereas those with irreparable damage undergo permanent arrest or apoptosis.

1.2.2.3 DDR-independent roles of ATM

Although ATM is best known for orchestrating the DDR in response to DSBs, growing evidence indicates that its functions extend beyond canonical genome surveillance. In addition to its nuclear role in maintaining chromosomal integrity, ATM also acts as a cytoplasmic stress sensor responsive to oxidative, metabolic, and organelle-derived perturbations. These non-canonical activities establish ATM as a versatile kinase that integrates diverse stress signals to regulate redox homeostasis, selective autophagy, and metabolic adaptation.

Oxidative and nitrosative stress sensing and signaling

Beyond DSB-induced activation, ATM can be directly activated by reactive oxygen species (ROS). Under oxidative stress, ATM forms intermolecular disulfide-linked dimers that are catalytically active but independent of MRN recruitment or autophosphorylation[125]. This

activation mode is mechanistically distinct from the monomerization triggered by DSBs. In addition, nitrosative stress can similarly engage ATM, further expanding its role in redox regulation[126].

Cytoplasmic ATM activated under oxidative conditions phosphorylates and activates liver kinase B1 (LKB1), which in turn stimulates AMP-activated protein kinase (AMPK). Activated AMPK phosphorylates tuberin (TSC2), a core component of the tuberous sclerosis complex (TSC) that functions as a GTPase-activating protein (GAP) for the small GTPase RHEB, the direct activator of mTORC1. Through this cascade, ATM indirectly suppresses mTORC1 signaling by promoting TSC2-dependent inhibition of RHEB, thereby restraining anabolic metabolism and inducing autophagy[126,127]. This DDR-independent pathway links oxidative stress to ATM activation and metabolic reprogramming via mTORC1 inhibition.

Selective autophagy of peroxisomes (pexophagy)

Peroxisomes are single-membrane organelles central to lipid metabolism and detoxification of ROS. Beyond its nuclear localization, ATM is also detected at peroxisomes, where it regulates their selective autophagic turnover (pexophagy)[128]. Upon oxidative stress, ATM is recruited to peroxisomes by peroxisomal biogenesis factor 5 (PEX5) and phosphorylates PEX5 at Ser141. This phosphorylation facilitates mono-ubiquitination of PEX5 at Lys209, which is recognized by the autophagy adaptor protein p62 that mediates sequestration of damaged peroxisomes into autophagosomes[128]. Through this mechanism, ATM directly links oxidative sensing to organelle quality control, highlighting its broader cytoplasmic role.

Mitochondrial homeostasis

ATM has also been implicated in maintaining mitochondrial integrity, as revealed by studies of ATM-deficient models. Loss of ATM leads to altered mitochondrial morphology, increased mitochondrial mass and ROS production, reduced respiratory efficiency, and impaired mitophagy[129]. These defects occur independently of nuclear DDR signaling, suggesting a mitochondria-associated pool of ATM with distinct regulatory functions. Partial rescue of

mitochondrial defects by allelic loss of Beclin-1–a key autophagy regulator–further supports a functional interplay between ATM and autophagic pathways in mitochondrial quality control.

Translation control and insulin signaling

ATM also contributes to translational control and insulin signaling. In response to insulin stimulation, ATM phosphorylates the eukaryotic initiation factor 4E-binding protein 1 (4E-BP1) at Ser111, thereby promoting cap-dependent translation[130]. In parallel, ATM activity is required for full activation of protein kinase B (AKT); inhibition or loss of ATM reduces phosphorylation of AKT at Ser473, impairing insulin-stimulated glucose uptake due to defective translocation of glucose transporter type 4 (GLUT4) to the plasma membrane[131-133]. Consistent with these cellular observations, ATM-deficient mice exhibit systemic glucose intolerance and insulin resistance[134].

These observations define ATM as a versatile stress sensor that extends its function beyond DNA damage signaling. By integrating redox, metabolic, and organelle-derived signals, ATM coordinates autophagy, translational control, and energy regulation, underscoring its broader role in maintaining cellular homeostasis.

1.3 mTORC1 signaling overview

The mechanistic target of rapamycin (mTOR) is a conserved serine/threonine kinase that assembles into two structurally and functionally distinct protein complexes: mTOR complex 1 (mTORC1) and mTOR complex 2 (mTORC2). Among these, mTORC1 serves as a central metabolic hub, integrating nutrient, growth factor, energy, and stress signals to coordinate anabolic and catabolic processes and maintain cellular homeostasis[5,135-137]. Through this integrative and regulatory control, mTORC1 governs core physiological functions such as growth, metabolism, and stress adaptation. Aberrant mTORC1 signaling is linked to ageing

and numerous age-related diseases, including cancer, metabolic disorders, and neurodegeneration, highlighting its central role in cellular and organismal physiology[6,135,138].

mTORC2, in contrast, regulates cytoskeletal organization and survival signaling primarily through phosphorylation of AGC-family kinases, including AKT (protein kinase B), SGK1 (serum- and glucocorticoid-induced protein kinase 1), and protein kinase C (PKC)[139-146]. Via AKT, mTORC2 can indirectly enhance mTORC1 activity by inhibiting the tuberous sclerosis complex (TSC), its main negative regulator[147]. Despite its physiological relevance, the functions and regulatory mechanisms of mTORC2 remain less well characterized compared to mTORC1.

Given the central relevance of mTORC1 to cellular metabolism and stress adaptation, this thesis focuses on how its activity is regulated in response to cellular stress and DNA damage signaling. The following sections therefore outline the principal functions of mTORC1 and the molecular mechanisms governing its regulation, establishing the framework for subsequent experimental investigations.

1.3.1 Core functions of mTORC1 signaling

mTORC1 is a multiprotein complex composed of the serine/threonine kinase mTOR together with the scaffolding protein RAPTOR (regulatory-associated protein of mTOR), the structural subunit mLST8 (mammalian lethal with SEC13 protein 8), and the regulatory proteins PRAS40 (proline-rich AKT substrate of 40kDa) and DEPTOR (DEP domain-containing mTOR-interacting protein)[148-152]. Among these, RAPTOR functions as a substrate-binding scaffold, recognizing a conserved TOR signaling (TOS) motif found in several downstream effectors, including ribosomal protein S6 kinase (S6K) and eukaryotic translation initiation factor 4E-binding protein1 (4E-BP1), and thereby facilitating their phosphorylation by the mTOR catalytic core[153]. While TOS-mediated interaction represents an important mode of substrate recruitment, many substrates including transcription factor EB (TFEB) and unc-51-like kinase (ULK1) lack this motif. Through phosphorylation of diverse

downstream substrates, mTORC1 exerts its growth-promoting role by stimulating anabolic processes, including protein, lipid, and nucleotide synthesis, while simultaneously suppressing catabolic programs such as lysosome biogenesis and autophagy. This dual regulation ensures that cellular metabolism is aligned with environmental conditions and nutrient supply[154]. Among the diverse downstream targets of mTORC1, two branches are most relevant to this thesis: control of protein synthesis and regulation of lysosomal biogenesis and autophagy.

1.3.1.1 Protein synthesis

Protein synthesis represents a major biosynthetic and energy-consuming process in eukaryotic cells and is tightly regulated to ensure that growth only proceeds under favorable conditions. mTORC1 functions as a pivotal signaling hub that coordinates translational control, thereby promoting cell growth and proliferation. This is achieved mainly through the phosphorylation of canonical substrates: ribosomal S6 kinase (S6K) and eukaryotic translation initiation factor 4E-binding protein1 (4E-BP1)[154,155]. Together, these effectors regulate translation initiation and ribosome biogenesis, ensuring that cells coordinate anabolic activity with nutrient and growth factor availability (Figure 1.3).

Regulation via 4E-BP1

Most capped mRNAs are translated via the eukaryotic translation initiation factor (eIF) 4F (eIF4F) complex, composed of the cap-binding protein eIF4E, the scaffolding protein eIF4G, and the RNA helicase eIF4A. One mechanism by which mTORC1 controls protein synthesis is through the phosphorylation of eukaryotic translation initiation factor 4E-binding protein 1 (4E-BP1). When dephosphorylated, 4E-BP1 binds with high affinity to the cap-binding protein eIF4E and thereby prevents its association with the scaffolding factor eIF4G. This competition blocks the assembly of the eIF4F complex, which is essential for recruitment of the 43S preinitiation complex to the 5’ cap of mRNAs, ultimately suppressing cap-dependent translation[156,157]. mTORC1-dependent phosphorylation of 4E-BP1 releases eIF4E and stimulates 5’ cap-dependent translation. Upon nutrient and growth factor stimulation,

mTORC1 phosphorylates 4E-BP1 in a hierarchical manner. Phosphorylation at Thr37 and Thr46 occurs first and serves as a priming event, which subsequently enables phosphorylation at Ser65 and Thr70[156,158]. This ordered phosphorylation progressively reduces the affinity of 4E-BP1 for eIF4E, releasing and allowing eIF4E to bind eIF4G and assemble the active eIF4F complex.

Regulation via S6K

The ribosomal S6 kinase (S6K) is a member of the AGC family of serine/threonine kinases and was the first substrate identified downstream of mTORC1[159,160]. Activation of S6K is biphasic: mTORC1 phosphorylates the hydrophobic motif site (Thr389), while phosphoinositide-dependent kinase 1 (PDK1) phosphorylates the activation-loop residue (Thr229), together yielding full catalytic activity[159-161]. Once activated, S6K phosphorylates a broad range of targets that collectively promote protein synthesis, ribosome biogenesis, and RNA processing.

A canonical substrate of S6K is ribosomal protein S6, a component of the 40S ribosomal subunit, which is phosphorylated on multiple serine residues (Ser235/236 and Ser240/244). While dispensable for global protein synthesis, S6 phosphorylation has been linked to cell-size control and the transcriptional induction of genes required for ribosome biogenesis[162,163].

S6K exerts major control over translation initiation and elongation. During initiation, S6K phosphorylates eIF4B, enhancing eIF4A helicase activity and promoting cap-dependent translation[164]. In parallel, S6K phosphorylates the translational repressor PDCD4 (programmed cell death protein 4), targeting it for proteasome-mediated degradation. PDCD4 loss relieves inhibition of eIF4A, further boosting initiation efficiency[165]. Additionally, S6K can associate with SKAR at exon-junction complexes, enhancing the translational efficiency of newly spliced mRNAs[166]. During elongation, S6K phosphorylates and inhibits eukaryotic elongation factor 1 kinase (eEF2K), thereby maintaining elongation factor 2 (eEF2) in its active form and facilitating efficient elongation[167].

Beyond its role in translation, S6K contributes to ribosome biogenesis by regulating ribosomal RNA (rRNA) and transfer RNA (tRNA) synthesis. It phosphorylates and activates upstream binding factor (UBF), a transcription factor essential for RNA polymerase I-mediated rRNA transcription, a major rate-limiting step in ribosome biogenesis[168]. In parallel, mTORC1 enhances RNA polymerase I activity through activation of transcription initiation factor 1A (TIF-1A)[169]. Furthermore, mTORC1 inactivates MAF1, a repressor of RNA polymerase III, increasing transcription of tRNAs and 5S rRNA[170,171].

Although mTORC1 regulates global translation through both S6K and 4E-BP1, it preferentially enhances the translation of mRNAs containing a 5' terminal oligopyrimidine (TOP) motif, which are enriched in ribosomal protein mRNAs, primarily through 4E-BP1-dependent mechanisms[172,173]. Together, the coordinated phosphorylation of S6K and 4E-BP1 allows mTORC1 to regulate multiple aspects of protein synthesis, from initiation and elongation to ribosome biogenesis.

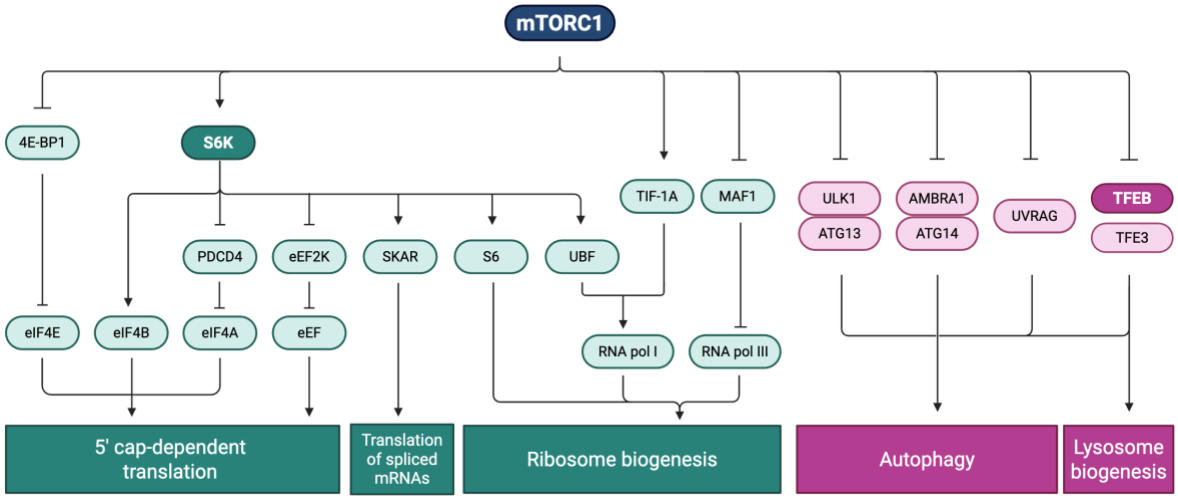

Figure 1.3 Schematic representation of major mTORC1 substrates and associated cellular processes.

mTORC1 promotes anabolic programs, such as cap-dependent translation and ribosome biogenesis (depicted in green), through phosphorylation of 4E-BP1, S6K, and associated translational regulators. Conversely, mTORC1 suppresses catabolic pathways, including autophagy and lysosome biogenesis (depicted in magenta), by phosphorylating TFEB, TFE3, ULK1, ATG13,

ATG14, AMBRA1, and UVRAG. Detailed descriptions of individual substrates and regulatory mechanisms are provided in the main text. Figure created with Biorender.com.

1.3.1.2 Lysosome biogenesis and autophagy

In addition to regulating anabolic programs like protein synthesis, mTORC1 also exerts negative control over catabolic processes, most prominently lysosome biogenesis and autophagy. These processes are essential for maintaining cellular homeostasis by recycling macromolecules and clearing damaged components. mTORC1 serves as the primary nutrient-sensitive brake on these pathways, suppressing autophagy and limiting lysosomal biogenesis under nutrient-replete conditions, while releasing this inhibition during starvation or stress. mTORC1 regulates this catabolic branch primarily through two mechanisms: (i) phosphorylation of the MiT/TFE transcription factors TFEB and TFE3, which control transcriptional programs for lysosome biogenesis and autophagy, and (ii) phosphorylation of core components of autophagy machinery that restrain autophagosome formation and maturation (Figure 1.3).

TFEB and TFE3: transcriptional control of lysosome- and autophagy-related genes

Among mTORC1 substrates, the transcription factor EB (TFEB) has emerged as a master regulator of the catabolic processes. Together with its closely related family member transcription factor E3 (TFE3), TFEB orchestrates the transcriptional network governing lysosome biogenesis and autophagy. TFEB and TFE3 are direct mTORC1 targets, whose phosphorylation controls their subcellular localization and transcriptional activity. Under nutrient sufficiency, the Rag GTPases recruit TFEB to lysosomes, where mTORC1 phosphorylates TFEB predominantly at Ser211 (and TFE3 at Ser321). This promotes 14-3-3 binding, thereby retaining the transcription factors in the cytoplasm[174-178]. During starvation and stress, TFEB is released from lysosomes and undergoes dephosphorylation, enabling its nuclear translocation. The phosphatase calcineurin, activated by lysosomal calcium release through the mucolipin-1 (MCOLN1/TRPML1) channel, contributes to TFEB dephosphorylation and activation in concert with protein phosphatase 2A (PP2A)[179-182].

Conversely, phosphorylation of TFEB at Ser142 and Ser138 promotes nuclear export during nutrient refeeding via a CRM1-dependent mechanism[183].

Once in the nucleus, TFEB and TFE3 recognize and bind the CLEAR (coordinated lysosomal expression and regulation) motif, a 10-base pair palindromic consensus sequence (5'-GTCACGTGAC-3'), via their basic helix-loop-helix leucine zipper domains[175]. CLEAR motifs are enriched in the promoters of more than 400 genes involving a wide variety of lysosomal and autophagy-related genes, collectively defined as the CLEAR network[174,184]. These include lysosomal hydrolases such as cathepsins D and B (CTSD, CTSB), β-hexosaminidase subunits (HEXA, HEXB), and α-glucosidase (GAA), and lysosomal acid lipase (LIPA), which enhance the degradative capacity of lysosomes. Lysosomal membrane proteins such as lysosome-associated membrane proteins 1 and 2 (LAMP1/2) and vacuolar H^+-vATPase subunits (ATP6V1/ATP6V0) maintain acidity and structural integrity, prerequisites for effective lysosome biogenesis and function. In addition to lysosomal genes, TFEB activates the expression of selective autophagy receptors, including sequestosome-1 (SQSTM1/p62) and neighbor of BRCA1 gene 1 protein (NBR1)[174]. Transcriptomic profiling further suggests that TFEB broadly influences the expression of autophagy-related genes (e.g., ATG5, ATG7, ATG12, ATG13, Beclin-1, and VPS34), although many of these remain putative targets that require experimental validation. Collectively, the TFEB/TFE3-driven transcriptional program increases both the number and the functional capacity of lysosomes, while simultaneously sustaining autophagic flux.

Post-translational control of autophagy regulators

Beyond its regulation of TFEB and TFE3, mTORC1 directly phosphorylates multiple autophagy regulators to suppress both autophagosome formation and maturation. Induction of autophagy requires formation of the initiation complex, composed of ULK1 (UNC-51-like kinase 1), ATG13 (autophagy-related protein 13), ATG101 (autophagy-related protein 101), and FIP200 (200k-Da FAK family kinase-interacting protein). At this stage, mTORC1 prevents activation of the complex by phosphorylating ULK1–thereby blocking its

activation by AMP-activated protein kinase (AMPK)–as well as ATG13[185-187]. When active, the ULK1 complex phosphorylates components of PI3KC3 (class III phosphatidylinositol 3-kinase; also known as VPS34) complex I, thereby facilitating phagophore nucleation. mTORC1 inhibits this step by phosphorylating AMBRA1 (autophagy/beclin-1 regulator 1) and ATG14, core subunits of the Beclin1–VPS34–AMBRA1–p115–ATG14 complex[188,189]. At later stages, mTORC1 also blocks autophagosome maturation by phosphorylating UVRAG (UV radiation resistance-associated gene protein), a key factor for autophagosome–lysosome fusion. mTORC1-mediated phosphorylation of UVRAG promotes binding to RUBICON, an inhibitor of autophagy[190].

Through regulation of TFEB/TFE3 and phosphorylation of autophagy regulators, mTORC1 establishes a multilayered system that coordinates lysosome biogenesis and autophagy with nutrient status. The transcriptional outputs of TFEB are particularly crucial, as they drive lysosomal biogenesis and determine autophagic potential, positioning TFEB as a central effector of this catabolic arm of mTORC1 signaling as a focal point of this thesis.

1.3.2 Regulation of mTORC1 signaling

mTORC1 activity is subject to a highly coordinated regulatory system that integrates growth-promoting signals with nutrient and energy availability while simultaneously responding to diverse stress conditions. Two major regulatory axes have been defined. The first is the TSC (tuberous sclerosis complex)–RHEB (Ras homolog enriched in brain) axis, which serves as a signaling hub for growth factors, cellular energy status, amino acids, and hypoxia, converging on the small GTPase RHEB, the immediate activator of mTORC1[154]. The second is the Rag GTPase–lysosome machinery, which governs the recruitment of mTORC1 to the lysosomal membrane in response to amino acids, glucose, and lipids, thereby promoting its activation by RHEB downstream and facilitating substrate phosphorylation. These two branches act in concert: spatial regulation by the Rag GTPases positions mTORC1 at the lysosome, while catalytic activation is dictated by the nucleotide-bound state of RHEB. In addition to these canonical mechanisms, an emerging body of work indicates that RHEB

itself is subject to direct post-translational modifications (PTMs), including phosphorylation, ubiquitination, and NEDDylation, which can modulate its localization, stability, and activity[191-194]. Although this layer of regulation is less well characterized, it points to a plausible mechanism by which stress pathways might fine-tune mTORC1 signaling independently of TSC.

1.3.2.1 TSC-RHEB axis

The tuberous sclerosis complex (TSC), composed of TSC1, TSC2, and TBC1D7, is a central negative regulator of mTORC1 activity. The complex functions as a GTPase-activating protein (GAP) for the small GTPase RHEB, stimulating its GTP hydrolysis[195]. Since RHEB in its GTP-loaded state directly stimulates the catalytic activity of mTOR, the GAP activity of TSC provides an effective means of suppressing mTORC1[196]. Conversely, when TSC is inhibited, RHEB remains in its active GTP-bound form, directly engaging the kinase domain of mTOR to stimulate its catalytic activity[154,196].

A wide variety of upstream signals converge on TSC, reflecting its role as a hub that integrates growth conditions and cellular stress. Growth factors (GFs) such as insulin and insulin-like growth factor (IGF) activate the phosphoinositide 3-kinase (PI3K)–AKT pathway, leading to phosphorylation of TSC2 on multiple serine and threonine residues (e.g., Ser939, Thr1462) and binding of 14-3-3 proteins, which suppress the GAP activity of the complex[147,197]. Similarly, extracellular signal-regulated kinase (ERK) and p90 ribosomal S6 kinase (RSK) phosphorylate TSC2 (e.g., Ser664, Ser1798), further inhibiting the complex in response to mitogenic cues[198-200]. In this way, growth factor signaling reduces TSC activity, favors RHEB–GTP accumulation, and drives mTORC1 activation.

By contrast, stress and energy-sensing pathways enhance TSC activity to suppress mTORC1. Under low energy conditions, AMP-activated protein kinase (AMPK), activated by the upstream kinase liver kinase B1 (LKB1), phosphorylates TSC2 on residues such as Ser1387 to stimulate its GAP activity[201-203]. AMPK also exerts an inhibitory phosphorylation on the

mTORC1 subunit RAPTOR, providing a parallel inhibitory mechanism[204]. Hypoxia similarly promotes TSC activity through the induction of regulated in development and DNA damage response protein (REDD1), which disrupts inhibitory 14-3-3 interactions with TSC2[205].

In addition to regulation by phosphorylation, the subcellular localization of the TSC complex regulates its inhibitory function toward mTORC1. TSC dynamically localizes to the lysosomal surface in response to stress signals, where it inhibits RHEB[206,207]. Growth factors promote dissociation of TSC from lysosomes, whereas stress conditions such as amino acid and energy deprivation or hypoxia enhance its lysosomal recruitment, thereby reinforcing repression of mTORC1. This spatial regulation adds another layer of control, ensuring that TSC activity is exerted precisely at the site where RHEB engages mTORC1.

The TSC–RHEB axis functions as a highly tunable regulatory module. By integrating biochemical modifications with dynamic changes in subcellular localization, it provides a versatile system through which nutrient availability and stress signals collectively shape mTORC1 signaling.

1.3.2.2 Regulation of RHEB by post-translational modifications

In addition to being regulated by the TSC through control of its GTP- and GDP-bound states, Ras homolog enriched in brain (RHEB) is also subject to diverse post-translational modifications (PTMs) that directly influence its function. These include farnesylation, ubiquitination, phosphorylation, and NEDDylation, each of which has been shown to alter RHEB's localization, stability, ability to bind and retain GTP, or capacity to activate mTORC1. Together, these modifications establish an additional layer of regulation beyond the canonical TSC–RHEB axis and demonstrate that RHEB activity can be directly controlled by PTMs in response to different cellular conditions.

Farnesylation

One essential modification is farnesylation of the C-terminal CaaX motif of RHEB, catalyzed by farnesyltransferase (FTase). Following farnesylation, RHEB undergoes endoproteolytic processing by Ras converting enzyme 1 (RCE1) and carboxylmethylation by isoprenylcysteine carboxyl methyltransferase (ICMT), yielding a farnesylcysteine that confers hydrophobicity to the C-terminus[208]. This modification enables weak, transient association of RHEB with endomembranes, including lysosomes, where mTORC1 resides. Loss of the CaaX motif or pharmacological inhibition of FTase prevents RHEB from activating mTORC1 in cells[209,210]. Thus, farnesylation is a prerequisite for RHEB to access and activate mTORC1.

Ubiquitination

RHEB is also subject to ubiquitination, which couples growth factor and amino acid inputs to its regulation. In the context of growth factor signaling, the lysosomal E3 ligase Ring Finger Protein 152 (RNF152) ubiquitinates RHEB and promotes its interaction with the TSC complex, thereby limiting mTORC1 activation[191]. Epidermal growth factor (EGF) stimulation activates AKT, which phosphorylates the deubiquitinase ubiquitin-specific protease 4 (USP4), enhancing its activity toward RHEB. Deubiquitination of RHEB by USP4 disrupts its interaction with TSC, thereby relieving inhibition and permitting mTORC1 activation. In this way, RNF152 and USP4 act in opposition to connect growth factor–receptor tyrosine kinase signaling to regulation of the TSC–RHEB axis.

A distinct mode of ubiquitination occurs in response to amino acid availability. Refeeding cells with amino acids induces polyubiquitination of RHEB, which increases its affinity for mTORC1 and promotes pathway activation[193]. During starvation, the deubiquitinase ataxin-3 (ATXN3) associates with inactive Rag GTPases at lysosomes and maintains RHEB in a deubiquitinated state. Upon amino acid stimulation, ATXN3 dissociates, allowing RHEB polyubiquitination, enhanced binding to mTORC1, and subsequent degradation of ubiquitinated RHEB to terminate the signal. Thus, ubiquitination serves as a versatile

modification that can either suppress or activate RHEB, depending on whether it is engaged by growth factor-linked or amino acid-linked pathways.

Phosphorylation

Another modification is phosphorylation of RHEB at Ser130, which directly attenuates its activity. Under energy-depleted conditions, p38β kinase activates p38-regulated/activated protein kinase (PRAK, also known as MAPKAPK5), which phosphorylates RHEB on Ser130[194]. This phosphorylation reduces ability of RHEB to load and retain GTP, weakening its capacity to stimulate mTORC1. As a result, phosphorylation at S130 serves as a rapid means of downregulating RHEB activity during metabolic stress, independently of TSC regulation.

NEDDylation

Finally, RHEB can be modified by NEDDylation, the conjugation of the ubiquitin-like protein NEDD8 (neural precursor cell expressed developmentally down-regulated protein 8). This modification occurs at Lys169 and is mediated by the NEDD8-conjugating E2 enzyme UBE2F together with the E3 ligase SAG[211]. NEDDylated RHEB shows enhanced localization to lysosomes and increased GTP-binding affinity, resulting in stronger stimulation of mTORC1. Pharmacological inhibition of the neddylation machinery, for example through blockade of NEDD8-activating enzyme (NAE), prevents RHEB NEDDylation and suppresses mTORC1 signaling. Moreover, RHEB NEDDylation has been implicated in tumorigenesis in an mTORC1-dependent manner.

Collectively, these findings demonstrate that RHEB is regulated not only by its nucleotide-bound state under the control of TSC, but also by a spectrum of PTMs that fine-tune its localization, stability, and ability to engage mTORC1. Despite this progress. It remains largely unknown how cellular stress signals–particularly DNA damage–reprogram the PTM landscape of RHEB. Addressing these knowledge gaps is essential to expand understanding of how stress signaling integrates with the mTORC1 pathway, and this question forms the central focus of the present thesis.

1.3.2.3 Lysosomes-associated regulation of mTORC1

Once regarded primarily as degradative organelles, lysosomes are now recognized as central hubs for nutrient signaling. In the context of the mTORC1 pathway, they provide the spatial platform where nutrient-derived signals converge to regulate the activity of the kinase complex. Recruitment of mTORC1 to lysosomes enables its activation by the lysosome-resident pool of RHEB. Moreover, lysosomal substrates of mTORC1, such as TFEB and TFE3, depend on lysosomal localization of both the kinase complex and the substrate. The Rag GTPases are central for this recruitment process, and their activity is governed by their nucleotide-binding state, which integrates upstream cues including amino acids, glucose, and lipid availability.

Rag GTPases and the LAMTOR complex

Central to mTORC1 recruitment to lysosomes are the Rag GTPases, which function as obligate heterodimers, formed by RagA or RagB in combination with RagC or RagD (Figure 1.4). Their activity is dictated by nucleotide loading: the configuration in which RagA/B is GTP-bound and RagC/D is GDP-bound constitutes the active state, enabling interaction with the mTORC1 subunit RAPTOR and promoting recruitment of the kinase complex at lysosomes[212,213]. This process is organized by the LAMTOR complex (also known as Ragulator), a pentameric assembly composed of late endosomal/lysosomal adaptor, MAPK and mTOR activator proteins 1-5 (LAMTOR1-5). Anchored to the lysosomal membrane through lipid modifications of LAMTOR1, the LAMTOR complex not only stabilizes the Rag GTPases at this location but also provides guanine nucleotide exchange factor (GEF)-like activity to activate RagA/B[214].

Regulation of the Rag GTPases by GATOR and KICSTOR complexes

The activity of Rag GTPases is further modulated by the GATOR complexes, which exert opposing functions. GATOR1, composed of DEPDC5, NPRL2, and NPRL3, acts as a GAP for RagA/B. In amino acid-poor conditions, GATOR1 stimulates GTP hydrolysis on RagA/B,

thereby inactivating the heterodimer and preventing mTORC1 recruitment to lysosomes[215]. In contrast, GATOR2–a complex of MIOS, WDR24, WDR59, SEH1L, and SEC13–functions as a positive regulator by inhibiting GATOR1. Through this hierarchical arrangement, GATOR2 functions as an upstream regulator of GATOR1, integrating inputs from nutrient sensing pathways (discussed below). The effective function of GATOR1 further requires proper lysosomal localization, which is ensured by the KICSTOR complex, composed of SZT2, KPTN, ITFG2, and C12orf66. KICSTOR anchors GATOR1 to the lysosomal membrane, a prerequisite for its inhibitory activity on Rag GTPases[216].

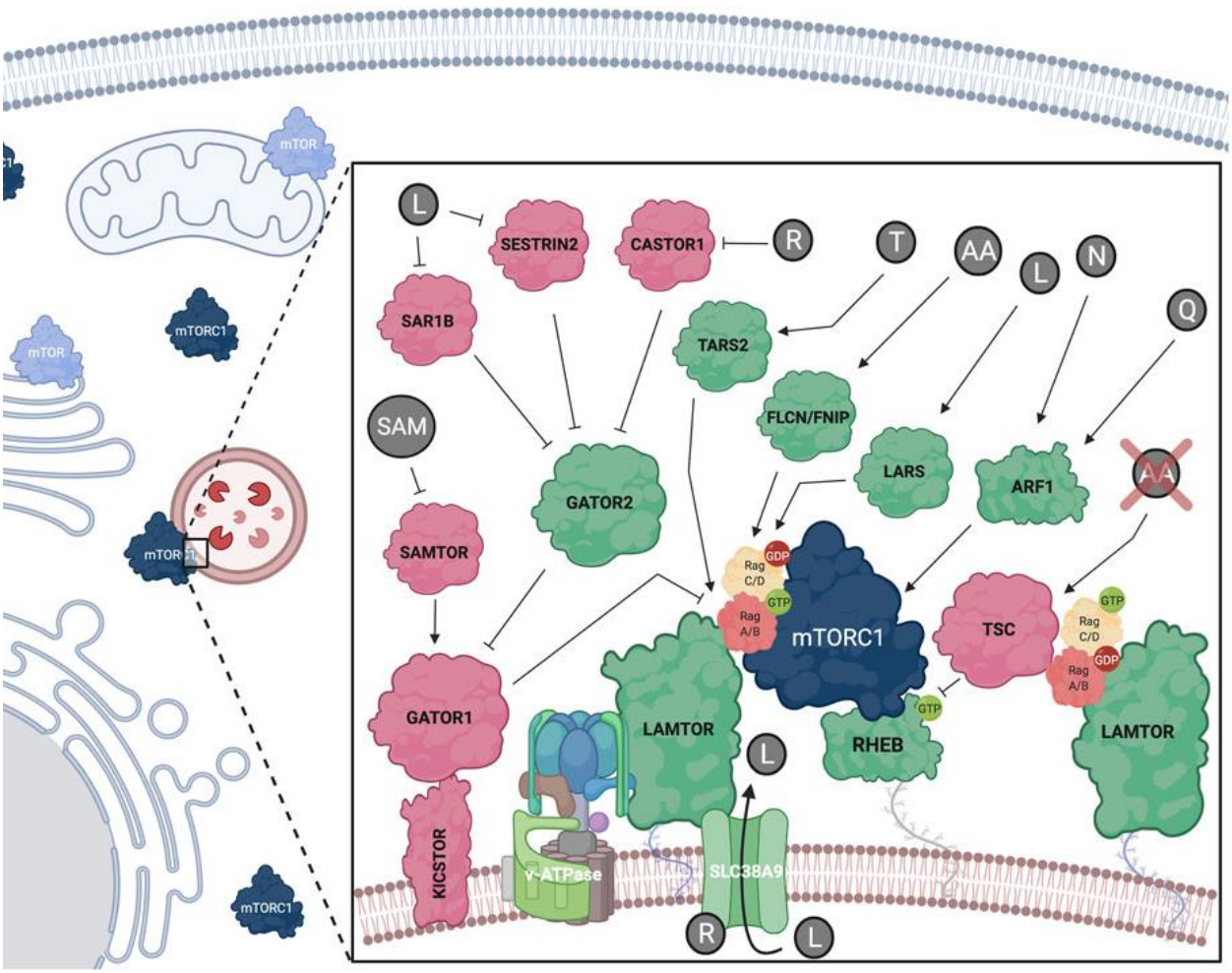

Figure 1.4 Lysosome-associated regulation of mTORC1 by Rag GTPases

mTORC1 localization on lysosomes is governed by RagA/B–RagC/D heterodimers anchored by the LAMTOR complex. Rag activity, determined by their nucleotide loading status, controls mTORC1 recruitment and serves as the convergence point for diverse nutreint cues. GATOR1 is the GAP for RagA/B: under amino-acid deprivation it catalyzes GTP hydrolysis on RagA/B, rendering inactive Rag dimer, and prevents mTORC1 recruitment. GATOR1 function requires lysosomal tethering by

KICSTOR. GATOR 2 inhibits GATOR 1; its activity is tuned by nutrient sensors (SESTRINs for leucine, CASTOR for arginine, and SAMTOR for S-adenosyl-methionine), thereby modulating RagA/B loading. In parallel, FLCN-FNIP acts as the GAP for Rag C/D, facilitating RagC/D–GDP state that favors lysosomal recruitment of mTORC1, with luminal inputs relayed by SLC38A9 and the v-ATPase. mTORC1 activator RHEB and inhibitor TSC are also depicted. See main text for details. Figure obtained and adapted from Fernandes *et al*[135].

FLCN, v-ATPase, and other lysosomal regulators

In addition to GATOR and KICSTOR, several other lysosomal factors fine-tune Rag GTPase activity. One such regulator is folliculin (FLCN)–FNIP1/2 complex, which functions as a GAP for RagC/D. By driving RagC/D into their GDP-bound state, FLCN–FNIP generates the nucleotide configuration that permits mTORC1 recruitment, a mechanism especially critical during amino-acid refeeding, when mTORC1 must be rapidly re-engaged[217].

Other lysosomal proteins contribute to nutrient sensing by linking the composition of the lysosomal lumen or the state of the lysosomal membrane to Rag activation. The vacuolar H^+-adenosine triphosphatase (v-ATPase) acidifies the lysosomal lumen and mechanistically couples luminal amino-acid availability to activation of the LAMTOR complex[218]. The lysosomal transmembrane protein SLC38A9 serves both as an arginine transporter and a nutrient sensor, transmitting luminal arginine levels to the LAMTOR-Rag axis[219,220]. Lipid metabolism also integrates into this pathway through Niemann-Pick type C proteins (NPC1 and NPC2), which mediate lysosomal cholesterol efflux. Under cholesterol-replete conditions, NPC1 promotes Rag-dependent mTORC1 activation, whereas loss of NPC1 dysregulates this signaling and leads to aberrant mTORC1 signaling[221,222]. Together with NPC1, SLC38A9 also contributes to lysosomal cholesterol sensing, further linking sterol availability to Rag GTPase activity[221,222].

Finally, lysosomal positioning within the cell provides an additional layer of regulation. The BORC complex and the small GTPase Arl8 direct lysosomal transport along microtubules, controlling whether lysosomes localize to the cell periphery or cluster in perinuclear regions[223]. Nutrient status influences this distribution, and peripheral positioning correlates

with higher mTORC1 signaling, whereas perinuclear clustering is associated with reduced activity[224].

Cytosolic amino-acid sensors

Cytosolic sensors directly couple amino-acid availability to the Rag GTPase machinery. Leucine is detected by Sestrin1 and Sestrin2, which in the absence of leucine bind and inhibit GATOR2, thereby allowing GATOR1 to inactivate RagA/B. Leucine binding to Sestrins disrupts this inhibitory interaction, releasing GATOR2 and enabling mTORC1 activation[225]. Arginine is monitored through two parallel systems: CASTOR1 (together with CASTOR2) binds and suppresses GATOR2 under arginine starvation, an effect relieved when arginine engages CASTOR1[226], while the lysosomal transceptor SLC38A9 senses luminal arginine and signals through the LAMTOR–Rag axis to activate mTORC1[219]. Methionine sufficiency is communicated through its metabolite S-adenosylmethionine (SAM), which is sensed by SAMTOR. Under SAM depletion, SAMTOR binds the GATOR1–KICSTOR complex to inactivate RagA/B; upon SAM binding, this interaction is released, permitting mTORC1 activation[227].

Other sensors have also been implicated in amino-acid signaling to mTORC1. Leucyl-tRNA synthetase (LARS) was initially proposed to function as a GAP for Rag D[228], but alternative models suggested that it may instead act as a scaffolding factor in leucine signaling. Glutamine can stimulate mTORC1 through Rag-dependent mechanisms involving the lysosomal transceptor SLC38A9[219], as well as through a Rag-independent pathway in which the Golgi-localized GTPase Arf1 mediates mTORC1 recruitment to the Golgi apparatus[229].

Other metabolic inputs that converge on the Rag–lysosome hub

In addition to amino acids, a range of other metabolic inputs converge on the Rag–lysosome signaling module. Glucose sufficiency sustains v-ATPase–LAMTOR activity, while glycolytic enzymes such as aldolase and metabolites including dihydroxyacetone phosphate (DHAP) link glucose metabolism to Rag-dependent regulation of mTORC1[230-232]. During glucose deprivation, the scaffold proteins AXIN and LKB1 are recruited to lysosomes, where they

activate AMPK and thereby reinforce mTORC1 inhibition[233]. Cholesterol availability, communicated through SLC38A9 and NPC1, further promotes Rag activation, whereas lipid stress disrupts this process[222]. Finally, lysosomal properties themselves modulate signaling: transporters such as SLC36A1 (PAT1) influence luminal pH and amino-acid efflux and Rag signaling[218].

Recruitment of mTORC1 and regulation of lysosomal substrates

Recruitment of mTORC1 to lysosomes by Rag GTPases not only enables its activation by RHEB but is particularly critical for a subset of lysosomal substrates, such as the transcription factors TFEB and TFE3, whose phosphorylation requires their Rag-dependent recruitment at the lysosomal surface. Under nutrient-rich conditions, RagC/D directly interacts with and retain TFEB and TFE3 at lysosomes, where they are phosphorylated by mTORC1 and consequently sequestered in the cytoplasm. Starvation disrupts this interaction, allowing their nuclear translocation and induction of lysosomal and autophagy genes[234]. In contrast, many canonical substrates–including S6K and 4E-BP1–do not require Rag-mediated recruitment to lysosomes for phosphorylation, underscoring a substrate-specific layer of spatial regulation within the pathway.

Rag-independent and non-lysosomal regulation

Although research on mTORC1 regulation has been centered on lysosomal machineries and Rag-dependent signaling, accumulating evidence indicates that mTORC1 also localizes to many other subcellular compartments, engaging different substrates and regulatory inputs. For example, glutamine can activate mTORC1 at the Golgi apparatus through Arf1 in a Rag-independent manner[229], and Golgi-resident substrates such as GRASP55 are phosphorylated by local mTORC1 pools[235]. In addition, canonical cytosolic substrates including S6K and 4E-BP1 can be phosphorylated independently of Rag-mediated lysosomal recruitment, reflecting the broad cytoplasmic distribution of mTORC1[236]. Moreover, active pools of mTORC1 have also been detected in the nucleus, where nuclear-targeted biosensors demonstrate growth factor-induced mTORC1 activity and nuclear

RHEB contributes to local regulation[237-239]. Together, these findings point to an emerging concept: beyond lysosome-based regulation, mTORC1 is organized into spatially distinct pools with differential substrate access.

1.4 Crosstalk between DDR and mTORC1 signaling pathways

An increasing number of studies indicate that the DDR and mTORC1 signaling are functionally interconnected. Evidence for this crosstalk arises from diverse experimental systems, including normal and cancer cell lines as well as mouse tissues, and spans a wide range of perturbations such as ionizing radiation, UV light, topoisomerase inhibitors, and replication stress. The reported outcomes vary from checkpoint activation and repair factor recruitment to alterations in translation and lysosomal programs. Collectively, these findings suggest the existence of bidirectional influences between the two pathways. However, the available evidence remains fragmented and difficult to integrate into a unifying model. The following subsections summarize the current knowledge, highlighting both established connections and the key limitations that define the present knowledge gap.

1.4.1 Regulation of mTORC1 pathway by DDR signaling

Cytoplasmic ATM represses mTORC1 activity through ATM–LKB1–AMPK–TSC2 axis during oxidative and nitrosative stresses, which was covered in Section 1.2.2.3.

ATR–cholesterol signaling to mTORC1

Beyond its canonical role in stabilizing stalled forks and signaling through CHK1, ATR increases *de novo* cholesterol synthesis through the phosphorylation and upregulation of lanosterol synthase (LSS), the enzyme essential for cholesterol synthesis pathway[240]. ATR affects mTORC1 activity through this pathway even in unperturbed cells without replication stress induction, also independently of CHK1 and the TSC complex. Moreover, activating ATR via induction of replication stress was sufficient to increase cholesterol levels, which enhanced mTORC1 lysosomal localization and activity, thereby linking ATR to mTORC1 pathway.

p53-driven transcriptional programs that restrain mTORC1 activity

Under genotoxic stress, the tumor suppressor p53 activates transcriptional programs that can suppress mTORC1 signaling. Among its targets, Sestrin1/2 and REDD1 (regulated in development and DNA damage responses 1) have been shown to repress mTORC1 activity[241-245]. Sestrins inhibit mTORC1 through two complementary mechanisms: (i) activation of AMPK, which phosphorylates and activates TSC2 to suppress RHEB-driven mTORC1 activity[246], and (ii) an AMPK-independent mechanism, in which Sestrins bind and inhibit GATOR2, thereby relieving GATOR1-mediated inhibition of Rag GTPases and preventing Rag-dependent recruitment of mTORC1 to lysosomes[243,244]. In parallel, REDD1 inhibits mTORC1 during hypoxia through a TSC-dependent mechanism[205,247]. Additionally, TSC2, AMPK β1 subunit, and PTEN (phosphatase and tensin homolog)–negative regulators of mTORC1 activity–have been identified as p53 targets, with their expression controlled in a stress-, cell-, and tissue-specific manner; however, functional relevance of this transcriptional regulation remains to be studied[248].

DNA-PK activity impinging on mTORC1 through AKT

DNA-PK physically interacts with and functionally engages mTORC2 (via SIN1, a component of mTORC2) to promote AKT Ser473 phosphorylation upon UV irradiation, thereby supporting cell survival[249]. DNA damage caused by ionizing radiation and topoisomerase inhibitors induce DNA-PK-dependent phosphorylation of SIN1, enabling its interaction with the guanine nucleotide exchange factor ECT2, which is required for full activation of AKT[250]. Inhibition of DNA-PK or disruption of mTORC2 diminished AKT Ser473 phosphorylation, which is required for full AKT activation. As AKT is an upstream activator of mTORC1 by inhibiting TSC2 and PRAS40, which negative regulate mTORC1 activity, DNA-PK signaling can impinge on mTORC1 activity through this mechanism.

1.4.2 Regulation of DDR by mTORC1 signaling

Accumulating evidence has suggested a role of mTORC1 in the DNA damage response, as mTORC1 inhibitors sensitized cells to DNA damage.

Opposing roles of S6K in DNA damage

S6K exerts dual functions in the DDR, acting as a negative regulator of DDR signaling while supporting DNA repair. On one hand, S6K phosphorylates the E3 ubiquitin ligase RNF168 at Ser60, thereby inhibiting its activity[251]. Since RNA168 is essential for propagating the DSB signaling and recruiting repair factors to sites of damage[24], this modification attenuates DDR signaling. Inhibition of S6K-mediated RNF168 phosphorylation restores signal amplification and repair initiation. On the other hand, S6K promotes DNA repair through cell cycle regulation and direct modification of repair proteins. It phosphorylates CDK1 at Ser39, enforcing a G2/M checkpoint arrest that facilitates homologous recombination, and phosphorylates MSH6 at Ser309, thereby enhancing mismatch repair[252]. Consistent with this pro-repair role, breast cancer cells with S6K gene amplifications display increased resistance to DNA-damaging therapeutics, and high S6K expression correlates with poor patient survival following chemotherapy[252]. By exerting both inhibitory and supportive functions within the DDR, S6K exemplifies the complexity of communication between genome maintenance pathways and metabolic signaling, an area that remains incompletely understood.

Translational control of checkpoint proteins

mTORC1 promotes cap-dependent translation and protein synthesis primarily through 4E-BP1 and S6K, as discussed above. This translational control influences the cellular abundance of checkpoint proteins. Inhibition of mTORC1, which suppresses protein synthesis, lowers CHK1 protein levels and sensitizes Ewing sarcoma cells to CHK1 inhibitors[253]. Notably, CHK1 inhibition activates 4E-BP1, thereby inhibiting protein synthesis and reducing CHK1 protein levels. Conversely, depletion of 4E-BP1 impairs checkpoint signaling after irradiation: 4E-BP1 knockdown reduces CHK2 phosphorylation, leading to an

incomplete G2 arrest, consistent with a reduced capacity to mount and maintain checkpoint responses[254]. In addition, both PI3K and DNA-PK inhibitors decrease 4E-BP1 protein levels via proteasomal degradation[254]. Although the full mechanisms remain to be defined, these lines of evidence support a role of mTORC1-regulated translation in controlling checkpoint proteins.

Lysosomal/TFEB–TFE3 programs intersect DDR outputs

The transcription factors TFEB and TFE3, mTORC1 substrates, are activated by genotoxic stress in a p53- and mTORC1-dependent manner[255]. Loss of TFEB and TFE3 reduces p53 stability and impairs p53-dependent transcriptional programs, with accompanying defects in cell-cycle control and apoptosis. TFEB is also also implicated in DNA repair: TFEB knockdown disrupts homologous recombination, leading to persistent γH2AX, and sensitizes cells to DNA damage-induced apoptosis[256]. In addition, inhibiting calcineurin (a TFEB phosphatase) increases apoptosis[256]. These effects are consistent with the downregulation of cell-cycle and homologous-recombination genes and the upregulation of pro-apoptotic genes upon TFEB knockdown. Although these studies indicate context-dependent effects of TFEB on apoptosis, they establish TFEB/TFE3 as transcriptional regulators within the DDR.

Although growing evidence points to crosstalk between the DDR and mTORC1 pathway, both operate within extensive signaling networks comprising numerous upstream regulators and downstream effectors. It is therefore not unexpected that components of one pathway can infuence, or be influenced by, elements of the other. However, the literature remains fragmented—reported effects are often context-dependent and difficult to integrate. A unifying framework is still lacking to explain how DDR inputs are transmitted to the principal regulators of mTORC1. This challenge is further compounded by the complexity of mTORC1 regulation itself, as the pathway integrates diverse nutrient, energy, and stress signals that can be indirectly affected by DNA damage.

1.5 Scientific question, hypothesis, and aims

The background outlined above highlights a critical gap in understanding how cells coordinate genome surveillance with metabolic regulation. Both the DDR and mTORC1 pathways are essential for maintaining cellular homeostasis and viability, and each has been extensively characterized. However, the direct molecular link between them remains incompletely understood. Although several studies have suggested indirect signaling from DDR kinases to upstream regulators of mTORC1, it is still unclear whether DNA damage influences mTORC1 through more direct mechanisms on its immediate regulators. More broadly, how DNA damage reshapes mTORC1 activity to meet the metabolic demands of genome maintenance remains unresolved.

The central question of this thesis is therefore: what is the molecular mechanism that connects the DNA damage response to mTORC1 signaling, enabling DNA damage to modulate metabolic outputs?

Given that the DDR represents an energy-intensive cellular program, I hypothesize that genome surveillance and metabolic control are coordinated through direct signaling mechanisms. Specifically, I propose that DDR kinases target proximal regulators of mTORC1, allowing cells to fine-tune its activity and promote adaptive cellular responses under genotoxic stress.

To test this hypothesis, the research presented in this thesis pursued three main aims:

(1) To determine whether DDR kinases directly modify core regulators of mTORC1, thereby establishing a mechanistic link between DNA damage signaling and mTORC1 activation.
(2) To define how this signaling connection modulates mTORC1 output in the context of DNA damage.
(3) To assess the functional consequences of this regulatory axis and elucidate how altered mTORC1 signaling influences cellular adaptation to genotoxic stress.

Chapter 2. Results

2.1 RHEB is phosphorylated in response to DNA damage

RHEB is best known as a direct activator of mTORC1, with its activity primarily governed by its nucleotide-binding state under the control of the TSC complex, the canonical GAP for RHEB[196,257-259]. While this GTP/GDP cycle is considered the dominant mode of RHEB regulation, several studies have revealed that RHEB is also subject to additional layers of control via post-translational modifications (PTMs), such as ubiquitylation and phosphorylation, that can modulate its activity towards mTORC1[191-194]. These observations raise the possibility that RHEB activity may be dynamically tuned by different PTMs under specific conditions. To systematically identify reported PTMs on RHEB, we queried the PhosphoSitePlus database (www.phosphosite.org)[260], which compiles multiple large-scale phospho-proteomics and proteomics datasets. This search revealed that human RHEB is modified by diverse PTMs, including phosphorylation, ubiquitylation and acetylation (Figure 2.1). Together, these data support the view that RHEB receives regulatory input beyond its canonical nucleotide-loading status.

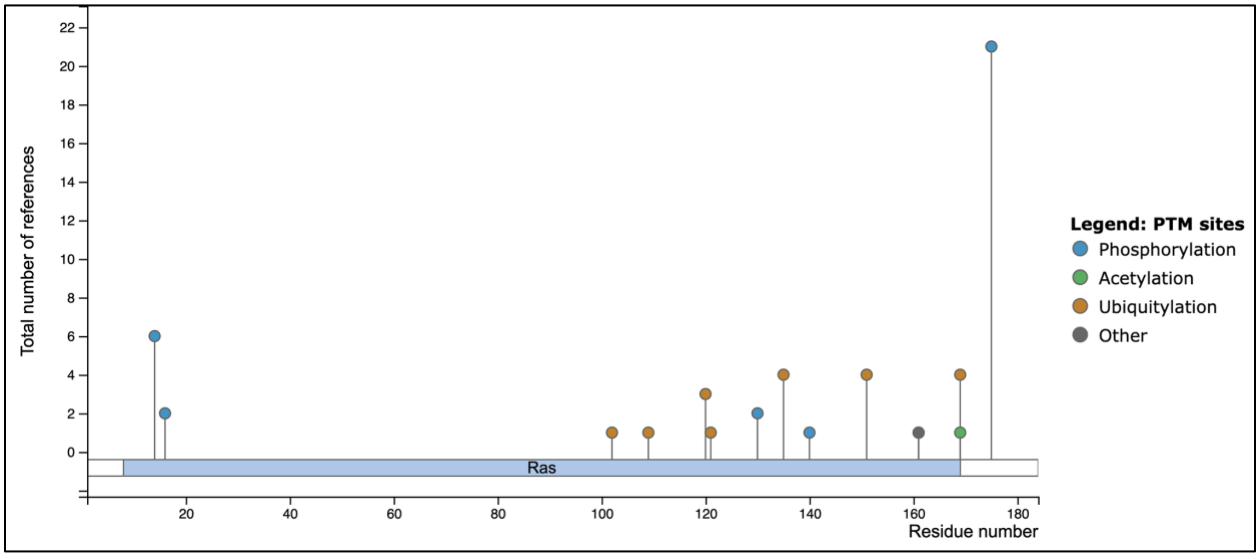

Figure 2.1 RHEB is subject to multiple post-translational modifications (PTMs).

The schematic summarizes reported PTMs mapped to the human RHEB protein. Residue numbers are shown along the x-axis, and the y-axis indicates the number of independent datasets in which each modification site has been identified. Distinct types of modifications are represented by colored circles: phosphorylation (blue), acetylation (green), and ubiquitylation (orange). Other less frequently reported PTMs, such as succinylation, are indicated in brown. Data were compiled from PhophoSitePlus (https://www.phosphosite.org), which integrates multiple proteomics studies.

Among the identified sites, serine 175 (S175), located near the C-terminal end of RHEB, stood out as it was consistently detected as phosphorylated across multiple cell types and conditions (Figure 2.2). Notably, many of the datasets reporting this modification were derived from phospho-proteomics screens designed to enrich for ATM/ATR substrates using antibodies that recognize phosphorylated serine/threonine followed by glutamine (pS/TQ)[192], the canonical consensus motif of ATM and ATR[260]. Since these kinases are central mediators of the DNA damage response (DDR), this observation raised the possibility that RHEB S175 (hereafter, RHEB^{S175}) phosphorylation occurs downstream of DDR signaling. We therefore hypothesized that RHEB^{S175} may be phosphorylated in response to genotoxic stress.

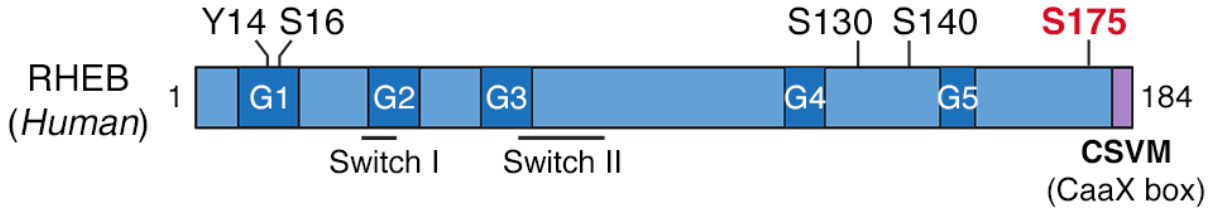

Figure 2.2 Schematic representation of phosphorylation sites on human RHEB.
Identified phosphorylation sites on human RHEB were compiled from publicly available phospho-proteomics datasets curated in the PhosphoSitePlus database[260]. The schematic also illustrates the positions of key structural features of RHEB, including the conserved GTP-binding motifs (G1-G5), the Switch I and Switch II regions that undergo conformational changes upon nucleotide exchange, and the C-terminal CaaX box motif, which undergoes farnesylation and is essential for membrane anchoring. Among the reported sites, serine 175 (S175), which is the focus of this study, is highlighted in red.

To test this hypothesis, we generated a phospho-specific antibody against RHEB^{S175} and validated its specificity using a non-phosphorylatable alanine mutant (RHEB^{S175A}) (Figure

2.3). This reagent enabled direct monitoring of RHEB^{S175} phosphorylation following DNA damage.

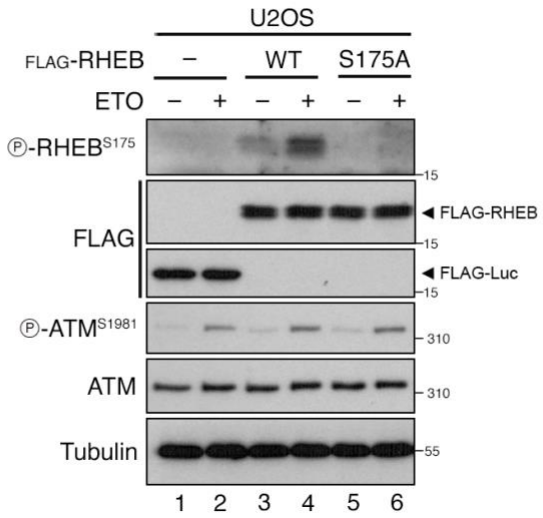

Figure 2.3 Validation of the phospho-specific RHEB S175 antibody.

U2OS cells were transiently transfected with FLAG-tagged Luciferase (–; transfection control), FLAG-tagged wild-type RHEB (WT), or the phospho-deficient RHEB S175A (S175A). Cells were treated with etoposide (ETO; 20 μM, 2 h) or with DMSO as vehicle control. Whole-cell lysates were subjected to immunoblotting and probed with the indicated antibodies, including the custom anti-phospho-RHEB S175 antibody. The phospho-specific antibody recognized WT RHEB upon etoposide treatment but not the S175A mutant, confirming its specificity.

Next, we examined whether RHEB^{S175} phosphorylation is induced by DNA damaging agents with distinct mechanisms of action. In human osteosarcoma U2OS cells expressing FLAG-tagged RHEB, etoposide (a topoisomerase II inhibitor[261]) robustly activated ATM, as indicated by Ser1981 autophosphorylation as expected, and markedly increased RHEB^{S175} phosphorylation from low basal levels (Figure 2.4a,b)[112]. Similar increases were observed after treatment with doxorubicin, another topoisomerase II inhibitor that also intercalates DNA[262], and hydroxyurea, which induces replication stress by depleting deoxyribonucleotides through inhibition of ribonucleotide reductase (Figure 2.4c-f)[263,264]. Ionizing radiation (IR) also produced a dose-dependent induction of RHEB^{S175} phosphorylation in RHEB knock-out (KO) human embryonic kidney HEK293FT cells reconstituted with FLAG-RHEB (Figure 2.4g,h).

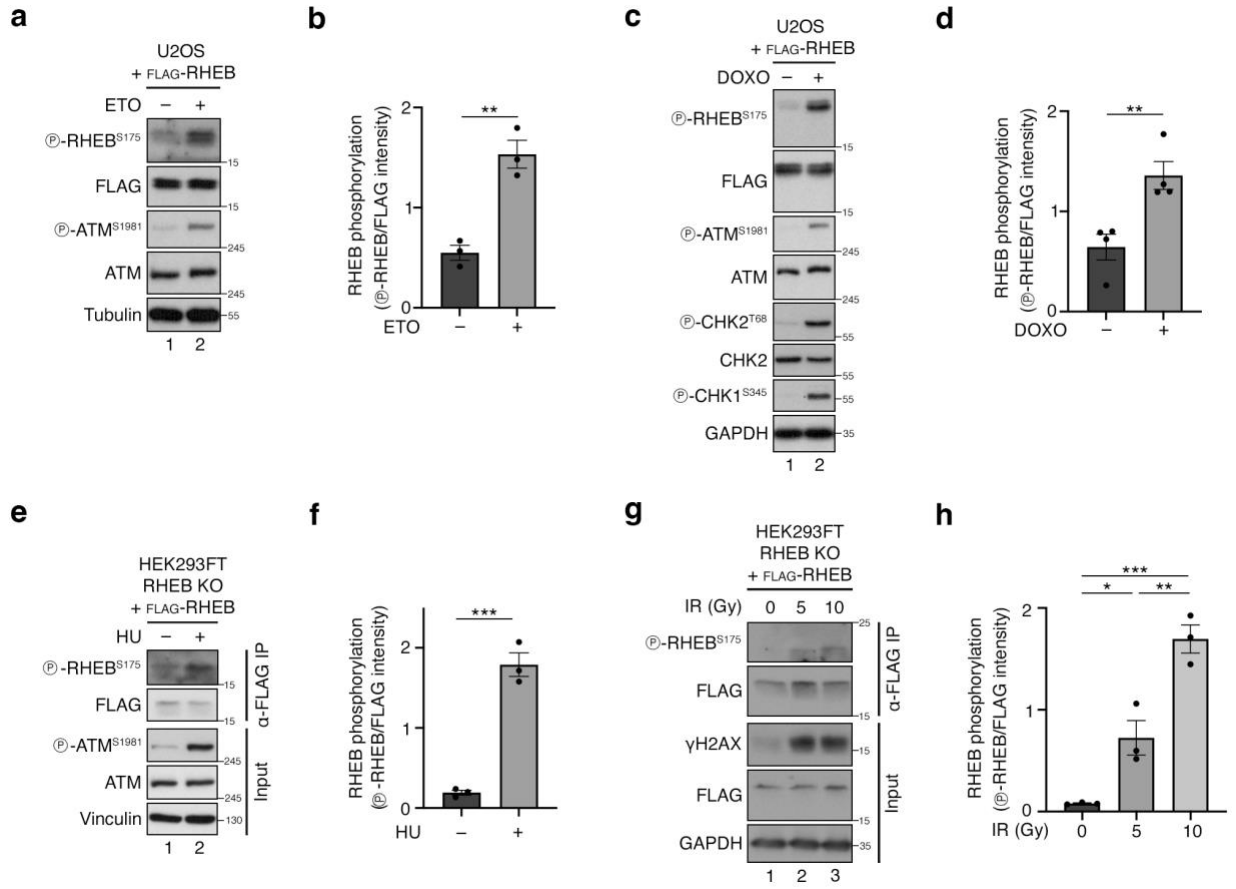

Figure 2.4 RHEB is phosphorylated at S175 in response to DNA damage.

(a-b) U2OS cells transiently expressing FLAG-tagged RHEB were treated with etoposide (ETO; 20 μM, 2 hr) or DMSO as vehicle control. Whole-cell lysates were subjected to immunoblotting with the indicated antibodies. Phosphorylation of ATM at Ser1981 was used as a marker for DDR activation (a). Quantification of RHEB phosphorylation (p-RHEB/FLAG signal) in (b). *n* = 3 independent experiments.

(c-d) Immunoblots with lysates from U2OS cells transiently expressing FLAG-tagged RHEB treated with doxorubicin (DOXO; 2 μM, 2 hr) or DMSO as control, probed with the indicated antibodies. Phosphorylation of ATM (ATM^{S1981}), CHK2 (CHK2^{T68}) and CHK1 (CHK1^{S345}) were used to confirm DDR induction (c). Quantification of RHEB phosphorylation (p-RHEB/FLAG signal) in (d). *n* = 4 independent experiments.

(e-f) RHEB KO HEK293FT cells stably expressing FLAG-tagged RHEB were treated with hydroxyurea (HU; 1 mM, 2 h) or with water as vehicle control. FLAG immunoprecipitates and input lysates were analyzed by immunoblotting with the indicated antibodies (e). Quantification of RHEB phosphorylation (p-RHEB/FLAG signal) in (f). *n* = 3 independent experiments.

(g-h) Immunoblots with lysates from RHEB KO HEK293FT cells stably expressing FLAG-tagged RHEB, left untreated or exposed to increasing doses of ionizing radiation (0-10 Gy), probed with the indicated antibodies (g). Quantification of RHEB phosphorylation (p-RHEB/FLAG signal) in (h). *n* = 3 independent experiments. Data in graphs shown as mean ± SEM. * $p < 0.05$, ** $p < 0.01$, *** $p < 0.001$.

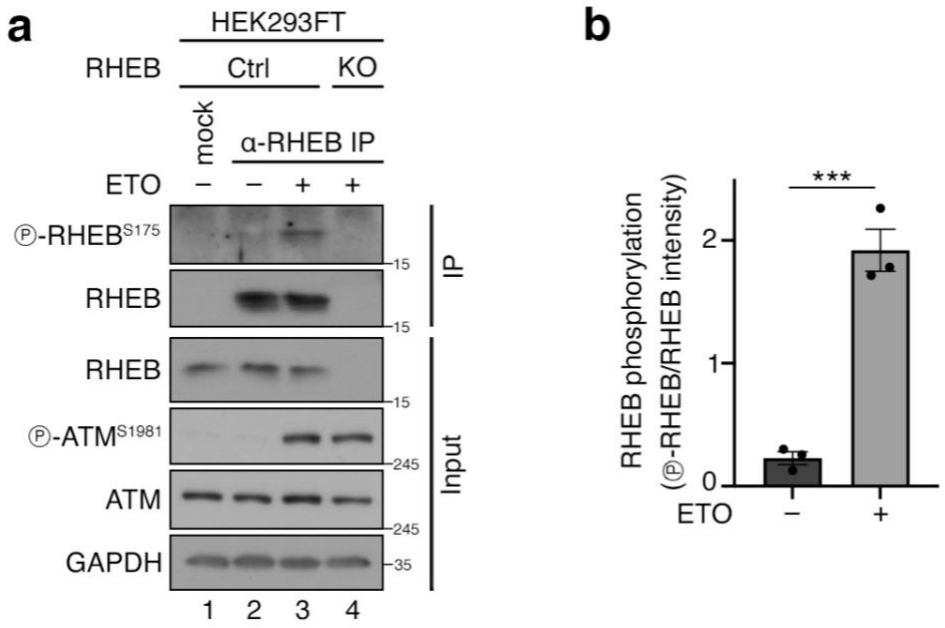

Figure 2.5 Endogenous RHEB is phosphorylated at S175 in response to DNA damage.
(a-b) Endogenous RHEB was immunoprecipitated from control HEK293FT cells (Ctrl) treated with etoposide (ETO; 20 μM, 2 hr) or DMSO as vehicle control, followed by immunoblotting with the indicated antibodies. RHEB knockout HEK293FT cells were included as a negative control to confirm antibody specificity (a). Quantification of endogenous RHEB phosphorylation (p-RHEB/RHEB) in (b). *n* = 3 independent experiments. Data in graph shown as mean ± SEM. *** $p < 0.001$.

Importantly, these findings were not restricted to exogenously expressed RHEB: immunopurified endogenous RHEB from HEK293FT cells also displayed increased S175 phosphorylation following etoposide treatment (Figure 2.5). Together, these data demonstrate that RHEB is phosphorylated at serine 175 in response to diverse forms of DNA damage, including topoisomerase inhibition, replication stress, and IR. This establishes RHEB^{S175} as a bona fide DNA damage-responsive phosphorylation site and suggests a potential regulatory role for this modification in the cellular response to genotoxic stress.

2.2 ATM mediates RHEB phosphorylation upon genotoxic stress

Having established that RHEB is phosphorylated at serine 175 in response to DNA damage, we next sought to identify the upstream kinase responsible for this modification. As RHEB

S175 lies within a consensus pS/TQ motif typically targeted by ATM/ATR kinases, and its phosphorylation was consistently detected in DNA damage-oriented phospho-proteomics screens, we next sought to determine whether one of the apical DDR kinases is responsible for RHEB phosphorylation.

To test whether ATM activity is required for RHEB phosphorylation, we treated U2OS cells expressing FLAG-RHEB with KU-60019, a selective ATM inhibitor. Under these conditions, etoposide-induced phosphorylation of RHEB^{S175} was completely abolished, which implicates ATM as the upstream kinase (Figure 2.6a). In contrast, pharmacological inhibition of ATR with VE-821 or of DNA-PK with NU7441 did not prevent the etoposide-induced phosphorylation of RHEB (Figure 2.6b).

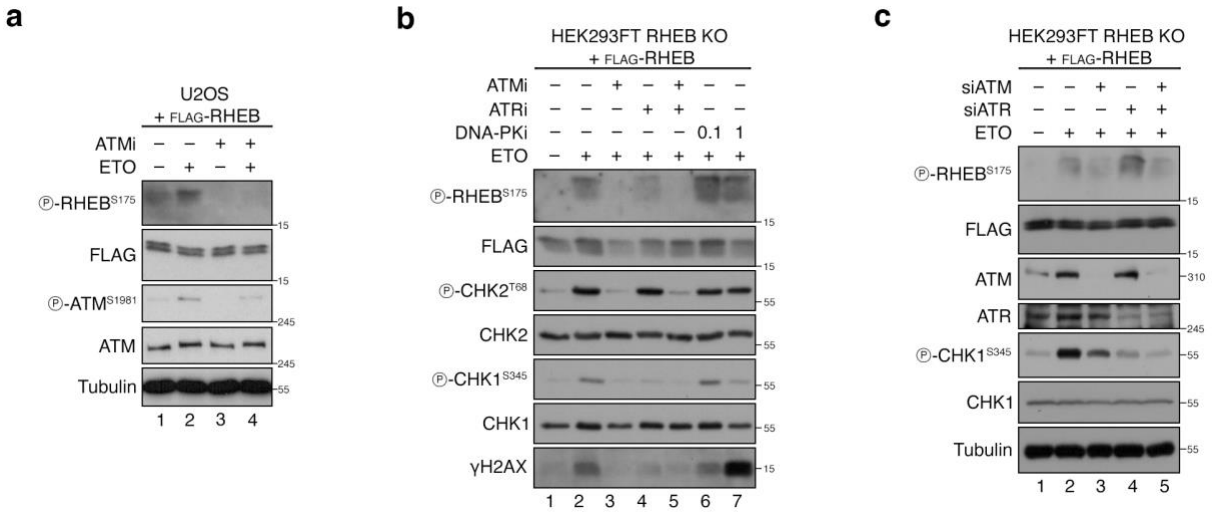

Figure 2.6 ATM, but not ATR or DNA-PK, mediates DNA damage-induced RHEB phosphorylation.
(a) Immunoblots with lysates from U2OS cells transiently expressing FLAG-tagged RHEB, pre-treated with ATM inhibitor (ATMi; KU-60019, 1 μM, 30 min), followed by treatment with etoposide (ETO; 20 μM, 2 hr), probed with the indicated antibodies. DMSO was used as control for all treatments. *n* = 3 independent experiments.
(b) Immunoblots with lysates from RHEB KO HEK293FT cells stably expressing FLAG-tagged RHEB, pre-treated with ATM inhibitor (ATMi; KU-60019; 1 μM), ATR inhibitor (ATRi; VE-832; 1 μM), or DNA-PK inhibitor (DNA-PKi; NU7441; 0.1 μM or 1 μM) for 30 min, followed by treatment with etoposide (ETO; 20 μM, 2 hr), probed with the indicated antibodies. DMSO was used as control for all treatments. *n* = 3 independent experiments.
(c) Immunoblots with lysates from RHEB KO HEK293FT cells stably expressing FLAG-tagged RHEB, transfected with siRNAs targeting ATM (siATM), ATR (siATR), or Luciferase as a control, probed with

the indicated antibodies. Cells were treated with etoposide (ETO; 20 μM, 2 hr), or DMSO as control, prior to lysis.

To further validate these observations, we employed genetic approaches. Small interfering RNA (siRNA)-mediated depletion of ATM markedly reduced etoposide-induced RHEB^{S175} phosphorylation, whereas ATR depletion had no detectable effect (Figure 2.6c). These results are consistent with the inhibitor studies and confirm that ATM, but not ATR or DNA-PK, is the principal kinase responsible for this modification. Together, these results suggest that RHEB phosphorylation lies downstream of canonical ATM signaling during genotoxic stress.

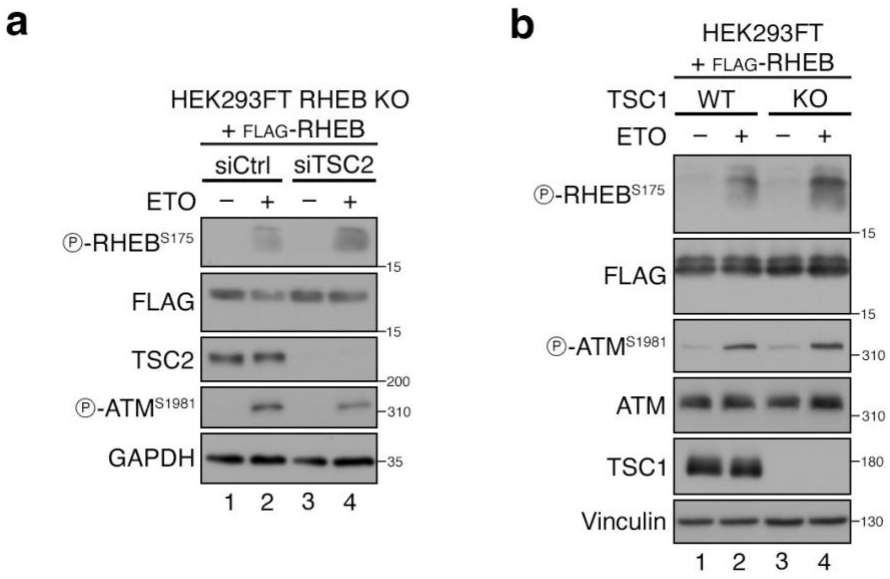

Figure 2.7 DNA damage-induced RHEB phosphorylation does not require the TSC.

(a) Immunoblots with lysates from RHEB KO HEK293FT cells stably expressing FLAG-tagged RHEB, transfected with siRNAs targeting TSC2 (siTSC2) or Luciferase as a control (siCtrl), probed with the indicated antibodies. Cells were treated with etoposide (ETO; 20 μM, 2 hr), or DMSO as control, prior to lysis.

(b) Immunoblots with lysates from HEK293FT WT or TSC1 KO cells transiently expressing FLAG-tagged RHEB, treated with etoposide (ETO; 20 μM, 2 hr) or DMSO as control, probed with the indicated antibodies.

ATM has previously been shown to regulate mTORC1 activity indirectly via the LKB1–AMPK–TSC2 axis in response to oxidative stress [126,127]. Because TSC2 is the core component of the

TSC complex and the cognate GAP for RHEB, we asked whether ATM influences RHEB phosphorylation indirectly through TSC. To address this possibility, we examined RHEB phosphorylation upon TSC2 knockdown or in TSC1 knockout cells following etoposide treatment. In both settings, RHEB phosphorylation was robustly induced by etoposide, indicating that this modification occurs independently of the TSC complex and of the previously-reported ATM–LKB1–AMPK–TSC2 signaling axis (Figure 2.7).

Together with the identification of RHEB^{S175} as a putative ATM-regulated phospho-site, these findings suggested that ATM may directly phosphorylate RHEB. Indeed, co-immunoprecipitation (co-IP) experiments demonstrated that exogenously expressed FLAG-tagged RHEB interacts with endogenous ATM protein (Figure. 2.8a), in line with previous observations[196] indicating an interaction between RHEB and a catalytic domain of ATM.

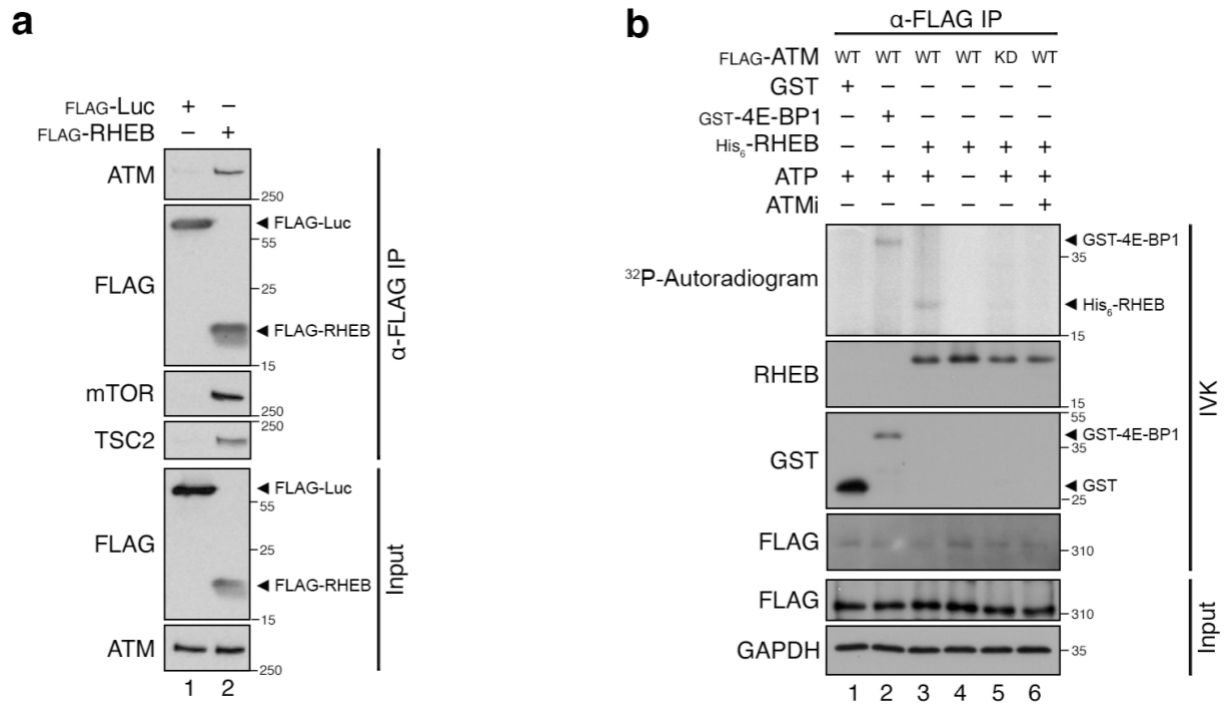

Figure 2.8 RHEB is a direct substrate of ATM: evidence from interaction and in vitro kinase assays.

(a) Co-immunoprecipitation between endogenous ATM and RHEB from HEK293FT cells transiently expressing FLAG-tagged RHEB or Luciferase (Luc) as a control. The input and IP samples were analyzed by immunoblotting with the indicated antibodies. *n* = 3 independent experiments.

(b) *In vitro* kinase assays with ATM immunopurified from HEK293FT cells transiently expressing FLAG-tagged WT or kinase-dead (KD) ATM, using recombinant His_6-tagged RHEB protein as a substrate. Cells were treated with etoposide (ETO; 20 μM, 2 hr) before lysis to activate ATM. Specificity of RHEB phosphorylation was confirmed by pre-treatment with an ATM inhibitor (ATMi; KU-60019; 1 μM, 30 min), or omitting ATP from the reaction. Recombinant GST or GST-4E-BP1 proteins were used as a negative or positive control, respectively. Substrate phosphorylation detected by autoradiography. *n* = 3 independent experiments.

Finally, we tested whether ATM is capable of directly phosphorylating RHEB. *In vitro* kinase (IVK) assays were performed using immunopurified FLAG-tagged ATM from etoposide-treated cells, in which ATM is robustly activated, together with recombinant His_6-tagged RHEB. As a positive control, recombinant GST-tagged 4E-BP1, a well-established ATM substrate, was included in parallel reactions and displayed robust phosphorylation, thereby validating the ATM activity of this experimental setup (Figure 2.8b). Under the same conditions, RHEB was also phosphorylated by ATM, demonstrating that it can serve as a direct substrate. This phosphorylation was strictly dependent on ATM catalytic activity, as it was abolished in the absence of ATP, in the presence of the selective ATM inhibitor KU-60019, or when a kinase-dead ATM mutant was used (Figure. 2.8b).

Together, these findings establish ATM as the upstream kinase mediating RHEB phosphorylation in response to DNA damage and provide biochemical evidence that RHEB is a direct substrate of ATM.

2.3 DNA damage triggers substrate-specific mTORC1 responses

mTORC1 coordinates cellular growth and stress adaptation by phosphorylating a wide range of downstream targets[138,154]. Among the most well-studied are ribosomal S6 kinase (S6K), which promotes protein synthesis[159], and the lysosome-associated transcription factor EB (TFEB), a master regulator of lysosome biogenesis and autophagy[176,181]. Increasing evidence demonstrates that mTORC1 activity is not applied uniformly across all substrates, but instead displays substrate-specific regulation[236,265-269]. For example, TFEB—an mTORC1 substrate that localizes to lysosomes—is regulated differently from cytosolic substrates

such as S6K, particularly when lysosomal function is perturbed or the Rag GTPases are genetically inactivated[236]. On the other hand, hyperactivation of mTORC1 following TSC loss leads to increased phosphorylation of S6K but decreased phosphorylation of TFEB, thereby promoting TFEB activation and lysosome biogenesis[266,267,270]. Accordingly, genetic ablation of RHEB induces the opposite pattern: diminished S6K phosphorylation and enhanced TFEB phosphorylation[265].

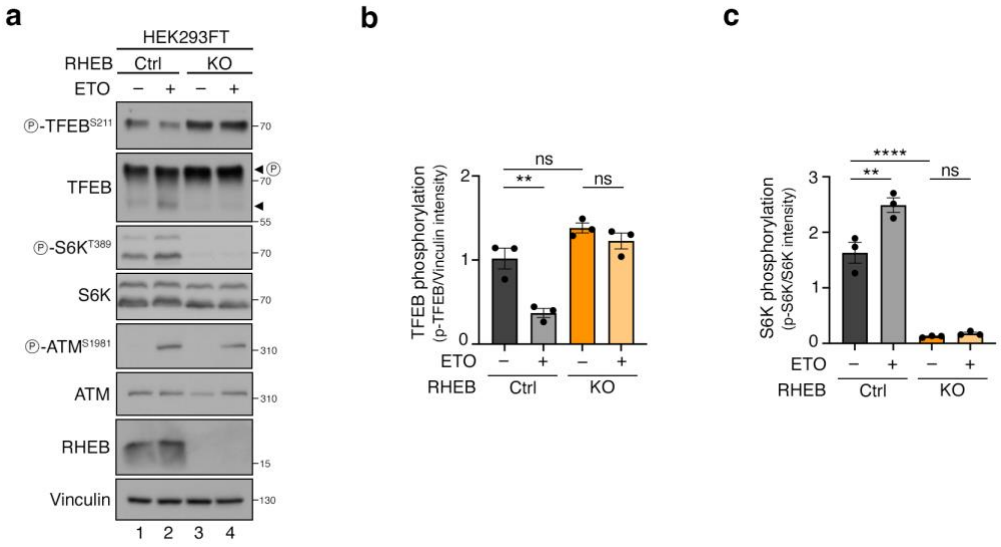

Figure 2.9 DNA damage rewires mTORC1 signaling to promote substrate-specific responses. **(a-c)** Immunoblots with lysates from control (Ctrl) and RHEB KO HEK293FT cells treated with etoposide (ETO; 20 μM, 8 h) or DMSO as vehicle control, probed with the indicated antibodies. Arrowheads indicate bands corresponding to phosphorylated (P) and non-phosphorylated TFEB forms (a). Quantification of TFEB phosphorylation (pTFEB/Vinculin) in (b) and S6K phosphorylation (p-S6K/total S6K) in (c). *n* = 3 independent experiments.

To determine how mTORC1 signaling responds to DNA damage in our setting, we examined the phosphorylation status of TFEB and S6K following etoposide treatment. In wild-type control cells, DNA damage induced a marked reduction in TFEB phosphorylation, while simultaneously causing an increase in S6K phosphorylation (Figure 2.9). Strikingly, the DNA damage-induced dephosphorylation of TFEB was strongly attenuated in RHEB knockout (KO) cells, indicating that this response is RHEB-dependent. By contrast, S6K phosphorylation was already minimal in RHEB KO cells and remained low regardless of DNA damage. These

observations demonstrate that DNA damage elicits substrate-specific remodeling of mTORC1 signaling, characterized by enhanced phosphorylation of S6K and RHEB-dependent dephosphorylation of TFEB.

2.4 TFEB is activated upon DNA damage in a RHEB-dependent manner

The activity of TFEB is tightly controlled by its phosphorylation status, which determines its subcellular localization. Under nutrient-rich conditions, mTORC1-mediated phosphorylation of TFEB retains it in the cytosol, preventing the nuclear import. Conversely, when TFEB is dephosphorylated, it translocates to the nucleus where it activates transcriptional programs that drive lysosomal biogenesis and autophagy[174,179,181,234,271,272].

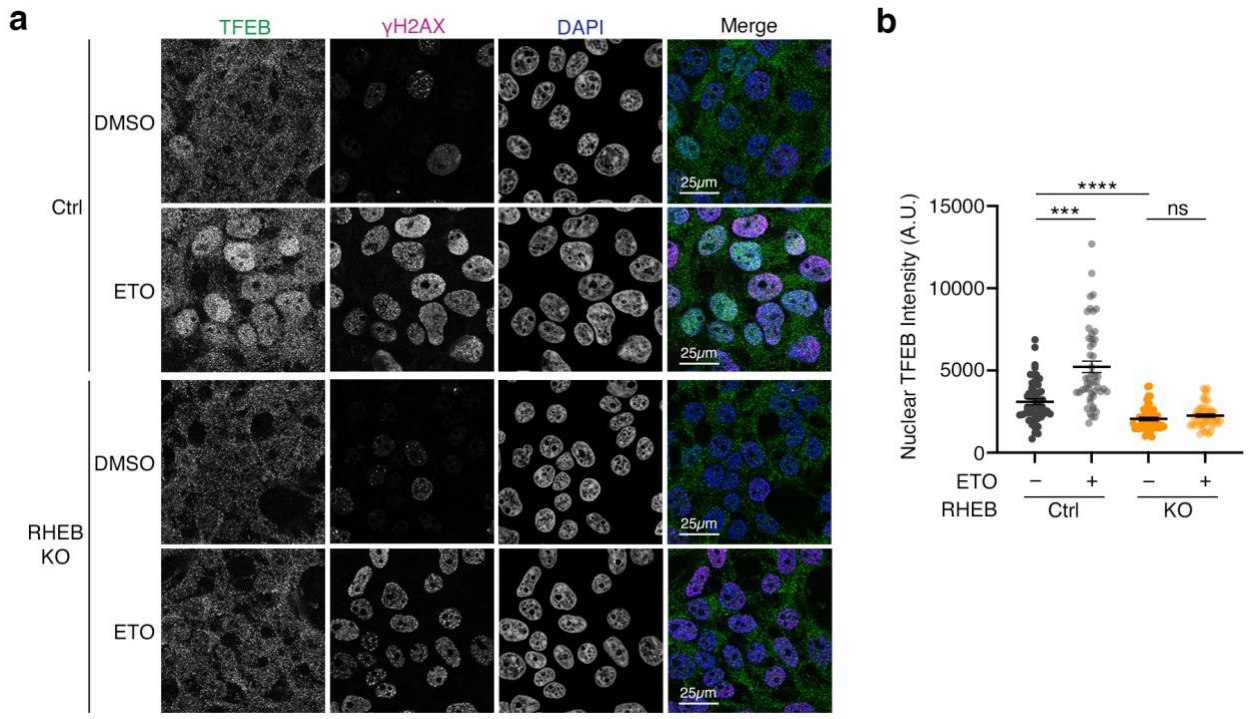

Figure 2.10 DNA damage induces nuclear translocation of TFEB in a RHEB-dependent manner. **(a-b)** Control (Ctrl) and RHEB knockout (RHEB KO) HEK293FT cells were treated with etoposide (ETO; 20 μM, 8 h) or with DMSO as vehicle control and analyzed by confocal microscopy. Cells were stained for TFEB (green) and γ-H2AX (red), with DAPI used to visualize nuclei (blue). γ-H2AX served as a marker for DDR induction. Representative images are shown in (a). Quantification of nuclear TFEB signal intensity (arbitrary units, A.U.) from 50 individual cells across 5 independent fields per condition is presented in (b). Scale bars = 25 μm. Data in graphs shown as mean ± SEM. Statistical

significance was determined using one-way ANOVA with multiple comparisons. *** $p < 0.001$, **** $p < 0.0001$; ns, non-significant.

As we observed a decrease in TFEB phosphorylation following DNA damage, we next examined whether this correlated with changes in TFEB localization. Immunofluorescence analysis revealed that etoposide treatment strongly enhanced nuclear accumulation of TFEB in wild-type cells, consistent with its dephosphorylation profile. In contrast, this DNA damage-induced nuclear translocation was markedly reduced in RHEB KO cells (Figure 2.10).

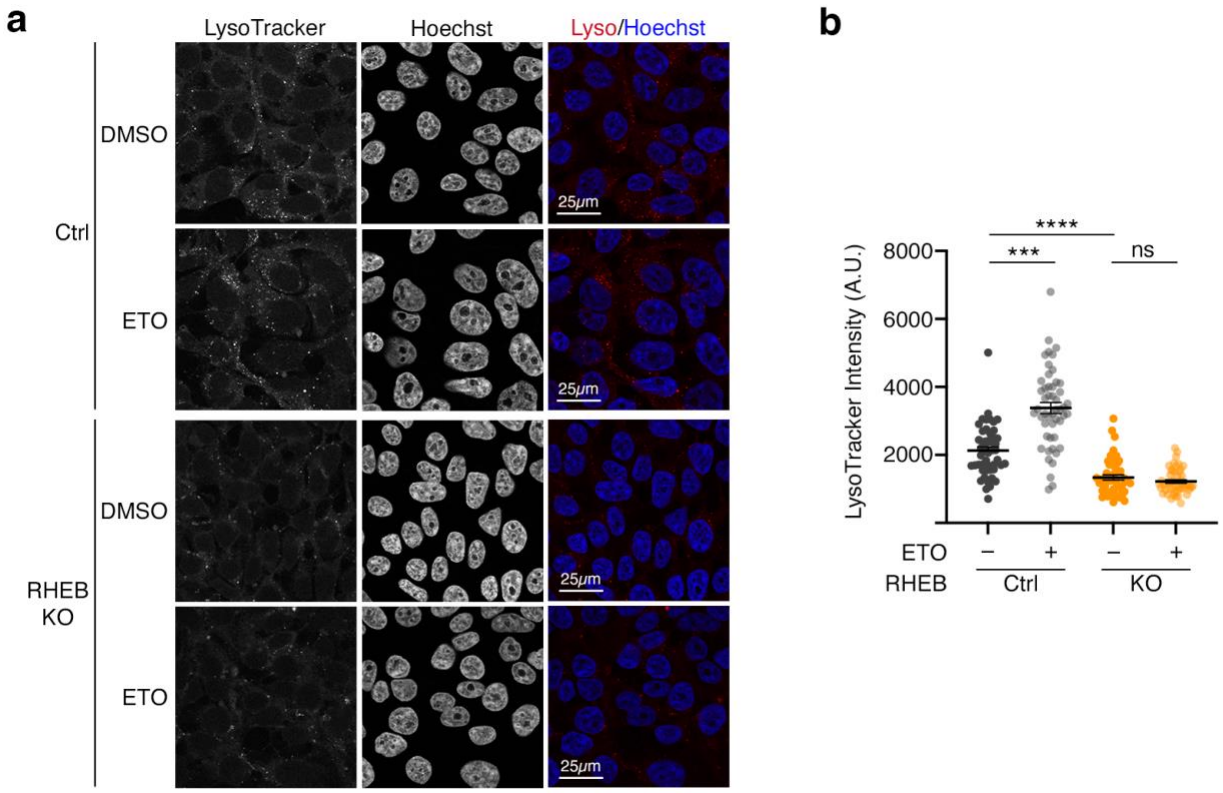

Figure 2.11 DNA damage increases lysosomal abundance in a RHEB-dependent manner.

(a-b) Control (Ctrl) and RHEB knockout (RHEB KO) HEK293FT cells were treated with etoposide (ETO; 20 μM, 8 h) or with DMSO as vehicle control and stained with LysoTracker (red) to assess lysosomal abundance by confocal microscopy. Nuclei were stained with Hoechst (blue). Representative images are shown in (a). Quantification of LysoTracker signal intensity (arbitrary units, A.U.) from 50 cells across 4-5 independent fields per condition is shown in (b). Scale bars = 25 μm. Data in graphs shown as mean ± SEM. Statistical significance was determined using one-way ANOVA with multiple comparisons. *** $p < 0.001$, **** $p < 0.0001$; ns, non-significant.

To assess whether nuclear translocation of TFEB is translated into activation of its transcriptional program, we measured lysosomal abundance using LysoTracker. In wild-type cells, etoposide treatment led to a pronounced increase in lysosomal signals, whereas this response was largely blunted in RHEB KO cells (Figure 2.11). Together, these findings indicate that genotoxic stress induces TFEB activation and lysosomal biogenesis in a manner that requires RHEB.

Table 1. Predicted kinases for RHEB phosphorylation sites identified by NetworKIN motif analysis. Predicted upstream kinases for individual RHEB phosphorylation sites were identified using NetworKIN, which integrates consensus kinase recognition motifs with contextual information from protein–protein interaction networks to increase prediction specificity. Scores represent the strength of the prediction.

Site	Predicted Kinase(s)	Score
S4	PKCepsilon	4.54
	PKCbeta	2.49
	PKCalpha	2.38
S6	**ATM**	14.43
S16	AMPKa2	2.71
S20	PKBalpha	2.76
	AMPKa2	2.75
T23	AMPKa2	2.77
T38	PDHK1	5.66
T42	PDHK1	2.67
T44	AMPKa2	2.79
T48	RSK3	2.7
	RSK1	2.62
T61	AMPKa2	2.79
S86	PDHK1	2.67
	PKCepsilon	2.54
T88	AMPKa2	2.77
S89	PKCepsilon	4.54
	PKCalpha	3.95
	PKCbeta	2.49
S92	PDHK1	9.38
S130	RSK3	2.76
	AMPKa2	2.73
	RSK1	2.62
	PDHK1	2.47
S149	PKCepsilon	4.54
	PKCbeta	2.49
S175	**ATM**	17.38
S182	PKCepsilon	4.1
	PKCbeta	2.05

2.5 RHEB phosphorylation is required for TFEB response upon genotoxic stress

Having established that TFEB activation in response to DNA damage is RHEB-dependent, we next asked whether phosphorylation of RHEB itself is necessary for this process. While phospho-proteomics studies identified serine 175 as a candidate ATM phosphorylation site, we reasoned that additional residues might also contribute to RHEB regulation. To address this, we applied NetworKIN, a computational tool that integrates kinase consensus motifs with protein-protein interaction networks to infer kinase-substrate relationships[273,274]. In addition to S175, NetworKIN predicted serine 6 (S6) as an additional putative ATM-regulated phosphorylation site on RHEB (Table 1).

To test the functional relevance of these sites, we generated a double phospho-deficient RHEB mutant (S6A/S175A; hereafter referred to as 'SSAA') and reconstituted RHEB knockout HEK293FT cells with either wild-type RHEB ($RHEB^{WT}$) or SSAA mutant RHEB ($RHEB^{SSAA}$). Stable expression of both $RHEB^{WT}$ or $RHEB^{SSAA}$ restored basal mTORC1 signaling in RHEB KO cells, as evidenced by recovery of S6K phosphorylation (Figure 2.12). This demonstrates that the $RHEB^{SSAA}$ mutant is competent to activate mTORC1 under steady-state conditions.

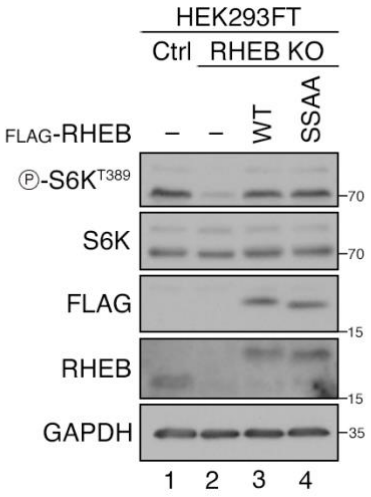

Figure 2.12 Re-expression of RHEB WT or phosphorylation-deficient RHEB S6A/S175A restores mTORC1 activity in RHEB knockout HEK293FT.

HEK293FT control (Ctrl), RHEB knockout (RHEB KO), and RHEB KO cells stably reconstituted with FLAG-tagged wild-type RHEB (WT) or the phosphorylation-deficient double mutant RHEB S6A/S175A (SSAA) were cultured under nutrient-replete conditions. Whole cell lysates were subjected to immunoblotting with the indicated antibodies to assess mTORC1 activity. *n* = 3 independent experiments.

We then examined how these cells respond to DNA damage. Upon etoposide treatment, $RHEB^{WT}$ cells exhibited a clear reduction in TFEB phosphorylation, whereas this response was strongly attenuated in $RHEB^{SSAA}$-expressing cells (Figure 2.13). In contrast, S6K phosphorylation was increased to a similar extent in both $RHEB^{WT}$ and $RHEB^{SSAA}$ cells, indicating that the defect is specific to the regulation of lysosomal mTORC1 signaling and TFEB phosphorylation (Figure 2.13).

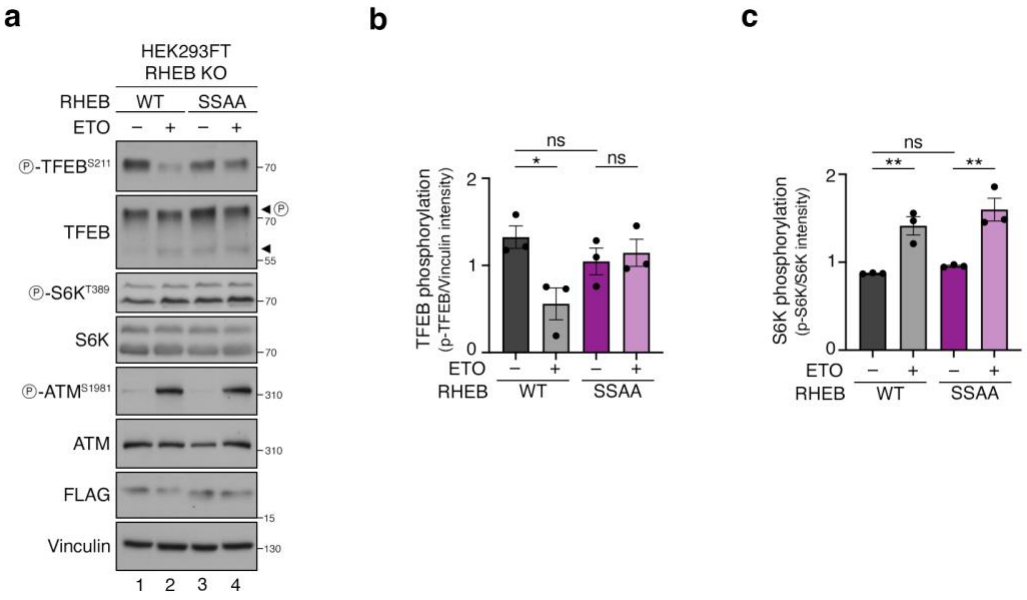

Figure 2.13 DNA damage-induced TFEB dephosphorylation requires RHEB phosphorylation.
(a-c) RHEB knockout (RHEB KO) HEK293FT cells stably expressing FLAG-tagged wild-type RHEB (WT) or the phosphorylation-deficient RHEB S6A/S175A double mutant (SSAA) were treated with etoposide (ETO; 20 µM, 8 h) or DMSO as vehicle control. Whole-cell lysates were subjected to immunoblotting with the indicated antibodies. Arrowheads indicate the slower-migrating phosphorylated (P) and faster-migrating dephosphorylated forms of TFEB (a). Quantification of TFEB phosphorylation (p-TFEB/Vinculin) in (b) and S6K phosphorylation (p-S6K/total S6K) in (c). *n* = 3 independent experiments. Data in graphs shown as mean ± SEM. Statistical significance was determined using one-way ANOVA with multiple comparisons. ** $p < 0.01$; ns, non-significant.

Consistent with the signaling results, TFEB nuclear translocation was induced by DNA damage in RHEB^{WT} cells but was markedly impaired in RHEB^{SSAA}-expressing cells (Figure 2.14). Similarly, etoposide-induced increase in lysosomal abundance, monitored by LysoTracker staining, was observed in RHEB^{WT}-reconstituted cells but absent in RHEB^{SSAA} cells (Figure 2.15).

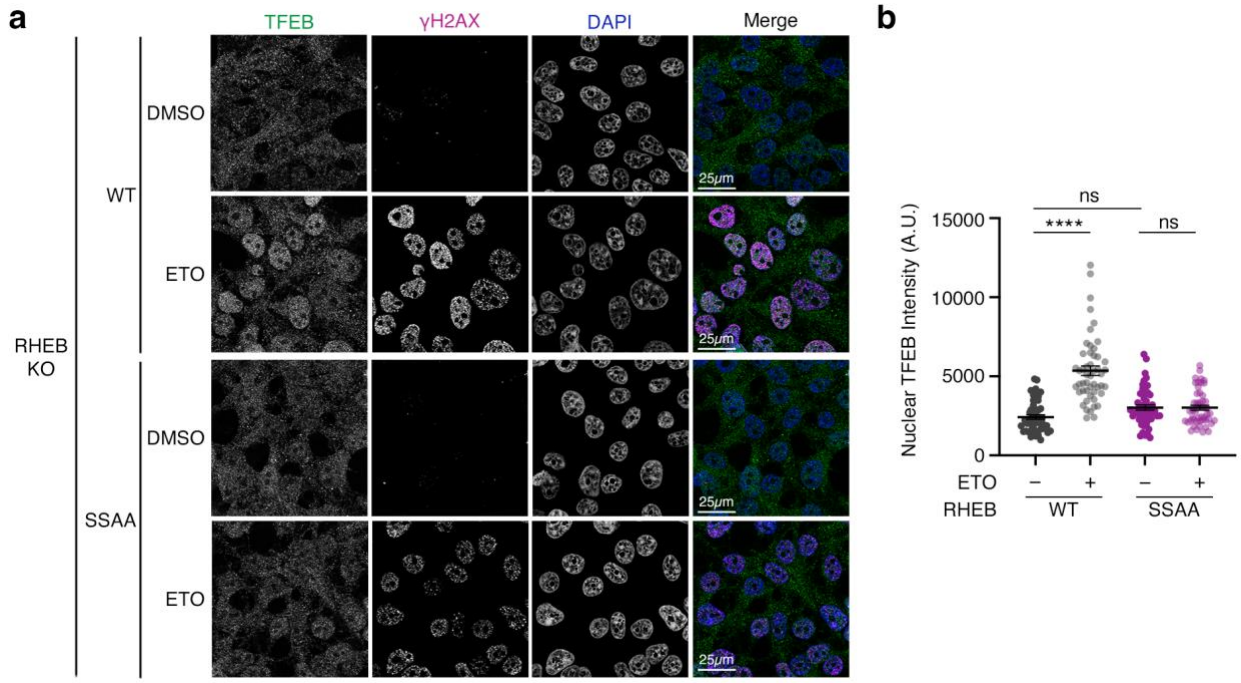

Figure 2.14 DNA damage-induced TFEB nuclear translocation requires RHEB phosphorylation. **(a-b)** RHEB knockout (RHEB KO) HEK293FT cells stably expressing FLAG-tagged wild-type RHEB (WT) or a phosphorylation-deficient RHEB$^{S6A/S175A}$ mutant (SSAA) were treated with etoposide (ETO; 20 μM, 8 h) or with DMSO as vehicle control. TFEB localization was analyzed by confocal microscopy. Cells were stained for TFEB (green) and γ-H2AX (red), with DAPI used to visualize nuclei (blue). γ-H2AX served as a marker for DDR induction. Representative images are shown in (a). Quantification of nuclear TFEB signal intensity (arbitrary units, A.U.) from 50 cells across 4-5 independent fields per condition is presented in (b). Scale bars = 25 μm. Data in graphs shown as mean ± SEM. Statistical significance was determined by one-way ANOVA with multiple comparisons. **** $p < 0.0001$; ns, non-significant.

Together, these data demonstrate that ATM-dependent phosphorylation of RHEB is required for activating the TFEB axis of mTORC1 signaling in response to DNA damage. While RHEB phosphorylation is dispensable for maintaining basal mTORC1 activity, it is required to couple DNA damage signals to TFEB activation and lysosome biogenesis.

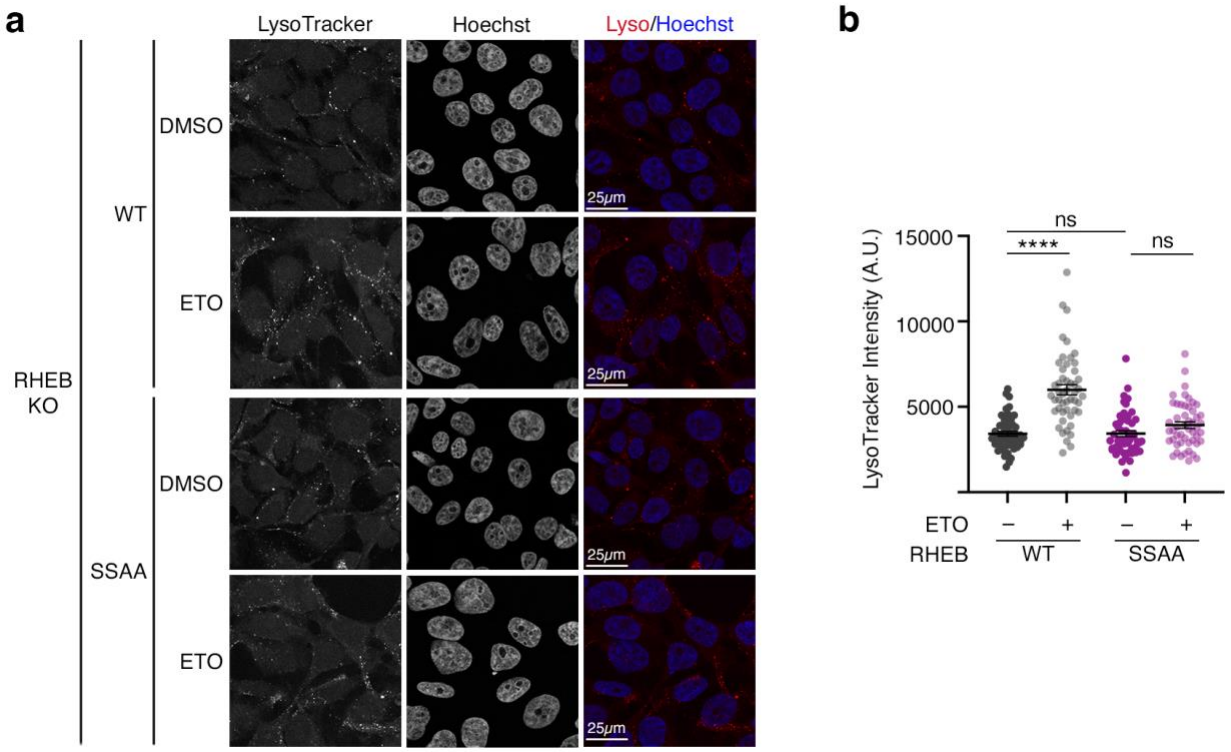

Figure 2.15 DNA damage-induced increase in lysosomal abundance requires RHEB phosphorylation.

(a-b) RHEB knockout (RHEB KO) HEK293FT cells stably expressing FLAG-tagged wild-type RHEB (WT) or the phosphorylation-deficient RHEB$^{S6A/S175A}$ mutant (SSAA) were treated with etoposide (ETO; 20 μM, 8 h) or with DMSO as vehicle control. Cells were stained with LysoTracker (red) to assess lysosomal abundance and with Hoechst (blue) to label nuclei. Representative confocal images are shown in (a). Quantification of LysoTracker signal intensity (arbitrary units, A.U.) from 50 cells across 4-5 independent fields per condition is shown in (b). Scale bars = 25 μm. Data in graphs shown as mean ± SEM. Statistical significance was determined using one-way ANOVA with multiple comparisons. **** $p < 0.0001$; ns, non-significant.

2.6 RHEB phosphorylation promotes TFEB-dependent proliferative recovery after DNA damage

Given the established role of mTORC1 in adapting cellular physiology to stress, we next asked whether RHEB-mediated TFEB activation contributes to the cellular response to DNA damage. To assess this, we monitored cell growth dynamics following ionizing radiation (IR) by measuring confluency over time. Wild-type cells displayed a transient pause in proliferation after exposure to 10 Gy IR, followed by recovery and resumption of growth

(Figure 2.16a). In contrast, RHEB knockout cells exhibited a marked defect in recovery, failing to resume proliferation after the transient growth arrest induced by irradiation. Importantly, this effect was specific to the cellular response to irradiation, as RHEB KO cells displayed similar growth kinetics to wild-type controls under basal conditions (Figure 2.16b).

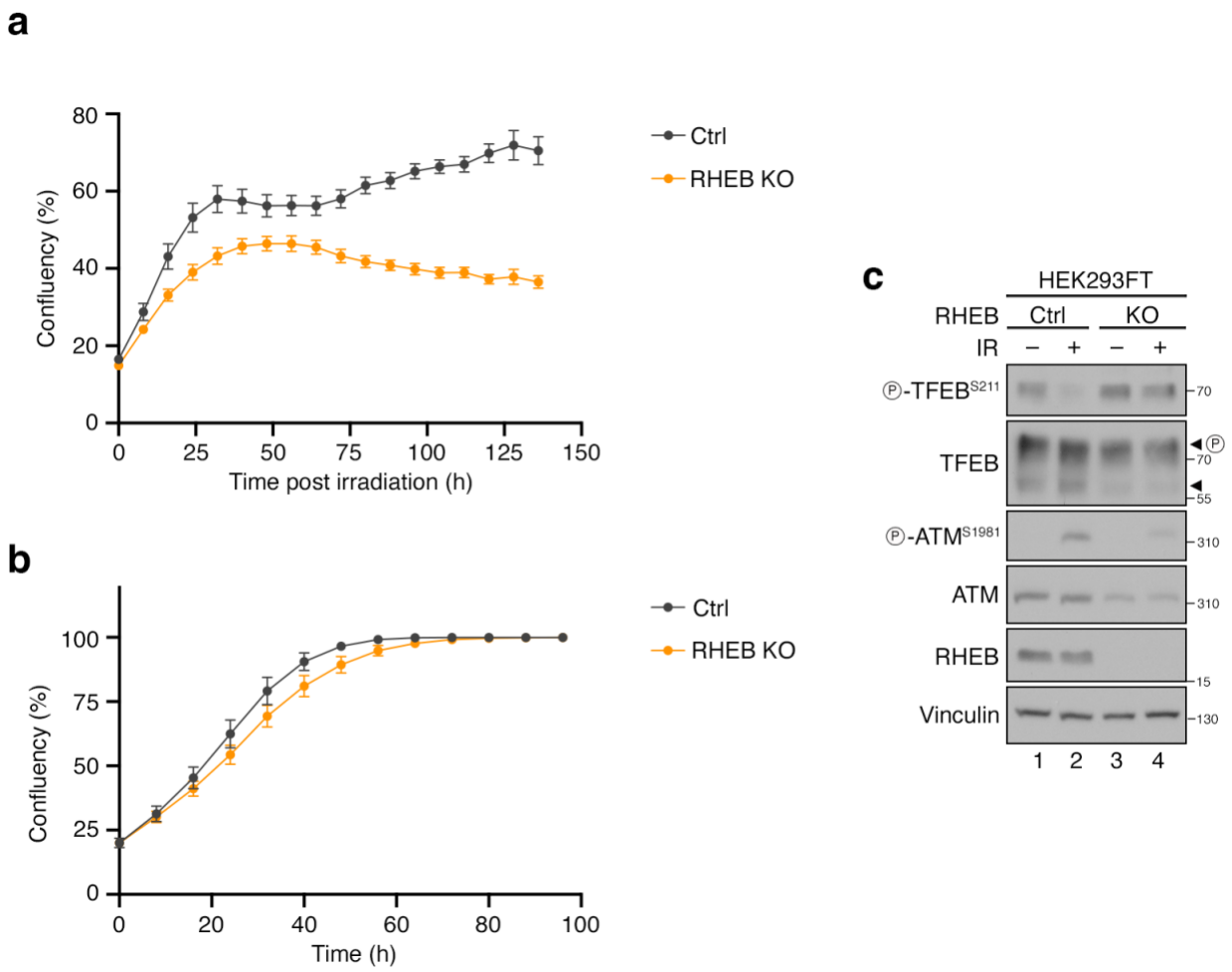

Figure 2.16 RHEB knockout cells display defective proliferative recovery and impaired TFEB signaling following irradiation.

(a,b) Time course of cell confluency (%) in control (Ctrl) and RHEB knockout (RHEB KO) HEK293FT cells following ionizing radiation (IR; 10 Gy) (a) or under standard culture conditions without irradiation (b). Cell confluency was quantified by time-lapse imaging using an Incucyte system, with images acquired every 8 h.

(c) Whole-cell lysates from control (Ctrl) and RHEB KO cells irradiated with 10 Gy or left untreated were collected 8 h post-irradiation and analyzed by immunoblotting with the indicated antibodies. In Ctrl cells, IR triggered a decrease in TFEB phosphorylation, consistent with TFEB activation, whereas this response was impaired in RHEB KO cells.

We next tested whether RHEB phosphorylation is required for this recovery process. Cells reconstituted with the non-phosphorylatable RHEB^{SSAA} mutant were more sensitive to irradiation than RHEB^{WT} cells, despite indistinguishable growth kinetics under unstressed conditions (Figure 2.17a,b). These results indicate that ATM-dependent phosphorylation of RHEB is critical for sustaining cell growth following genotoxic stress.

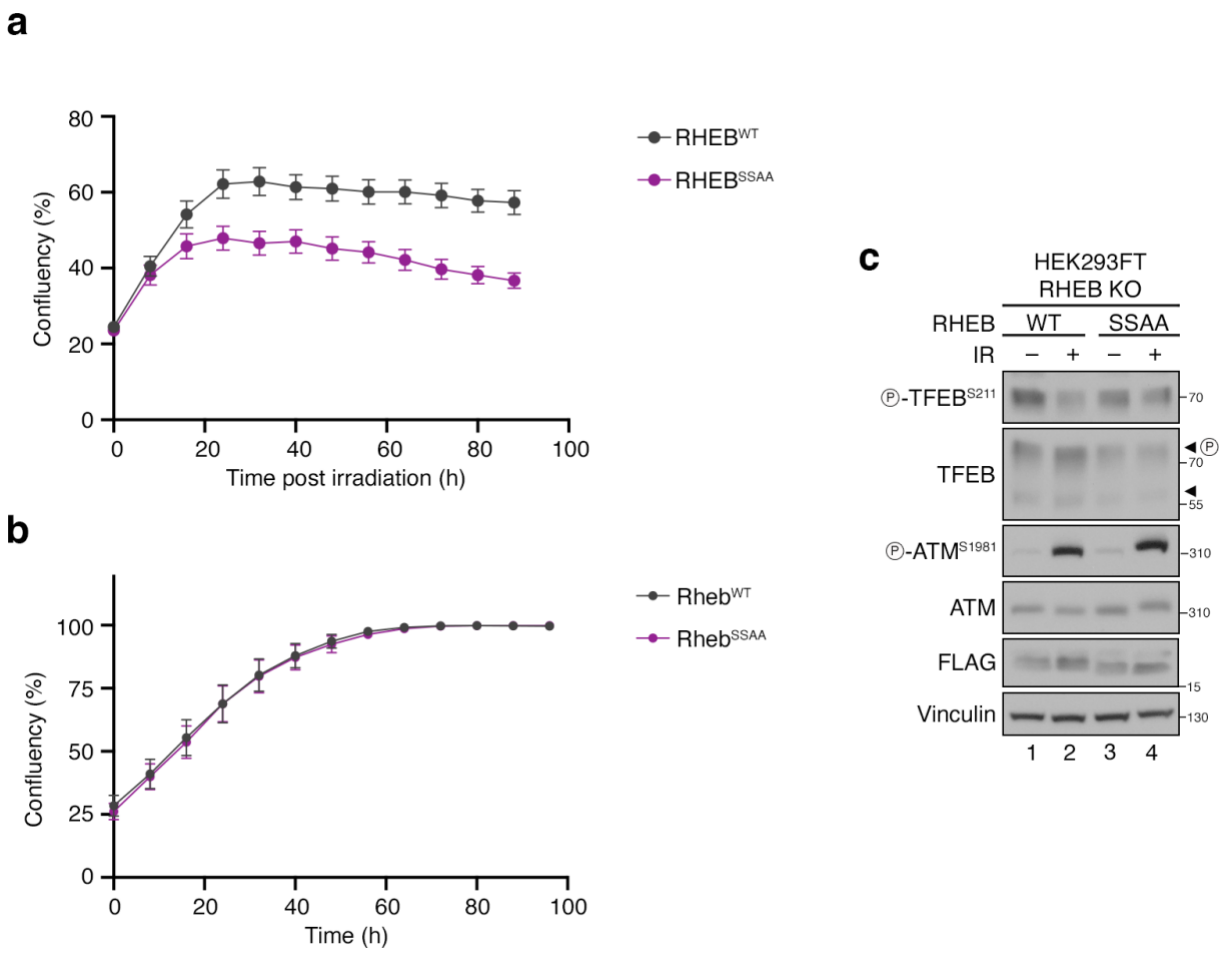

Figure 2.17 Phosphorylation-deficient RHEB (S6A/S175A) disrupts TFEB signaling and proliferation following irradiation.

(a,b) RHEB knockout HEK293FT cells stably expressing FLAG-tagged wild-type RHEB (RHEB^{WT}) or the phosphorylation-deficient RHEB S6A/S175A mutant (RHEB^{SSAA}) were monitored for cell confluency (%) after exposure to ionizing radiation (IR; 20 Gy) (a) or under standard culture conditions without irradiation (b). Cell confluency was quantified by time-lapse imaging using an Incucyte system, with images acquired every 8 h.

(c) Whole-cell lysates from RHEB knockout HEK293FT cells stably expressing wild-type RHEB (RHEB^{WT}) or the phosphorylation-deficient RHEB S6A/S175A (RHEB^{SSAA}) either irradiated with 20 Gy or left untreated, were collected 8 h post-irradiation and analyzed by immunoblotting with the

indicated antibodies. IR induced a decrease in TFEB phosphorylation in RHEB^{WT}-expressing cells, whereas this response was impaired in RHEB^{SSAA} cells.

Since both RHEB KO and RHEB^{SSAA} cells exhibited defective TFEB activation upon DNA damage (Figure 2.16c and 2.17c), we hypothesized that impaired TFEB signaling may underlie their defective growth recovery. Consistent with this idea, S6K phosphorylation was unaffected in RHEB^{SSAA} cells exposed to etoposide (Figure 2.13a,c), suggesting that the phenotype is not explained by defects in canonical cytosolic mTORC1 signaling.

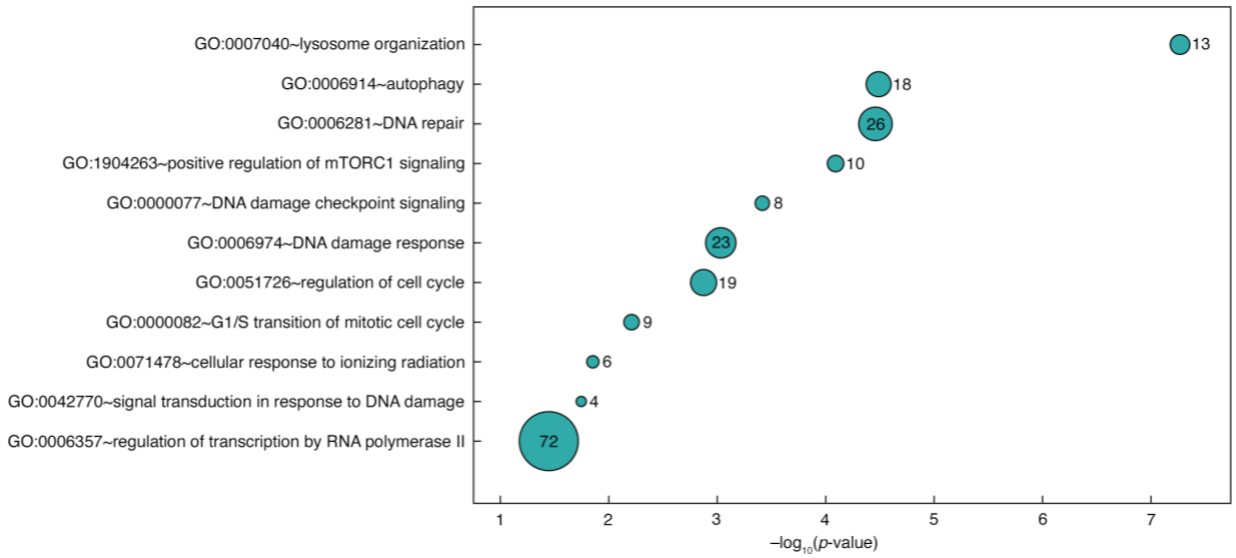

Figure 2.18 Gene Ontology biological process (BP) analysis of TFEB target genes identifies enrichment of DNA damage-related pathways.

Dot plot summarizing the results of GO biological process (BP) enrichment analysis performed on a curated set of TFEB target genes. The x-axis represents statistical significance of enrichment expressed as $-\log_{10}(p\text{-value})$. Each circle corresponds to an enriched GO term, with circle size proportional to the number of TFEB target genes associated with that term; gene counts are indicated inside or next to the circles. Terms are displayed on the y-axis. Several top-ranking categories were linked to DNA damage responses including DNA repair, checkpoint signaling, and cellular response to ionizing radiation, suggesting that TFEB target genes are functionally coupled to DDR pathways.

In further support of our hypothesis, prior studies have implicated TFEB in mediating DDR and DNA repair pathways[255,256,275,276]. To explore this possibility further, we performed gene ontology (GO) term enrichment analysis using a curated list of TFEB target genes. As

expected, the analysis revealed enrichment of canonical TFEB-regulated biological processes such as lysosome organization (GO:0007040), autophagy (GO:0006914), and mTORC1 signaling (GO:1904263) (Figure 2.18). Interestingly, we also observed significant enrichment of biological processes linked to the DDR, including DNA repair (GO:0006281), DNA damage checkpoint signaling (GO:0000077, GO:0006974, GO:0042770), response to radiation (GO:0071478), and cell cycle regulation (GO:0051726, GO:0000082), among others (Figure 2.18).

To directly test whether the impaired TFEB response accounts for the defective growth recovery of RHEB KO cells, we manipulated the Rag GTPases, which anchor TFEB on lysosomes and restrict its nuclear translocation. As S6K phosphorylation is regulated in a Rag-independent manner in the presence of exogenous amino acids[236,268], this strategy selectively impacts TFEB signaling.

Knockdown of RagA and RagB in RHEB KO cells led to a complete loss of TFEB phosphorylation and, strikingly, restored their ability to proliferate following irradiation (Figure 2.19a-c). Notably, under basal conditions without irradiation, RagA/B knockdown modestly reduced proliferation compared to both control and RHEB KO cells, highlighting that its growth-promoting effect is specific to genotoxic stress. This result indicates that relieving TFEB from lysosomal retention is sufficient to compensate for the absence of RHEB during the DNA damage response.

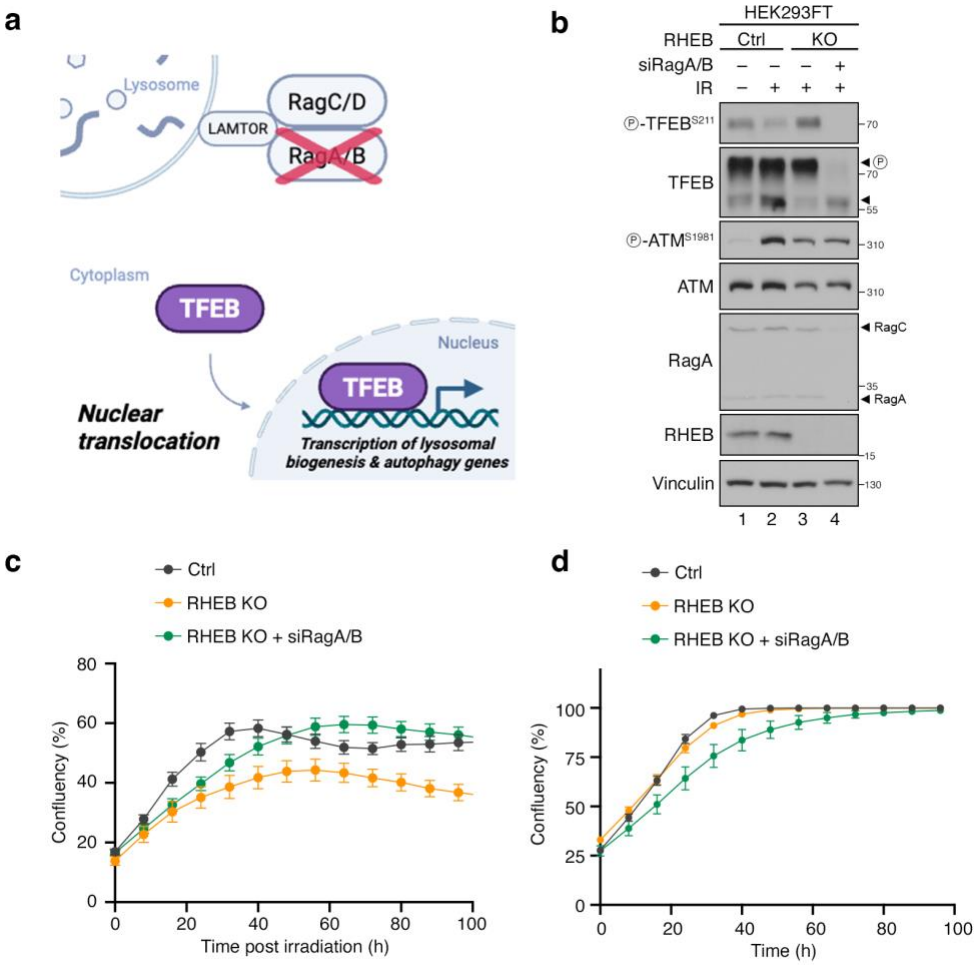

Figure 2.19 RagA/B knockdown in RHEB KO cells induces TFEB dephosphorylation and rescues impaired growth following DNA damage.

(a) Schematic representation of RagA/B knockdown. Loss of RagA/B liberates TFEB from the lysosomal surface, allowing its nuclear translocation.

(b) Immunoblots with lysates from control (Ctrl), RHEB knockout (RHEB KO), and RHEB KO HEK293FT cells with RagA/B knockdown (RHEB KO + siRagA/B), either left untreated or irradiated with 10 Gy and harvested 8 h later. RagA/B knockdown abolished TFEB phosphorylation, which implies TFEB activation.

(c,d) Time course of HEK293FT cell confluency (%) in control (Ctrl), RHEB knockout (RHEB KO), and RHEB KO cells with RagA/B knockdown (RHEB KO + siRagA/B) following irradiation (10 Gy) (c) or under standard culture conditions without irradiation (d). Cell confluency was quantified by time-lapse imaging using an Incucyte system, with images acquired every 8 h. RagA/B knockdown rescued the proliferative defect of RHEB KO cells after irradiation (c), while under basal conditions it modestly slowed proliferation compared to Ctrl and RHEB KO cells (d).

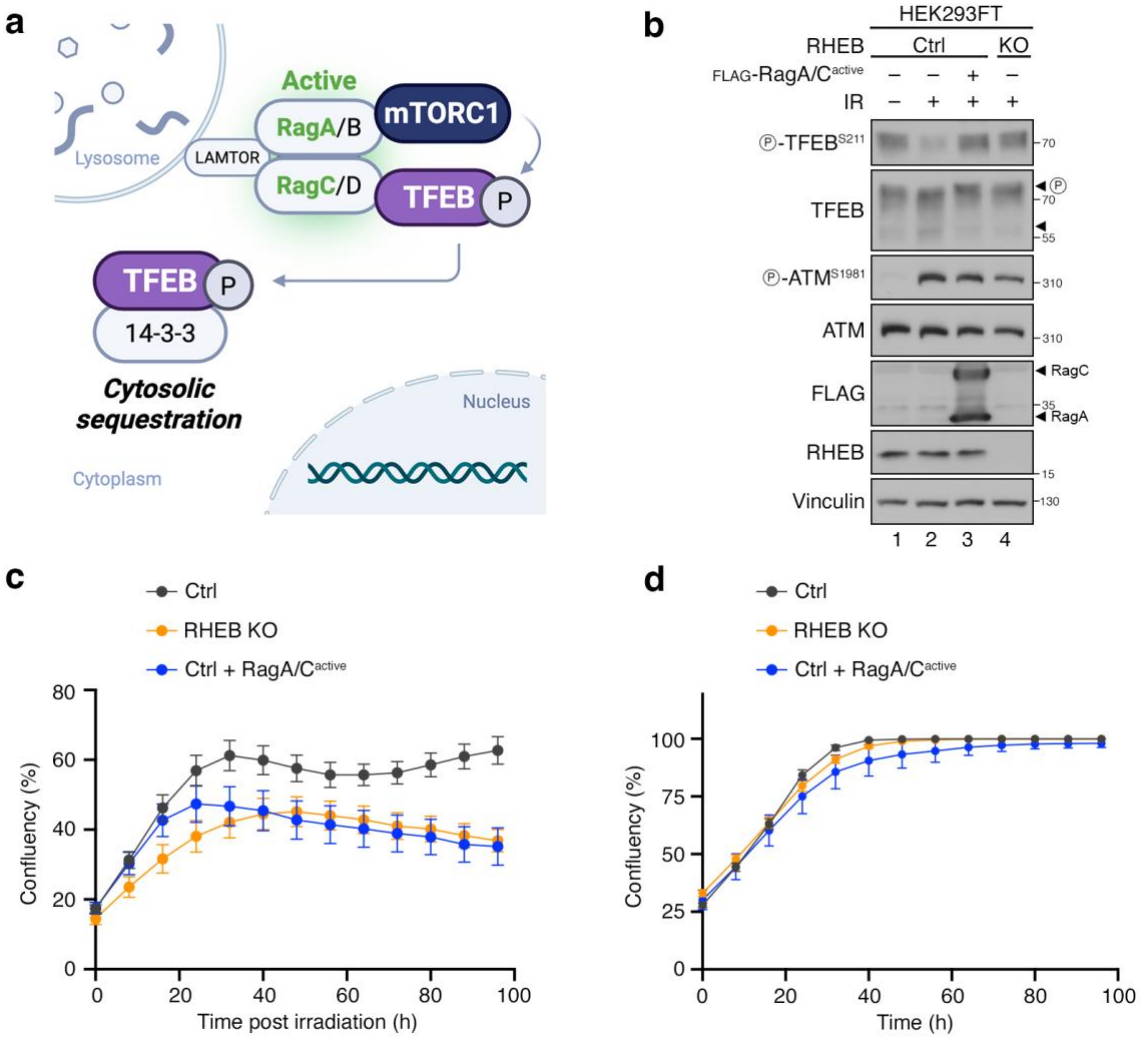

Figure 2.20 Constitutively active RagA/C increases TFEB phosphorylation and impairs proliferative recovery following DNA damage.

(a) Schematic representation of constitutively active RagA/C dimer expression (RagA Q66L, GTP-locked; RagC S75N, GDP-locked). Active RagA/C recruits TFEB and mTORC1 more strongly on lysosomes, leading to enhanced TFEB phosphorylation. Phosphorylated TFEB is sequestered in the cytoplasm through binding to 14-3-3 proteins, thereby preventing its nuclear translocation.

(b) Immunoblots with lysates from control (Ctrl), RHEB knockout (RHEB KO), and control HEK293FT cells transiently expressing constitutively active RagA/C dimer (RagA/C^{active}; RagA Q66L and RagC S75N), either left untreated or irradiated with 10 Gy and harvested 8 h later. Expression of active RagA/C increased TFEB phosphorylation even after irradiation.

(c,d) Time course of cell confluency (%) in control (Ctrl), RHEB knockout (RHEB KO), and control HEK293FT cells transiently expressing a constitutively active RagA/C dimer (Ctrl + RagA/C^{active}; RagA Q66L and RagC S75N), either following irradiation (10 Gy) (c) or under standard culture conditions without irradiation (d). Cell confluency was quantified by time-lapse imaging using an Incucyte system, with images acquired every 8 h.Expression of constitutively active RagA/C in control cells

impaired proliferative recovery after irradiation, resulting in a phenotype comparable to that of RHEB KO cells.

Conversely, in wild-type cells, expression of a constitutively active RagA/C dimer, which increases both mTORC1 and TFEB recruitment to lysosomes thereby enhancing TFEB phosphorylation and preventing its nuclear translocation[176,181,272], caused sustained TFEB phosphorylation even after irradiation (Figure 2.20a,b). This perturbation phenocopied the impaired growth recovery observed in RHEB KO cells, underscoring the importance of TFEB activation in enabling cellular adaptation to DNA damage (Figure 2.20c). Importantly, both RagA/B depletion and active RagA/C overexpression had only minimal effects on basal proliferation in unstressed conditions (Figure 2.19d and Figure 2.20d), highlighting the role of TFEB regulation in modulating the cellular adaptation to genotoxic stress.

Collectively, these findings identify TFEB activation as a critical component of the cellular recovery program following DNA damage. They demonstrate that this process requires ATM-dependent phosphorylation of RHEB, which specifically enables the mTORC1–TFEB signaling axis to promote lysosome biogenesis and support proliferative recovery after genotoxic stress.

2.7 Summary and working model

In this project, I investigated how RHEB, the direct activator of mTORC1, is regulated in the context of the DNA damage response (DDR) and how this regulation influences downstream signaling and cellular recovery. The data presented establish that RHEB is phosphorylated in response to diverse genotoxic stimuli, including topoisomerase inhibition, replication stress and ionizing radiation. Using both pharmacological inhibitors and genetic ablation, we identified ATM as the upstream kinase, and *in vitro* kinase assays confirmed that RHEB is a direct ATM substrate (Figure 2.6 and Figure 2.8).

DNA damage elicits substrate-specific outputs of mTORC1 signaling: phosphorylation of TFEB is reduced, whereas phosphorylation of S6K is enhanced. ATM-dependent

phosphorylation of RHEB is selectively required for the TFEB branch of this response, but dispensable for S6K regulation. Thus, RHEB phosphorylation provides a mechanism by which DNA damage signals are specifically coupled to the lysosomal mTORC1-TFEB axis, while canonical cytosolic substrates such as S6K remain independently regulated (Figure 2.9 and Figure 2.13).

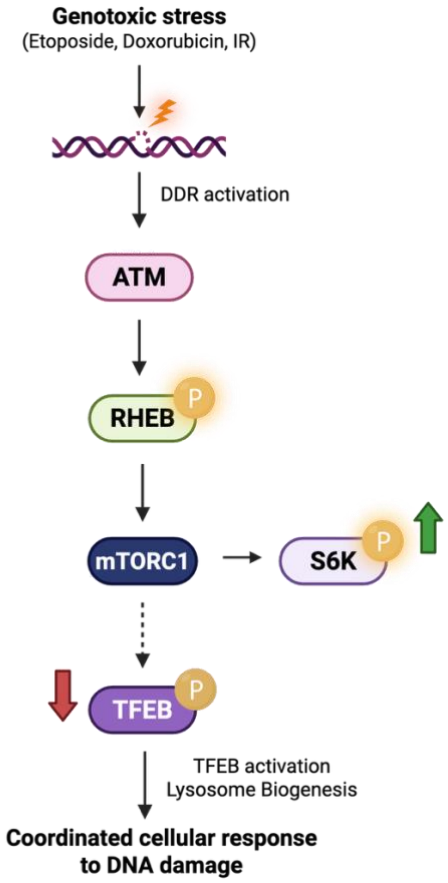

Figure 2.21 Working model of the ATM–RHEB–mTORC1–TFEB signaling axis in the DNA damage response.

Schematic representation of the proposed signaling pathway linking ATM, RHEB, and mTORC1 to TFEB regulation under genotoxic stress. DNA damage induced by etoposide, doxorubicin or ionizing radiation (IR) activates ATM, which directly phosphorylates RHEB. This modification selectively attenuates mTORC1 activity toward TFEB, causing TFEB dephosphorylation and nuclear translocation, while phosphorylation of S6K remains sustained. Nuclear TFEB promotes lysosomal biogenesis in a manner dependent on RHEB phosphorylation. A proper TFEB response is essential for coordinating cellular response to genotoxic stress (see also text for details).

Functionally, phosphorylation-deficient RHEB mutants impaired TFEB activation and lysosomal biogenesis following DNA damage, without affecting basal mTORC1 activity or S6K phosphorylation. These defects translated into reduced proliferative recovery after irradiation. Manipulation of Rag GTPases further demonstrated that the TFEB branch is critical for this adaptive response: releasing TFEB from lysosomal retention rescued the growth defect of RHEB-deficient cells, while preventing TFEB nuclear translocation reproduced the impaired recovery phenotype.

Taken together, these findings support a model in which ATM phosphorylates RHEB to enable activation of the TFEB branch of mTORC1 signaling in the context of DNA damage. This pathway promotes lysosome biogenesis and contributes to recovery of cellular growth following genotoxic stress.

Chapter 3. Discussion

The work presented in this thesis uncovers a previously unrecognized regulatory mechanism linking DNA damage signaling to mTORC1. Specifically, I demonstrate that RHEB is directly phosphorylated by ATM, and this modification is required for regulation of the TFEB branch of mTORC1 signaling. Through this mechanism, DNA damage promotes TFEB activation, lysosomal biogenesis, and recovery of cellular growth, whereas canonical cytosolic mTORC1 substrate S6K is regulated independently. These findings expand the current understanding of mTORC1 regulation and establish ATM-dependent phosphorylation of RHEB as a mechanism that fine-tunes mTORC1 signaling during genotoxic stress, engaging the TFEB axis without perturbing S6K control.

The following sections place these findings in the context of RHEB regulation, substrate-specific mTORC1 signaling, and cellular adaptation to DNA damage, and conclude with broader implications, limitations and future perspectives.

3.1 RHEB as a PTM-integrating hub upstream of mTORC1

RHEB is a well-established direct activator of mTORC1, with its function controlled by the GTP/GDP cycle under the regulation of the TSC complex. Most upstream cues that impinge on mTORC1 activity—including amino acids, growth factors, and energy status—converge on this axis, positioning RHEB as the principal effector of TSC-mediated control. However, accumulating evidence indicates that RHEB is not solely a nucleotide-regulated switch. Post-translational modifications (PTMs) such as ubiquitylation, phosphorylation, acetylation and NEDDylation have been identified on RHEB, pointing to additional layers of regulation that may fine-tune its activity in a context-dependent manner. For example, PRAK (p38-regulated/activated protein kinase; also known as MAPK5)-mediated phosphorylation at S130 was shown to reduce RHEB activity under energetic stress, highlighting how stress-responsive kinases can directly impinge on RHEB function[194].

The findings presented in this study extend this concept by identifying a novel ATM-dependent RHEB phosphorylation as a stress-responsive PTM. Unlike the GTP/GDP cycle, which broadly determines whether RHEB is competent to activate mTORC1, DNA damage-induced RHEB phosphorylation modifies mTORC1 signaling output in a substrate-specific manner. This dual regulation underscores the role of RHEB as an integrating hub that not only conveys growth factor and nutrient signals through its nucleotide state, but also accommodates stress inputs through targeted PTMs. In this way, RHEB can diversify mTORC1 signaling outputs depending on cellular context.

Our data further demonstrate that ATM-mediated phosphorylation of RHEB occurs independently of the TSC complex, distinguishing this mode of regulation from previously described ATM-LKB1-AMPK-TSC2 signaling axis[126,127]. Prior studies reported that oxidative and nitrosative stresses inhibit mTORC1 through this indirect axis[126,127]. By contrast, the present work shows that ATM can also act directly on RHEB in response to DNA damage, thereby bypassing TSC and providing an alternative means to modulate mTORC1 activity. The ATM-dependent phosphorylation described here adds to the known modes of RHEB regulation through PTMs, demonstrating how stress-activated kinases can rewire its function to reshape downstream mTORC1 signaling.

Together with previous reports identifying a range of PTMs on RHEB, the findings presented here expand its role beyond that of a passive effector of the TSC complex[191,193,194,211]. Instead, RHEB emerges as a dynamic signaling hub that integrates diverse cellular cues to regulate mTORC1 activity. By identifying ATM as an upstream kinase that directly phosphorylates RHEB in response to genotoxic stress, this work further underscores the versatility of RHEB as a regulatory node within the broader mTORC1 signaling network.

3.2 Substrate-specific mTORC1 signaling during DNA damage

The data presented in this thesis reveal that DNA damage induces a substrate-specific rewiring of mTORC1 signaling. Following genotoxic stress, TFEB phosphorylation is reduced, resulting in its nuclear translocation and activation of lysosomal biogenesis program. In contrast, phosphorylation of canonical, non-lysosomal substrate S6K is enhanced. These divergent outputs demonstrate that mTORC1 is not uniformly activated or inhibited under stress but is instead rewired toward specific substrates in a context-dependent manner.

Mechanistically, DNA damage induces a substrate-specific rewiring of mTORC1 signaling in which TFEB dephosphorylation requires ATM-dependent phosphorylation of RHEB. Cells lacking RHEB or expressing a non-phosphorylatable RHEB mutant failed to induce TFEB dephosphorylation or trigger its nuclear translocation upon DNA damage. As a result, these cells were unable to upregulate lysosomal content under genotoxic stress and support growth recovery following irradiation. In contrast, the increase in S6K phosphorylation following DNA damage was unaffected by loss of RHEB phosphorylation, demonstrating that the ATM-RHEB axis selectively controls the lysosomal mTORC1-TFEB branch, while cytosolic substrates such as S6K remain regulated independently.

Functionally, attenuation of the TFEB response–whether in RHEB KO cells, $RHEB^{SSAA}$ mutants, or in cells expressing constitutively active RagA/C dimers–compromises proliferative recovery after genotoxic stress. By contrast, cells with intact ATM-RHEB-mTORC1-TFEB signaling manage genomic stress more effectively by transiently arresting, presumably initiating repair, and resuming proliferation. These findings build on the concept of substrate-specific mTORC1 regulation and position RHEB phosphorylation as a conditional switch that enables activation of lysosomal mTORC1 signaling during DNA damage, while cytosolic mTORC1 outputs remain independently regulated.

These findings are consistent with a growing body of evidence that mTORC1 activity is not uniformly propagated across its substrates[178,236,265-271,277-279]. We and others have previously

demonstrated that mTORC1 exhibits substrate-specific regulation, particularly evident when comparing lysosomal versus non-lysosomal targets. For instance, lysosomal mTORC1 substrates such as TFEB and TFE3 require Rag GTPases and proper lysosomal function for phosphorylation, whereas cytosolic substrates including S6K and 4E-BP1 are largely Rag- and lysosome-independent under basal culture conditions[236]. Accordingly, genetic or pharmacological perturbation of lysosomal function preferentially affects the lysosomal branch without altering non-lysosomal targets[236,269]. In line with this, cancer-associated activating RagC mutants selectively enhance TFEB phosphorylation with little effect on S6K[268]. Furthermore, TSC-null models display hyperphosphorylation of cytosolic targets and hypophosphorylation of the lysosomal substrates[266,267,270], whereas RHEB KO cells show the reverse phenotype[265].

The present work extends these paradigms into the DNA damage setting. mTORC1 again displays substrate-specific outputs, with lysosomal and cytosolic substrates responding in opposite directions. Importantly, ATM-dependent RHEB phosphorylation is required for TFEB regulation but dispensable for S6K upon DNA damage, underscoring the independence of these two arms of mTORC1 signaling. Together, these findings highlight DNA damage as another context in which mTORC1 acts not as a binary switch but as a substrate-selective signaling node, with ATM-RHEB axis serving as the molecular link between genotoxic stress and the lysosomal mTORC1-TFEB arm.

3.3 Reconciling divergent reports on DDR-mTORC1 signaling

Previous studies investigating the impact of DNA damage on mTORC1 signaling have reported mixed results, with some describing pathway inhibition and other observing maintained or even increased activity[7,255,256,280-282]. These discrepancies likely reflect differences in cell types, experimental conditions, DNA-damage-inducing protocols, or the read-outs used to assess mTORC1 activity.

Our findings help reconcile these divergent observations by demonstrating that mTORC1 is regulated in a substrate-specific manner during the DNA damage response. Under genotoxic stress, lysosomal substrates such as TFEB are dephosphorylated and activated, while phosphorylation of cytosolic targets like S6K is enhanced. This substrate-selective regulation provides a unifying explanation for why studies relying on different read-outs reached contradictory conclusions about the status of mTORC1 following DNA damage. In addition, experiments in this thesis focused on the early response (2–8 h post DNA damage induction), and it will be important to explore how mTORC1 activity evolves at later stages of DDR. Different phases of the DDR are likely to engage distinct mTORC1-dependent processes, particularly during transitions from DNA repair toward long-term outcomes such as senescence and apoptosis.

3.4 Functional implications of substrate-specific mTORC1 signaling

The divergent regulation of TFEB and S6K during DNA damage also points to distinct functional outcomes. Increased S6K phosphorylation aligns with previous studies implicating this kinase in DNA damage-associated processes, including the promotion of G2/M arrest through CDK1 (cyclin dependent kinase 1) modulation, enhancement of mismatch repair via MSH6 (mutS homolog 6) phosphorylation, and stabilization of p53[252,281,282]. Furthermore, the involvement of the translational machinery, especially through 4E-BP1, in regulating checkpoint protein levels and signaling suggests that S6K may act in a complementary or reinforcing manner[253,254]. Together, these findings support a model in which elevated S6K activity may contribute to transient proliferation arrest, thereby allowing efficient DNA repair.

In parallel, our results firmly position TFEB as a crucial mediator of cellular adaptation to genotoxic stress. Numerous studies have shown that TFEB activation promotes lysosome biogenesis and autophagy, while also regulating DNA repair, checkpoint signaling, cell cycle arrest, and apoptosis[255,256,275,276]. These diverse functions are mediated in part through TFEB-dependent regulation of multiple key components involved in these processes, including

p21, MDM2 and p53[255,256,275,276]. The impaired recovery that we observe in models with defective TFEB activation (e.g., in RHEB KO, RHEB^{SSAA}, or active RagA/C-expressing cells) further supports this role. Conversely, release of TFEB from lysosomal retention by RagA/B knockdown restored proliferation even in the absence of RHEB, directly linking TFEB activity to cellular recovery after DNA damage.

3.5 Lysosomal biogenesis as an adaptive response to DNA damage

An important aspect of TFEB activation, particularly relevant for this study, is its association with increased lysosomal abundance. This raises the possibility that enhanced lysosomal function or abundance contributes to cellular adaptation during DNA damage. Indeed, lysosomes and autophagy have been shown to be important for DDR protein recruitment to DNA lesions and efficient DNA repair[283-288]. Our results are consistent with this view, as cells with defective TFEB activation fail to increase lysosomal content and display impaired growth recovery after irradiation. These observations suggest that induction of lysosomal biogenesis through the ATM–RHEB–mTORC1–TFEB axis may provide a survival advantage under genotoxic stress by sustaining repair and promoting recovery of proliferation.

Although the precise mechanisms by which increased lysosomal abundance aids recovery remain to be clarified, we speculate that lysosomes contribute to the DDR through both degradative and signaling functions. As recycling machineries, they promote protein turnover and provide metabolic substrates and building blocks to meet the elevated demands of DNA repair, checkpoint activation, and chromatin remodeling. Enhanced lysosomal activity could ensure a steady supply of amino acids, lipids and other precursors to sustain protein synthesis, nucleotide production, and membrane remodeling. For instance, nucleotides may be in particularly high demand to support DNA synthesis during repair, lipid precursors may be required for nuclear envelop dynamics at repair foci, and amino acids may fuel translation of repair proteins. Lysosomal degradation can also generate metabolites that feed the TCA cycle and restore ATP levels, thereby meeting the energy requirements of the DDR. In parallel, increased lysosomal abundance may mitigate

oxidative stress by facilitating removal of damaged organelles and buffering the accumulation of reactive oxygen species, which are frequently generated during genotoxic stress. Beyond these degradative functions, lysosomes serve as signaling hubs: AMPK is activated at the lysosomal surface via recruitment of LKB1 and AXIN in response to low energy, while lysosomal Ca^{2+} release through TRPML1 activates calcineurin, which regulates transcription factors and metabolic adaptation. Taken together, these degradative and signaling functions may allow cells to cope with the combined metabolic and oxidative burden of DNA damage, thereby supporting proliferative recovery.

In sum, the findings presented in this thesis demonstrate that DNA damage does not produce a global, uniform change in mTORC1 activity but instead exhibits differential effects on distinct substrates. Enhanced phosphorylation of S6K and activation of TFEB occur in parallel, with the latter critically dependent on ATM-mediated RHEB phosphorylation. This framework provides a basis to reconcile previous divergent findings and to consider how selective regulation of mTORC1 outputs contributes to cellular recovery upon genotoxic stress. The next section addresses the limitations of these findings and directions for future work.

3.6 Future perspectives

The findings presented in this thesis establish ATM-dependent phosphorylation of RHEB as a previously unrecognized mechanism that links the DDR to selective mTORC1 outputs, thereby enabling TFEB activation and proliferative recovery. While these results provide strong evidence for a direct ATM–RHEB connection, further investigation will be required to define the underlying mechanisms and to determine the broader physiological relevance of this pathway.

One consideration is the reliance on phosphorylation-deficient mutants to study the role of RHEB modification. In this study, functional analyses were performed using a double mutant (S6A/S175A), raising the question whether these sites act cooperatively,

redundantly, or independently. Testing individual single-site mutants would allow a clearer resolution of site-specific contributions. In addition, phospho-mimetic mutants could provide complementary insights, although their interpretation is often less straightforward: unlike phospho-dead mutants, which reliably prevent modification, phospho-mimetics do not always recapitulate the structural and regulatory effects of true phosphorylation. Moreover, constitutive mimetics may mask functions that depend on dynamic phosphorylation-dephosphorylation cycles. An intriguing possibility is that RHEB phosphorylation, like that of CHK2 regulated downstream of ATM, may undergo cycles of phosphorylation and dephosphorylation during different phases of the DDR. Exploring such temporal dynamics would clarify whether RHEB functions as a transient molecular switch or a sustained signaling hub.

RHEB is subject to multiple post-translational modifications (PTMs), including ubiquitylation, farnesylation, and NEDDylation and it is plausible that phosphorylation by ATM may either prime or antagonize these additional modifications. Such cross-talk could influence the stability, localization, or signaling output of RHEB. A systematic analysis of how ATM-dependent phosphorylation interacts with other RHEB PTMs, particularly under stress conditions, would provide a deeper understanding of how RHEB integrates diverse regulatory inputs.

The precise subcellular location of RHEB phosphorylation by ATM is an important open question. RHEB has been reported in the nucleus, cytoplasm, and at endomembrane compartments, including lysosomes, while ATM is established as a nuclear kinase but also functions in the cytoplasm, mitochondria, mitochondria-associated membranes, and peroxisomes. Therefore, it is possible that ATM phosphorylates RHEB directly at lysosomes, or alternatively within other compartments before influencing lysosomal mTORC1 signaling. Exploring these possibilities through approaches such as immunofluorescence co-localization analysis, biochemical fractionation, and live-cell imaging will help clarify the spatial dynamics of this regulatory event.

To fully elucidate the mechanism of the ATM–RHEB–mTORC1–TFEB axis described in this thesis, future studies should determine how ATM-mediated phosphorylation of RHEB confers specificity toward TFEB regulation while leaving canonical mTORC1 outputs unaffected. Several mechanistic models can be envisioned, which are not mutually exclusive and collectively provide a framework for future investigation. One possibility is spatial regulation, whereby phosphorylation alters RHEB distribution across compartments (nucleus, cytoplasm, lysosomes, other endomembranes), changing the fraction of RHEB-activated mTORC1 complexes at lysosomes, where TFEB is phosphorylated, versus in the cytoplasm, where S6K is regulated. A related explanation is subcellular localization of mTORC1 itself: DNA damage may bias mTORC1 positioning away from lysosomes and toward cytosolic pools, thereby dampening TFEB phosphorylation while preserving or even enhancing S6K phosphorylation. A second mechanism could involve scaffolding at lysosomes, whereby phosphorylated RHEB influences how mTORC1 engages with the LAMTOR–Rag GTPase machinery. While RHEB does not directly bind the Rags, its phosphorylation could indirectly modulate RAPTOR–Rag interaction or alter the stability of this association. A third possibility relates to the local phosphatase microenvironment at lysosomes: lysosome-localized phosphatases such as calcineurin or protein phosphatase 2A (PP2A) oppose mTORC1-mediated phosphorylation of TFEB, and phosphorylated RHEB may shift the balance between kinase and phosphatase activity in this compartment. A fourth explanation may be nutrient signaling, since prior studies established that phosphorylation of lysosomal substrates requires functional lysosomes and Rag GTPases, whereas phosphorylation of cytosolic substrates is largely Rag-independent in the presence of exogenous amino acids. Therefore, DDR-driven RHEB phosphorylation could bias how mTORC1 integrates Rag-mediated nutrient inputs, selectively affecting lysosomal but not cytosolic substrates. Finally, substrate binding and conformational bias may also contribute: unlike S6K, which binds to RAPTOR through a canonical TOS motif, TFEB interacts via non-canonical route. RHEB phosphorylation could induce subtle conformational changes within the mTORC1 complex (e.g., mTOR–RAPTOR assembly) that

preferentially impact non-TOS substrates, thereby explaining the selectivity toward TFEB. Discriminating between these models will require future work, combining imaging of mTORC1 localization, structural and biochemical analyses of RHEB–mTOR interactions, and perturbation of phosphatases and LAMTOR–Rags.

As discussed in Section 3.5, lysosomal biogenesis emerges as a critical adaptive response to DNA damage, and our data show that cells unable to mount this program exhibit defective proliferative recovery. While this strongly implicate lysosomes in the recovery process, the precise mechanisms remain to be further investigated. Future work should test whether increased lysosomal abundance supports recovery by (i) metabolic recycling–supplying amino acids and precursors for protein and nucleotide synthesis; (ii) replenishing TCA intermediates and ATP; (iii) maintaining redox homeostasis by clearing damaged organelles and limiting reactive oxygen species; and/or (iv) engaging lysosome-centered signaling (AMPK activation via LKB1–AXIN; Ca^{2+}/calcineurin signaling via TRPML1). These possibilities can be addressed by selectively impairing lysosomal degradation (e.g., pharmacological inhibition of lysosomal acidification or genetic disruption of key hydrolases or v-ATPase subunits) while assaying proliferative recovery, metabolic flux, and redox status. In parallel, the contribution of lysosomal signaling can be addressed by disrupting AMPK activation at the lysosomal surface (for example, by interfering with LKB1–AXIN recruitment or using pharmacological AMPK modulators) and by preventing TRPML1-dependent Ca^{2+} release (through genetic or pharmacological perturbation), while monitoring proliferative recovery after DNA damage.

Beyond lysosomal biogenesis, TFEB regulates a broad transcriptional program that may also be relevant to DDR. Gene ontology analysis of TFEB targets revealed enrichment for categories related to DNA repair, checkpoints and cell cycle control, and signal transduction during DDR, suggesting that TFEB activity could influence genome maintenance more directly than previously appreciated. TFEB also induces autophagy-related genes and metabolic regulators, including PGC1α (peroxisome proliferator-

activated receptor gamma coactivator 1-alpha) and PPARα (peroxisome proliferator-activated receptor alpha)[289], which control mitochondrial biogenesis and lipid metabolism, as well as signaling molecules such as RagD that modulate mTORC1 activity. Dissecting whether proliferative recovery depends primarily on lysosomal biogenesis or whether these additional TFEB-driven pathways–autophagy, metabolic rewiring, and genome maintenance programs–play critical roles will be essential for defining the full scope of TFEB function in the DDR.

Although TFEB emerged as the central substrate in this work, other mTORC1 targets may contribute to the cellular response to DNA damage. Beyond TFEB and S6K, mTORC1 regulates pathways essential for repair and survival, including nucleotide biosynthesis through CAD (carbamoylphosphate synthetase 2) and ATF4 (activating transcription factor 4), protein synthesis via 4E-BP1, autophagy initiation through ULK1, and lipid metabolism through SREBP1/2 (sterol regulatory element-binding proteins 1 and 2), which may supply membranes for nuclear envelope remodeling and the stabilization of DNA repair foci, where chromatin reorganization and assembly of repair complexes increase membrane demand. Targeted immunoblotting of these substrates under DNA-damaging conditions, complemented by unbiased phosphoproteomics, would broaden the view of how mTORC1 integrates genotoxic stress.

Temporal aspects of mTORC1 regulation during the DDR also remain to be explored. This study primarily assessed early responses within 2-8 hours following DNA damage induction, when ATM activation is robust. However, the severity and duration of damage are likely to shape downstream signaling, influencing whether cells commit to repair and recovery, senescence, or apoptosis. Longitudinal analyses across DDR progression, coupled with studies examining different levels of DNA damage, would provide insight into how mTORC1 signaling adapts to different damage contexts and cell fate outcomes.

Finally, it is important to consider whether ATM-dependent phosphorylation of RHEB may extend beyond the DDR. ATM is increasingly recognized as a sensor of oxidative stress, mitochondrial dysfunction, and peroxisomal homeostasis, in addition to its canonical role in DNA repair. It is therefore conceivable that RHEB phosphorylation serves as a broader integrative mechanism, coupling diverse stress-related cues to mTORC1 signaling. Testing RHEB phosphorylation under non-DDR stress conditions, such as oxidative or metabolic stress, may reveal wider physiological relevance for this pathway.

In conclusion, while this thesis establishes a central role for ATM-dependent phosphorylation of RHEB in connecting DNA damage signaling to selective mTORC1 regulation, it raises many questions for further study. Addressing these questions will not only strengthen the mechanistic basis of the current model but may also uncover general principles by which RHEB integrates stress signals to fine-tune mTORC1 activity. Such insights will broaden our understanding of cellular adaptation to genotoxic stress and other stress conditions.

3.7 Conclusions

This thesis identifies ATM-dependent phosphorylation of RHEB as a novel post-translational modification that connects the DNA damage response (DDR) to mTORC1 signaling. Through this pathway, DNA damage selectively engages the TFEB branch of mTORC1 signaling, promoting lysosome biogenesis and enabling proliferative recovery after genotoxic stress. These findings highlight a direct mechanism by which DDR modulates mTORC1, linking genome stability pathways with cellular metabolic control.

RHEB phosphorylation was observed in response to diverse DNA-damaging stimuli, including topoisomerase inhibition, replication stress, and ionizing radiation. This modification was validated using a phospho-specific antibody against RHEB S175 in both overexpressed and endogenous RHEB. Pharmacological inhibition, genetic depletion, and *in vitro* kinase assays demonstrated that ATM is the upstream kinase responsible for this

phosphorylation. Importantly, the modification is independent of the TSC complex and of the previously described indirect ATM–LKB1–AMPK–TSC2 axis, thereby establishing a direct mode of RHEB regulation by DDR signaling.

ATM-dependent phosphorylation of RHEB was required for DNA damage-induced TFEB activation, as cells lacking RHEB or expressing phosphorylation-deficient mutants failed to dephosphorylate and activate TFEB, showed reduced lysosomal abundance, and exhibited impaired proliferative recovery following irradiation, despite maintaining mTORC1 activity toward canonical substrates. Manipulation of Rag GTPases further confirmed TFEB as the critical downstream effector of this pathway: knockdown of RagA/B, which prevents TFEB recruitment to lysosomes, abolished its phosphorylation and restored proliferative recovery, whereas constitutively active RagA/C maintained TFEB phosphorylation and cytoplasmic retention after DNA damage, reproducing the proliferative defect.

Together, these results establish ATM-dependent phosphorylation of RHEB as a novel post-translational modification that provides a direct molecular link from DDR to mTORC1 pathway. This link modifies mTORC1 outputs in response to DNA damage by engaging the TFEB-lysosome signaling branch, thereby contributing to cellular adaptation and recovery following genotoxic stress. mTORC1 signaling and the DNA damage response are both tightly linked to ageing and age-related disorders, primarily through their dysregulation. Imbalances in these pathways contribute to cancer, neurodegeneration and other age-associated conditions, and inhibitors targeting components of both pathways are currently being explored in various clinical settings. Within this context, the identification of ATM-dependent phosphorylation of RHEB and its role in TFEB regulation provides additional mechanistic insight into how DNA damage modulates mTORC1 activity. This underscores RHEB phosphorylation as a potential marker to study the induction of genotoxic stress in cells. In summary, these findings highlight a previously unrecognized mode of mTORC1 regulation by genotoxic stress, adding to the mechanistic understanding of how these two major pathways interact in contexts relevant to ageing and human disease.

Chapter 4. Materials and methods

Cell culture

All cell lines used in this study were maintained under standard mammalian tissue culture conditions at 37 °C in a humidified incubator with 5% CO_2. Human female embryonic kidney HEK293FT cells (#R70007, Invitrogen; RRID: CVCL_6911) were cultured in high-glucose Dulbecco's Modified Eagle Medium (DMEM; #41965039, Gibco) supplemented with 10% fetal bovine serum (FBS; #F7524, Sigma; #P30-3306, PAN-Biotech; #FBS.HP.0500, Bio&SELL) and 1× Penicillin-Streptomycin (#15140122, Gibco; #P4333-100ML, Sigma). Human osteosarcoma U2OS cells (#HTB-96, ATCC; RRID: CVCL_0042) were cultured in high-glucose DMEM GlutaMAX (#61965026, Gibco) with 10% FBS and 1× Penicillin-Streptomycin.

HEK293FT cells were purchased from Invitrogen, while U2OS cells were kindly provided by Nils-Göran Larsson (Max Planck Institute for Biology of Ageing, Cologne, Germany). Authentification of the HEK293FT cell line was performed using the Multiplex human Cell Line Authentication test (Multiplexion GmbH), which employs a single nucleotide polymorphism (SNP)-based genotyping approach, as described at www.multiplexion.de. No commonly misidentified cell lines were used in this study. All cell lines were regularly tested for *Mycoplasma* contamination using a PCR-based detection method and consistently tested negative throughout the course of this work.

Cell culture treatments

For drug treatments, cells were exposed to the following agents and concentrations unless otherwise specified in individual figure legends. Etoposide (#E1383, Sigma) was used at 20 μM for 2 or 8 h, doxorubicin (#D1515, Sigma) at 2 μM for 2 h, and hydroxyurea (#H8627, Sigma) at 2 mM for 2 h. These agents were used to induce DNA damage thorugh distinct mechanisms: etoposide and doxorubicin act as topoisomerase II inhibitors and DNA

intercalators, while hydroxyurea causes replication stress by depleting deoxyribonucleotide pools.

To inhibit DDR kinase activity, cells were pretreated for 30 min with KU-60019 (ATM inhibitor; #S1570, Selleckchem; 1 μM), VE-821 (ATR inhibitor; #S8007, Selleckchem; 1 μM), or NU7441 (DNA-PK inhibitor; #S2638, Selleckchem; 0.1 or 1 μM), prior to the addition of DNA-damaging agents. DMSO (#4720.1, Roth) was used as vehicle control for all treatments except for hydroxyurea, for which sterile water was used.

Plasmid DNA transfections

Transient plasmid DNA transfections were carried out using Effectene transfection reagent (#301425, QIAGEN), according to the manufacturer's instructions. Cells were seeded at approximately 25% confluency one day prior to transfection. Plasmid DNA was mixed with EC buffer and Enhancer, incubated for 5 min at room temperature, and subsequently combined with Effectene reagent. The DNA–reagent complexes were incubated for an additional 10 min before being added dropwise to the culture medium. Following transfection, cells were maintained in complete growth medium under standard culture conditions. Expression of the introduced constructs was assessed 36–48 h later by immunoblotting of whole-cell lysates.

Gene silencing experiments

Transient knockdown of *ATM, ATR, TSC2, RRAGA* and *RRAGB* was performed using siGENOME (pool of 4) gene-specific siRNAs (Horizon Discoveries). An siRNA duplex targeting the *R. reniformis* luciferase gene (RLuc) (#P-002070-01-50, Horizon Discoveries) was used as a control. Transfections were performed using 20 nM siRNA and the Lipofectamine RNAiMAX transfection reagent (#13778075, Invitrogen), according to the manufacturer’s instructions. Cells were harvested 72 hours post-transfection and knockdown efficiency was verified by immunoblotting. Sequences of all siRNAs used in this study are summarized in Table 2.

Table 2. siRNA sequences used in this study.

Target	Sequence
TSC2	GCAUCAACCCCAGUUUCGU
	GCAUUAAUCUCUUACCAUA
	UGGUCAAAUUCAAUAGCUG
	GGCUCAUCAAGAAGUAUAG
RRAGA	GGUCGAUAAUCUUCGCCAA
	CUUUAAACAUUGGACGCUA
	CCUCAAAUACGUACGUGAU
	GAACUCUCCUGACGCCAAA
RRAGB	UAUCGAAGCUGAUGAAGUA
	GGGAUGAAACCCUCUAUAA
	GGGACAACAUCUUCCGAAA
	GAAGAAGAUUUGAGGCGUU
ATM	GCAAAGCCCUAGUAACAUA
	GGGCAUUACGGGUGUUGAA
	UCGCUUAGCAGGAGGUGUA
	UGAUGAAGAGAGACGGAAU
ATR	GAACAACACUGCUGGUUUG
	GCAACUCGCCUAACAGAUA
	UCUCAGAAGUCAACCGAUU
	GAAUUGUGUUGCAGAGCUU

Generation of knockout cell lines

The HEK293FT RHEB and TSC1 knockout (KO) cell lines used in this study were described previously[265,290]. RHEB KO cells were generated by Dr. Aishwarya Acharya (MPI-AGE, Cologne) and TSC1 KO cells were generated by Dr. Andreas Lamprakis (MPI-AGE, Cologne), using CRISPR/Cas9-mediated genome editing based on the pX459 plasmid system, as originally described by Ran *et al*.[291]. Briefly, cells were transfected with pX459 vectors encoding Cas9 and single guide RNAs (sgRNAs) targeting either the RHEB or TSC1 coding sequence. Following puromycin selection, single-cell clones were isolated and expanded. Successful knockout was verified by genomic sequencing of the targeted locus and by immunoblotting to confirm loss of RHEB or TSC1 protein expression. The generated clones were maintained in parallel with wild-type HEK293FT controls for all experiments.

Generation of stable cell lines

Polyclonal HEK293FT RHEB knockout cells stably expressing FLAG-tagged RHEB wild-type (WT) or the non-phosphorylatable double mutant S6A/S175A (SSAA) were generated using a doxycycline-inducible sleeping-beauty-based transposon system[235,292]. For stable integration, RHEB KO cells were co-transfected with either pITR-FLAG-RHEB WT or SSAA expression constructs together with the pCMV-Trp transposase vector at a 10:1 ratio. Thirty-six hours post-transfection, cells were selected in medium containing 2 µg/ml puromycin (#A1113803, Gibco). To confirm successful genomic integration of the transposons, expression was induced with increasing concentrations of doxycycline (#D9891, Sigma) and monitored by immunoblotting. Under basal conditions, low-level leaky expression was detectable in the absence of doxycycline. As the leaky expression levels were comparable across constructs and closely matched endogenous RHEB level, all subsequent experiments were performed without doxycycline induction.

Antibodies

Information about all primary and secondary antibodies used in this thesis can be found in Table 3 and Table 4, respectively. The custom-made, rabbit polyclonal phospho-specific antibody recognizing RHEB when phosphorylated at S175 (phospho-RHEB^{S175}) was produced by immunizing animals with a synthetic KLH (Keyhole Limpet Hemocyanin)-conjugated phospho-peptide corresponding to residues around S175 of human RHEB: MDGAA(pS)QGKSSC. Peptide synthesis was performed by Peptide Specialty Laboratories GmbH (Heidelberg, Germany), and antibody generation was outsourced to ProSci incorporated (Poway, CA, USA). Antibodies were purified by coupling to NHS-Activated Sepharose 4 Fast Flow resin (#17090601, Cytiva), alternating acid-base washing steps, and elution with 0.2 M glycine (pH 2.8). Eluted fractions were normalized by 0.4 M Na_2HPO_4 (pH 8.2), and antibodies were stored in 50% glycerol, 0.1% BSA at -20 °C.

Table 3. Primary antibodies used in this study.

Antibody	Dilution	Supplier	Catalog Number
Rabbit monoclonal anti-phospho-p70 S6 Kinase (Thr389) (D5U1O)	1:1,000 (WB)	Cell Signaling Technology	97596
Rabbit polyclonal anti-S6 Kinase	1:1,000 (WB)	Cell Signaling Technology	9202
Rabbit monoclonal anti-phospho-TFEB (Ser211) (E9S8N)	1:1,000 (WB)	Cell Signaling Technology	37681
Rabbit polyclonal anti-TFEB	1:1,000 (WB); 1:200 (IF)	Cell Signaling Technology	4240
Rabbit monoclonal anti-GAPDH (14C10)	1:6,000 (WB)	Cell Signaling Technology	2118
Rabbit monoclonal anti-mTOR (7C10)	1:1,000 (WB)	Cell Signaling Technology	2983
Mouse monoclonal anti-α-Tubulin (DM1A)	1:1,000 (WB)	Sigma-Aldrich	T9026
Rabbit polyclonal anti-DYKDDDK tag	1:6,000 (WB)	Proteintech	20543-1-AP
Rabbit monoclonal anti-phospho-ATM (Ser1981) (D25E5)	1:1,000 (WB)	Cell Signaling Technology	13050
Rabbit monoclonal anti-ATM (D2E2)	1:1,000 (WB)	Cell Signaling Technology	2873
Rabbit monoclonal anti-phospho-CHK2 (Thr68) (C13C1)	1:1,000 (WB)	Cell Signaling Technology	2197
Rabbit monoclonal anti-CHK2 (D9C6)	1:1,000 (WB)	Cell Signaling Technology	6334
Rabbit monoclonal anti-phospho-CHK1 (Ser345) (133D3)	1:1,000 (WB)	Cell Signaling Technology	2348
Mouse monoclonal anti-CHK1 (2G1D5)	1:1,000 (WB)	Cell Signaling Technology	2360
Mouse monoclonal anti-phospho-Histone H2A.X (Ser139), clone JBW301	1:1000 (WB); 1:500 (IF)	Sigma-Aldrich	05-636
Rabbit polyclonal anti-phospho-RHEB (Ser175)	1:500 (WB)	N/A	This study
Mouse monoclonal anti-RHEB (B-12)	1:500 (WB)	Santa Cruz Biotechnology	sc-271509
Rabbit polyclonal anti-ATR	1:1,000 (WB)	Cell Signaling Technology	2790
Rabbit monoclonal anti-Tuberin/TSC2 (28A7)	1:6,000 (WB)	Cell Signaling Technology	3635
Rabbit polyclonal anti-Hamartin/TSC1	1:1,000 (WB)	Cell Signaling Technology	4906
Rabbit monoclonal anti-Vinculin (E1E9V)	1:6,000 (WB)	Cell Signaling Technology	13901
Rabbit polyclonal anti-GST tag	1:3,000 (WB)	Proteintech	10000-0-AP

Rabbit monoclonal anti-RagA (D8B5)	1:1,000 (WB)	Cell Signaling Technology	4357

Table 4. Secondary antibodies used in this study.

Antibody	Dilution	Supplier	Catalog Number
Peroxidase AffiniPure Donkey Anti-Rabbit IgG (H+L)	1:10,000 (WB)	Jackson ImmunoResearch	711-035-152
Peroxidase AffiniPure Donkey Anti-Mouse IgG (H+L)	1:10,000 (WB)	Jackson ImmunoResearch	715-035-151
Alexa Fluor 488 AffiniPure Donkey Anti-Rabbit IgG (H+L)	1:400 (IF)	Jackson ImmunoResearch	711-545-152
Alexa Fluor 594 AffiniPure Donkey Anti-Mouse IgG (H+L)	1:400 (IF)	Jackson ImmunoResearch	715-585-151

Identification of phosphorylation sites on RHEB

Phosphorylation sites on RHEB were identified using curated phospho-proteomics data and computational predictions. A putative phosphorylation site (RHEB^{S175}) was retrieved from the PhosphoSitePlus database (www.phosphosite.org)[260], based on unpublished high-throughput phospho-proteomics data generated by Cell Signaling Technology (CST). Kinase-substrate predictions were performed using NetworKIN[274], which integrates consensus phosphorylation motifs with contextual information, including protein-protein interactions, co-expression data, and subcellular localization, to predict upstream kinases for candidate phosphorylation sites. Human RHEB (UniProt ID: Q15382) was used as input, and high-confidence predictions were prioritized for further investigation.

Plasmids and Molecular Cloning

The pcDNA3-FLAG-RHEB WT and pcDNA3-FLAG-Luc (FLAG-tagged firefly Luciferase; used as a negative control) plasmids were described previously[293]. The pcDNA3-FLAG-RHEB S175A and the pcDNA3-FLAG-RHEB S6A/S175A were generated by site-directed mutagenesis using appropriate oligos, and the resulting PCR products were cloned into the EcoRI and NotI restriction sites of the pcDNA3-FLAG-RHEB WT vector. The FLAG-RHEB WT and FLAG-RHEB S6A/S175A mutant were subcloned into the sleeping-beauty-based, doxycycline-inducible pITR-TTP2 vector (based on pITR-TTP[235,265,292], with a more expanded

multiple cloning site feature) using the PvuII/NotI restriction sites, while also removing the additional start codon from the RHEB cDNA. The pETM11-RHEB used for recombinant His_6-tagged RHEB protein production was generated by PCR-amplifying human RHEB cDNA using appropriate primers and subcloning into the NcoI/NotI restriction sites of the pETM11 vector.

The pcDNA3.1(+) Flag-His-ATM wt (plasmid #31985) and the pcDNA3.1(+) Flag-His-ATM kd (plasmid #31986) were purchased from Addgene (both deposited by Michael Kastan and described in[294]). The pcDNA3-FLAG-RagA Q66L (GTP-locked) and the pcDNA3-FLAG-RagC S75N (GDP-locked) were described previously[206]. All restriction enzymes were purchased from Fermentas/Thermo Scientific. The integrity of all constructs was verified by sequencing. All DNA oligonucleotides used in this study are listed in Table 5.

Table 5. Sequences of oligos used in this study.

Name	**Sequence** (5'-to-3')
PCR oligos for site-directed mutagenesis of RHEB S175A and RHEB S6A/S175A	
WT_EcoRI_fwd	GCGgaattcATGCCGCAGTCCAAGTCCCGGAAGATC
S175A_NotI_rev	GCGgcggccgcTCACATCACCGAGCATGAAGACTTGCCTTGTGcAGC TGC
S6A_EcoRI_fwd	GCGgaattcCCGCAGTCCAAGgCCCGGAAGATCGCGATC
WT_NotI_rev	GCGgcggccgcTCACATCACCGAGCATGAAGACTTGC
PCR oligos for removing the start codon from RHEB WT and S6A/S175A cDNA	
WT_EcoRI_fwd	GCGgaattcCCGCAGTCCAAGTCCCGGAAGATCGCGATC
S6A_EcoRI_fwd	GCGgaattcCCGCAGTCCAAGgCCCGGAAGATCGCGATC
PCR oligos for subcloning RHEB into the pITR-TTP2 vector	
PvuII_FLAG_EcoRI_Rheb_fwd	TAAGCAcagctgATGGACTACAAGGACGACGACGACAAGGAATTC
NotI_Rheb_rev	GCTCGAgcggccgcTCACATCAC
PCR oligos for subcloning RHEB into the pETM11 vector	
BspHI_Rheb_fwd	GCGtcatgacgCCGCAGTCCAAGTCCCGGAAGATCG
Rheb_NotI_rev	GCGgcggccgcTCACATCACCGAGCATGAAGACTTGC

Cell lysis and immunoblotting

For standard SDS-PAGE and immunoblotting experiments, cells from one well of a 6-well plate were lysed in 300 µl ice-cold Triton lysis buffer (50 mM Tris pH 7.5, 1% Triton X-100, 150 mM NaCl, 50 mM NaF, 2 mM Na-vanadate, 0.011 gr/ml beta-glycerophosphate) or RIPA buffer (50 mM Tris pH 7.5, 1% Triton X-100, 150 mM NaCl, 0.1% SDS, 0.5 % sodium deoxycholate, 50 mM NaF, 2 mM Na-vanadate, 0.011 gr/ml beta-glycerophosphate), supplemented with 1x PhosSTOP phosphatase inhibitors (#04906837001, Roche) and 1x cOmplete protease inhibitors (#11697498001, Roche). Lysates were incubated for 10 minutes on ice and clarified by centrifugation (15000 rpm, 15 min, 4 °C). Protein concentration was measured using Protein Assay Dye Reagent (#5000006, Bio-Rad). Normalized samples were boiled in 1x SDS sample buffer for 5 min at 95 °C (6x SDS sample buffer: 350 mM Tris-HCl pH 6.8, 30% glycerol, 600 mM DTT, 12.8% SDS, 0.12% bromophenol blue).

Protein samples were subjected to electrophoretic separation on SDS-PAGE and analyzed by standard Western blotting techniques. In brief, proteins were transferred to nitrocellulose membranes (#10600002 or #10600001, Amersham) and stained with 0.2% Ponceau solution (#33427-01, Serva) to confirm equal loading. Membranes were blocked with 5% skim milk powder (#42590, Serva) in PBS-T [1x PBS, 0.1% Tween-20 (#A1389, AppliChem)] for 1 hour at room temperature, washed three times for 5 min with PBS-T and then incubated with primary antibodies [in PBS-T, 5% bovine serum albumin (BSA; #10735086001, Roche; #8076, Carl Roth)] overnight at 4 °C. The next day, membranes were washed three times for 5 min with PBS-T and incubated with the appropriate HRP-conjugated secondary antibodies (1:10000 in 5% milk in PBS-T) for 1 hour at room temperature. Signals were detected by enhanced chemiluminescence (ECL), using ECL Western Blotting Substrate (#W1015, Promega); or SuperSignal West Femto Substrate (#34095, Thermo Scientific) for weaker signals. Immunoblot images were captured on films (#28906835, GE Healthcare; #4741019289, Fujifilm). Blots were scanned and then quantified using GelAnalyzer 19.1.

Immunoprecipitation and co-immunoprecipitation (co-IP)

For ATM and FLAG-RHEB co-immunoprecipitation experiments, cells from a near-confluent 6-well plate were lysed in 500 µl CHAPS IP buffer (50 mM Tris pH 7.5, 0.3% CHAPS, 150 mM NaCl, 50 mM NaF, 2 mM Na-vanadate, 0.011 gr/ml beta-glycerophosphate) supplemented with 1x PhosSTOP phosphatase inhibitors (#04906837001, Roche) and 1x cOmplete protease inhibitors (#11697498001, Roche) for 10 minutes on ice. For anti-RHEB immunoprecipitation experiments, cells from a near-confluent 10-cm dish were lysed in 1 ml Triton IP buffer (50 mM Tris pH 7.5, 1% Triton X-100, 150 mM NaCl, 50 mM NaF, 2 mM Na-vanadate, 0.011 gr/ml beta-glycerophosphate), supplemented with 1x PhosSTOP phosphatase inhibitors (#04906837001, Roche) and 1x cOmplete protease inhibitors (#11697498001, Roche). Samples were clarified by centrifugation (15000 rpm, 15 min, 4 °C) and a fraction of the samples was taken as input. For anti-FLAG IPs, the remaining supernatants were incubated with 30 µl of pre-washed anti-FLAG M2 affinity gel (#A2220, Sigma) at 4 °C on a rotating mixer for 3 h. For anti-RHEB IPs, the supernatant was incubated with 3 µl anti-RHEB antibody (#SC-271509, Santa Cruz) at 4 °C on a rotating mixer overnight (16 h), followed by incubation with 30 µl pre-washed Protein G Agarose bead slurry (#11719416001, Roche) for an additional hour at 4 °C on a rotating mixer. For all IPs, beads were then washed four times with the respective IP wash buffer (50 mM Tris pH 7.5, 0.3% CHAPS; or 1% Triton X-100, 150 mM NaCl, 50 mM NaF) and boiled in 2x SDS loading buffer. Samples were analyzed by SDS-PAGE and the presence of co-immunoprecipitated proteins was detected by immunoblotting with appropriate specific antibodies.

***In vitro* kinase assay**

In vitro ATM kinase assays were developed based on previous reports[192,294], using FLAG-ATM immunopurified from HEK29FT cells treated with etoposide (20 µM, 2 h). In brief, cells of two near-confluent wells of a 6-well plate were lysed with modified TGN buffer (50 mM Tris pH 7.5, 150 mM NaCl, 1% Tween-20, 0.3% Nonidet P-40, 1 mM NaF, 1mM mM Na-vanadate), supplemented with 1x PhosSTOP phosphatase inhibitors (#04906837001, Roche) and 1x cOmplete protease inhibitors (#11697498001, Roche) for 10 min on ice. Samples were

clarified by centrifugation (15000 rpm, 15 min, 4 °C), supernatants were subjected to immunoprecipitation by incubation with 30 µl pre-washed anti-FLAG M2 affinity gel (#A2220, Sigma) for 3 h (4 °C, rotating). Beads were then washed with TGN buffer with high salt (0.5 M NaCl), followed by two washes with kinase buffer (20 mM HEPES, pH 7.5, 50 mM NaCl, 10 mM $MgCl_2$, 1 mM DTT, 10 mM $MnCl_2$). Finally, the reactions were prepared by resuspending the beads in kinase buffer containing 125 µM unlabeled ATP, 6 µCi of [γ-^{32}P] ATP (#SRP-301; Hartmann Analytic) and 1 µg of recombinant proteins as indicated in the figure. The kinase reaction was conducted at 30 °C for 1 h and stopped by addition of one volume 2x SDS sample buffer and boiling for 5 min at 95 °C. Samples were run on SDS-PAGE, the gel was dried (GD2000, Amersham) and radio-labeled proteins were visualized on PhosphorImager (Typhoon FLA9500, GE Healthcare).

Production of recombinant His_6-tagged RHEB

Production of GST and GST-4E-BP1 were described in a previous report[235]. Recombinant His_6-tagged RHEB protein was produced by transforming *E. coli* Rosetta electrocompetent bacteria with the pETM11-RHEB vector, according to standard procedures. In brief, protein expression was induced with isopropyl-β-D-thiogalactopyranoside (IPTG) for 4 h at 37 °C, and His_6-RHEB was purified using Ni-NTA agarose (#1018244, Qiagen) and eluted with 333 mM imidazole (#A1073, Applichem).

Immunofluorescence and confocal microscopy

Immunofluorescence/confocal microscopy experiments were performed as described previously[206,290]. In brief, cells were seeded on glass coverslips coated with fibronectin (#A8350, Applichem) or poly-L-Lysine (sc-286689, Santa Cruz), treated as described in the figure legends, and fixed with 4% paraformaldehyde (PFA) (#28908, Thermo Scientific) in 1x PBS (10 min, room temperature), followed by a permeabilization step with 0.1% Triton in PBS for 10 min. Cells were blocked in blocking buffer (1% BSA in PBS) for 45 minutes. Staining with anti-TFEB (#4240, Cell Signaling Technology) and anti-γH2AX (#05-636, Sigma) antibodies (1:200 and 1:500, respectively in blocking buffer) was performed by incubation

for 16 h at 4 °C. After staining with primary antibodies, coverslips were washed three times with PBS and then stained with highly cross-adsorbed fluorescent secondary antibodies (Donkey anti-Rabbit Alexa Fluor 488, Donkey anti-Mouse Alexa Fluor 594; both from Jackson ImmunoResearch) diluted 1:400 in blocking buffer for 1 hour at room temperature. Nuclei were stained with DAPI (#A1001, VWR) (1:2000 in PBS) for 10 min and coverslips were washed three times for 10 min with PBS before mounting on glass slides with Fluoromount-G (#00-4958-02, Invitrogen). All images were acquired on an SP8 Leica confocal microscope (TCS SP8 X or TCS SP8 DLS, Leica Microsystems) using a 63x oil objective lens. Image acquisition was performed using the LAS X software (Leica Microsystems). Images from single channels are shown in grayscale, whereas in merged images, Alexa Fluor 488 is shown in green and Alexa Fluor 594 in magenta. Brightness and contrast were adjusted for visualization purposes using Fiji (https://imagej.net/software/fiji/downloads)[295]. Alterations were applied to the entire image, keeping the parameters identical between all images of the same channel in each panel.

LysoTracker staining

For LysoTracker staining experiments, cells were seeded on fibronectin- or poly-L-lysine-coated coverslips and grown until they reached 80-90% confluency. Lysosomes were stained by the addition of 100 nM LysoTracker Red DND-99 (#L7528, Invitrogen) in the treatment media for 1 hour. Nuclei were stained by Hoechst 33342 (#1351304, Bio-Rad). Cells were then fixed with 4% PFA in PBS for 10 min at room temperature, washed and permeabilized with PBT solution (1x PBS, 0.1% Tween-20) for 10 min. Coverslips were mounted on slides using Fluoromount-G (#00-4958-02, Invitrogen). All images were captured on an SP8 Leica confocal microscope (TCS SP8 X or TCS SP8 DLS, Leica Microsystems) using a 63x oil objective lens. Image acquisition was performed using the LAS X software (Leica Microsystems). Brightness and contrast were adjusted for visualization purposes using Fiji[295]. Alterations were applied to the entire image, keeping the parameters identical between all images of the same channel.

Cell confluency measurements

Changes in cell confluency were measured using an IncuCyte S3 live-cell imaging and analysis System (Sartorius). In brief, cells were cultured in 12-well plates and images from nine different regions per well were acquired at regular intervals (8 h) with a 10x objective in an IncuCyte apparatus. Images were analyzed using the IncuCyte software.

Statistical analysis

Statistical analysis and presentation of quantification data was performed using GraphPad Prism (versions 9 and 10). Data in all graphs are shown as mean ± SEM. For graphs with only two conditions shown, significance was calculated using Student's t-test (unpaired, two-tailed). For all other graphs, significance for the indicated pairwise comparisons was calculated using one-way ANOVA with *post hoc* Tukey's multiple comparisons test. Sample sizes (*n*) and significance values are indicated in figure legends (* $p < 0.05$, ** $p < 0.01$, *** $p < 0.001$, **** $p < 0.0001$, ns: non-significant).

All findings were reproducible over multiple independent experiments, within a reasonable degree of variability between replicates. For most experiments, at least three independent replicates were performed. The sample size for microscopy experiments (number of individual cells used in quantifications) is provided in the respective figure legends. No statistical method was used to predetermine sample size, which was determined in accordance with standard practices in the field. No data were excluded from the analyses. The experiments were not randomized, and the investigators were not blinded to allocation during experiments and outcome assessment.

Quantification of nuclear TFEB and LysoTracker intensities

Signal intensities were calculated using the Fiji software[295]. For nuclear TFEB quantification, nuclei were selected as regions-of-interest (ROIs) for approximately 50-60 cells over 4-5 independent representative images per condition acquired from one representative experiment (out of 3 independent replicate experiments) and integrated density was

calculated, representing the sum of the values of all pixels in the given ROI. For quantification of LysoTracker signal, ROIs (which were individual cells) were determined for approximately 50-60 cells over 4-5 independent representative images per condition and integrated density was calculated, representing the sum of the values of all pixels in the given ROI.

References

1. Kolch, W., Halasz, M., Granovskaya, M., and Kholodenko, B.N. (2015). The dynamic control of signal transduction networks in cancer cells. Nat Rev Cancer *15*, 515-527. 10.1038/nrc3983.
2. Su, J., Song, Y., Zhu, Z., Huang, X., Fan, J., Qiao, J., and Mao, F. (2024). Cell-cell communication: new insights and clinical implications. Signal Transduct Target Ther *9*, 196. 10.1038/s41392-024-01888-z.
3. Blackford, A.N., and Jackson, S.P. (2017). ATM, ATR, and DNA-PK: The Trinity at the Heart of the DNA Damage Response. Mol Cell *66*, 801-817. 10.1016/j.molcel.2017.05.015.
4. Huang, R., and Zhou, P.K. (2021). DNA damage repair: historical perspectives, mechanistic pathways and clinical translation for targeted cancer therapy. Signal Transduct Target Ther *6*, 254. 10.1038/s41392-021-00648-7.
5. Laplante, M., and Sabatini, D.M. (2012). mTOR signaling in growth control and disease. Cell *149*, 274-293. 10.1016/j.cell.2012.03.017.
6. Panwar, V., Singh, A., Bhatt, M., Tonk, R.K., Azizov, S., Raza, A.S., Sengupta, S., Kumar, D., and Garg, M. (2023). Multifaceted role of mTOR (mammalian target of rapamycin) signaling pathway in human health and disease. Signal Transduct Target Ther *8*, 375. 10.1038/s41392-023-01608-z.
7. Ma, Y., Vassetzky, Y., and Dokudovskaya, S. (2018). mTORC1 pathway in DNA damage response. Biochim Biophys Acta Mol Cell Res *1865*, 1293-1311. 10.1016/j.bbamcr.2018.06.011.
8. Danesh Pazhooh, R., Rahnamay Farnood, P., Asemi, Z., Mirsafaei, L., Yousefi, B., and Mirzaei, H. (2021). mTOR pathway and DNA damage response: A therapeutic strategy in cancer therapy. DNA Repair (Amst) *104*, 103142. 10.1016/j.dnarep.2021.103142.
9. Chatzidoukaki, O., Goulielmaki, E., Schumacher, B., and Garinis, G.A. (2020). DNA Damage Response and Metabolic Reprogramming in Health and Disease. Trends Genet *36*, 777-791. 10.1016/j.tig.2020.06.018.
10. Ciccia, A., and Elledge, S.J. (2010). The DNA damage response: making it safe to play with knives. Mol Cell *40*, 179-204. 10.1016/j.molcel.2010.09.019.
11. Jackson, S.P., and Bartek, J. (2009). The DNA-damage response in human biology and disease. Nature *461*, 1071-1078. 10.1038/nature08467.
12. Dall'Agnese, G., Dall'Agnese, A., Banani, S.F., Codrich, M., Malfatti, M.C., Antoniali, G., and Tell, G. (2023). Role of condensates in modulating DNA repair pathways and its implication for chemoresistance. J Biol Chem *299*, 104800. 10.1016/j.jbc.2023.104800.
13. Lee, J.H., and Paull, T.T. (2005). ATM activation by DNA double-strand breaks through the Mre11-Rad50-Nbs1 complex. Science *308*, 551-554. 10.1126/science.1108297.
14. Stracker, T.H., and Petrini, J.H. (2011). The MRE11 complex: starting from the ends. Nat Rev Mol Cell Biol *12*, 90-103. 10.1038/nrm3047.

15. Uziel, T., Lerenthal, Y., Moyal, L., Andegeko, Y., Mittelman, L., and Shiloh, Y. (2003). Requirement of the MRN complex for ATM activation by DNA damage. EMBO J *22*, 5612-5621. 10.1093/emboj/cdg541.
16. Zou, L., and Elledge, S.J. (2003). Sensing DNA damage through ATRIP recognition of RPA-ssDNA complexes. Science *300*, 1542-1548. 10.1126/science.1083430.
17. Cimprich, K.A., and Cortez, D. (2008). ATR: an essential regulator of genome integrity. Nat Rev Mol Cell Biol *9*, 616-627. 10.1038/nrm2450.
18. Mimori, T., and Hardin, J.A. (1986). Mechanism of interaction between Ku protein and DNA. J Biol Chem *261*, 10375-10379.
19. Walker, J.R., Corpina, R.A., and Goldberg, J. (2001). Structure of the Ku heterodimer bound to DNA and its implications for double-strand break repair. Nature *412*, 607-614. 10.1038/35088000.
20. Sibanda, B.L., Chirgadze, D.Y., and Blundell, T.L. (2010). Crystal structure of DNA-PKcs reveals a large open-ring cradle comprised of HEAT repeats. Nature *463*, 118-121. 10.1038/nature08648.
21. Rogakou, E.P., Pilch, D.R., Orr, A.H., Ivanova, V.S., and Bonner, W.M. (1998). DNA double-stranded breaks induce histone H2AX phosphorylation on serine 139. J Biol Chem *273*, 5858-5868. 10.1074/jbc.273.10.5858.
22. Stucki, M., Clapperton, J.A., Mohammad, D., Yaffe, M.B., Smerdon, S.J., and Jackson, S.P. (2005). MDC1 directly binds phosphorylated histone H2AX to regulate cellular responses to DNA double-strand breaks. Cell *123*, 1213-1226. 10.1016/j.cell.2005.09.038.
23. Mailand, N., Bekker-Jensen, S., Faustrup, H., Melander, F., Bartek, J., Lukas, C., and Lukas, J. (2007). RNF8 ubiquitylates histones at DNA double-strand breaks and promotes assembly of repair proteins. Cell *131*, 887-900. 10.1016/j.cell.2007.09.040.
24. Doil, C., Mailand, N., Bekker-Jensen, S., Menard, P., Larsen, D.H., Pepperkok, R., Ellenberg, J., Panier, S., Durocher, D., Bartek, J., et al. (2009). RNF168 binds and amplifies ubiquitin conjugates on damaged chromosomes to allow accumulation of repair proteins. Cell *136*, 435-446. 10.1016/j.cell.2008.12.041.
25. Mattiroli, F., Vissers, J.H., van Dijk, W.J., Ikpa, P., Citterio, E., Vermeulen, W., Marteijn, J.A., and Sixma, T.K. (2012). RNF168 ubiquitinates K13-15 on H2A/H2AX to drive DNA damage signaling. Cell *150*, 1182-1195. 10.1016/j.cell.2012.08.005.
26. Ng, H.M., Wei, L., Lan, L., and Huen, M.S. (2016). The Lys63-deubiquitylating Enzyme BRCC36 Limits DNA Break Processing and Repair. J Biol Chem *291*, 16197-16207. 10.1074/jbc.M116.731927.
27. Nicassio, F., Corrado, N., Vissers, J.H., Areces, L.B., Bergink, S., Marteijn, J.A., Geverts, B., Houtsmuller, A.B., Vermeulen, W., Di Fiore, P.P., and Citterio, E. (2007). Human USP3 is a chromatin modifier required for S phase progression and genome stability. Curr Biol *17*, 1972-1977. 10.1016/j.cub.2007.10.034.
28. Poulsen, M., Lukas, C., Lukas, J., Bekker-Jensen, S., and Mailand, N. (2012). Human RNF169 is a negative regulator of the ubiquitin-dependent response to DNA double-strand breaks. J Cell Biol *197*, 189-199. 10.1083/jcb.201109100.

29. Kumagai, A., and Dunphy, W.G. (2000). Claspin, a novel protein required for the activation of Chk1 during a DNA replication checkpoint response in Xenopus egg extracts. Mol Cell *6*, 839-849. 10.1016/s1097-2765(05)00092-4.
30. Matsuoka, S., Rotman, G., Ogawa, A., Shiloh, Y., Tamai, K., and Elledge, S.J. (2000). Ataxia telangiectasia-mutated phosphorylates Chk2 in vivo and in vitro. Proc Natl Acad Sci U S A *97*, 10389-10394. 10.1073/pnas.190030497.
31. Yazdi, P.T., Wang, Y., Zhao, S., Patel, N., Lee, E.Y., and Qin, J. (2002). SMC1 is a downstream effector in the ATM/NBS1 branch of the human S-phase checkpoint. Genes Dev *16*, 571-582. 10.1101/gad.970702.
32. Ashley, A.K., Shrivastav, M., Nie, J., Amerin, C., Troksa, K., Glanzer, J.G., Liu, S., Opiyo, S.O., Dimitrova, D.D., Le, P., et al. (2014). DNA-PK phosphorylation of RPA32 Ser4/Ser8 regulates replication stress checkpoint activation, fork restart, homologous recombination and mitotic catastrophe. DNA Repair (Amst) *21*, 131-139. 10.1016/j.dnarep.2014.04.008.
33. Liaw, H., Lee, D., and Myung, K. (2011). DNA-PK-dependent RPA2 hyperphosphorylation facilitates DNA repair and suppresses sister chromatid exchange. PLoS One *6*, e21424. 10.1371/journal.pone.0021424.
34. Olson, E., Nievera, C.J., Klimovich, V., Fanning, E., and Wu, X. (2006). RPA2 is a direct downstream target for ATR to regulate the S-phase checkpoint. J Biol Chem *281*, 39517-39533. 10.1074/jbc.M605121200.
35. Chowdhury, D., Xu, X., Zhong, X., Ahmed, F., Zhong, J., Liao, J., Dykxhoorn, D.M., Weinstock, D.M., Pfeifer, G.P., and Lieberman, J. (2008). A PP4-phosphatase complex dephosphorylates gamma-H2AX generated during DNA replication. Mol Cell *31*, 33-46. 10.1016/j.molcel.2008.05.016.
36. Feng, J., Wakeman, T., Yong, S., Wu, X., Kornbluth, S., and Wang, X.F. (2009). Protein phosphatase 2A-dependent dephosphorylation of replication protein A is required for the repair of DNA breaks induced by replication stress. Mol Cell Biol *29*, 5696-5709. 10.1128/MCB.00191-09.
37. Lu, X., Nannenga, B., and Donehower, L.A. (2005). PPM1D dephosphorylates Chk1 and p53 and abrogates cell cycle checkpoints. Genes Dev *19*, 1162-1174. 10.1101/gad.1291305.
38. Nakada, S., Chen, G.I., Gingras, A.C., and Durocher, D. (2025). Author Correction: PP4 is a gammaH2AX phosphatase required for recovery from the DNA damage checkpoint. EMBO Rep *26*, 1184-1185. 10.1038/s44319-024-00338-9.
39. Oliva-Trastoy, M., Berthonaud, V., Chevalier, A., Ducrot, C., Marsolier-Kergoat, M.C., Mann, C., and Leteurtre, F. (2007). The Wip1 phosphatase (PPM1D) antagonizes activation of the Chk2 tumour suppressor kinase. Oncogene *26*, 1449-1458. 10.1038/sj.onc.1209927.
40. Shreeram, S., Demidov, O.N., Hee, W.K., Yamaguchi, H., Onishi, N., Kek, C., Timofeev, O.N., Dudgeon, C., Fornace, A.J., Anderson, C.W., et al. (2006). Wip1 phosphatase modulates ATM-dependent signaling pathways. Mol Cell *23*, 757-764. 10.1016/j.molcel.2006.07.010.
41. Bartek, J., and Lukas, J. (2003). Chk1 and Chk2 kinases in checkpoint control and cancer. Cancer Cell *3*, 421-429. 10.1016/s1535-6108(03)00110-7.

42. Smith, J., Tho, L.M., Xu, N., and Gillespie, D.A. (2010). The ATM-Chk2 and ATR-Chk1 pathways in DNA damage signaling and cancer. Adv Cancer Res *108*, 73-112. 10.1016/B978-0-12-380888-2.00003-0.
43. Mailand, N., Falck, J., Lukas, C., Syljuasen, R.G., Welcker, M., Bartek, J., and Lukas, J. (2000). Rapid destruction of human Cdc25A in response to DNA damage. Science *288*, 1425-1429. 10.1126/science.288.5470.1425.
44. Falck, J., Mailand, N., Syljuasen, R.G., Bartek, J., and Lukas, J. (2001). The ATM-Chk2-Cdc25A checkpoint pathway guards against radioresistant DNA synthesis. Nature *410*, 842-847. 10.1038/35071124.
45. Bartek, J., and Lukas, J. (2001). Pathways governing G1/S transition and their response to DNA damage. FEBS Lett *490*, 117-122. 10.1016/s0014-5793(01)02114-7.
46. Sherr, C.J., and Roberts, J.M. (1999). CDK inhibitors: positive and negative regulators of G1-phase progression. Genes Dev *13*, 1501-1512. 10.1101/gad.13.12.1501.
47. Parker, L.L., and Piwnica-Worms, H. (1992). Inactivation of the p34cdc2-cyclin B complex by the human WEE1 tyrosine kinase. Science *257*, 1955-1957. 10.1126/science.1384126.
48. Perry, J.A., and Kornbluth, S. (2007). Cdc25 and Wee1: analogous opposites? Cell Div *2*, 12. 10.1186/1747-1028-2-12.
49. Nicolai, S., Rossi, A., Di Daniele, N., Melino, G., Annicchiarico-Petruzzelli, M., and Raschella, G. (2015). DNA repair and aging: the impact of the p53 family. Aging (Albany NY) *7*, 1050-1065. 10.18632/aging.100858.
50. Chapman, J.R., Taylor, M.R., and Boulton, S.J. (2012). Playing the end game: DNA double-strand break repair pathway choice. Mol Cell *47*, 497-510. 10.1016/j.molcel.2012.07.029.
51. Singleton, B.K., Torres-Arzayus, M.I., Rottinghaus, S.T., Taccioli, G.E., and Jeggo, P.A. (1999). The C terminus of Ku80 activates the DNA-dependent protein kinase catalytic subunit. Mol Cell Biol *19*, 3267-3277. 10.1128/MCB.19.5.3267.
52. Kurosawa, A., Koyama, H., Takayama, S., Miki, K., Ayusawa, D., Fujii, M., Iiizumi, S., and Adachi, N. (2008). The requirement of Artemis in double-strand break repair depends on the type of DNA damage. DNA Cell Biol *27*, 55-61. 10.1089/dna.2007.0649.
53. Capp, J.P., Boudsocq, F., Bertrand, P., Laroche-Clary, A., Pourquier, P., Lopez, B.S., Cazaux, C., Hoffmann, J.S., and Canitrot, Y. (2006). The DNA polymerase lambda is required for the repair of non-compatible DNA double strand breaks by NHEJ in mammalian cells. Nucleic Acids Res *34*, 2998-3007. 10.1093/nar/gkl380.
54. Mahajan, K.N., Nick McElhinny, S.A., Mitchell, B.S., and Ramsden, D.A. (2002). Association of DNA polymerase mu (pol mu) with Ku and ligase IV: role for pol mu in end-joining double-strand break repair. Mol Cell Biol *22*, 5194-5202. 10.1128/MCB.22.14.5194-5202.2002.
55. Grawunder, U., Wilm, M., Wu, X., Kulesza, P., Wilson, T.E., Mann, M., and Lieber, M.R. (1997). Activity of DNA ligase IV stimulated by complex formation with XRCC4 protein in mammalian cells. Nature *388*, 492-495. 10.1038/41358.

56. Heyer, W.D., Ehmsen, K.T., and Liu, J. (2010). Regulation of homologous recombination in eukaryotes. Annu Rev Genet *44*, 113-139. 10.1146/annurev-genet-051710-150955.
57. Sartori, A.A., Lukas, C., Coates, J., Mistrik, M., Fu, S., Bartek, J., Baer, R., Lukas, J., and Jackson, S.P. (2007). Human CtIP promotes DNA end resection. Nature *450*, 509-514. 10.1038/nature06337.
58. Gravel, S., Chapman, J.R., Magill, C., and Jackson, S.P. (2008). DNA helicases Sgs1 and BLM promote DNA double-strand break resection. Genes Dev *22*, 2767-2772. 10.1101/gad.503108.
59. Mimitou, E.P., and Symington, L.S. (2008). Sae2, Exo1 and Sgs1 collaborate in DNA double-strand break processing. Nature *455*, 770-774. 10.1038/nature07312.
60. Nimonkar, A.V., Genschel, J., Kinoshita, E., Polaczek, P., Campbell, J.L., Wyman, C., Modrich, P., and Kowalczykowski, S.C. (2011). BLM-DNA2-RPA-MRN and EXO1-BLM-RPA-MRN constitute two DNA end resection machineries for human DNA break repair. Genes Dev *25*, 350-362. 10.1101/gad.2003811.
61. Moynahan, M.E., Pierce, A.J., and Jasin, M. (2001). BRCA2 is required for homology-directed repair of chromosomal breaks. Mol Cell *7*, 263-272. 10.1016/s1097-2765(01)00174-5.
62. Sy, S.M., Huen, M.S., and Chen, J. (2009). PALB2 is an integral component of the BRCA complex required for homologous recombination repair. Proc Natl Acad Sci U S A *106*, 7155-7160. 10.1073/pnas.0811159106.
63. Xia, B., Sheng, Q., Nakanishi, K., Ohashi, A., Wu, J., Christ, N., Liu, X., Jasin, M., Couch, F.J., and Livingston, D.M. (2006). Control of BRCA2 cellular and clinical functions by a nuclear partner, PALB2. Mol Cell *22*, 719-729. 10.1016/j.molcel.2006.05.022.
64. Raynard, S., Bussen, W., and Sung, P. (2006). A double Holliday junction dissolvasome comprising BLM, topoisomerase IIIalpha, and BLAP75. J Biol Chem *281*, 13861-13864. 10.1074/jbc.C600051200.
65. Wu, L., Bachrati, C.Z., Ou, J., Xu, C., Yin, J., Chang, M., Wang, W., Li, L., Brown, G.W., and Hickson, I.D. (2006). BLAP75/RMI1 promotes the BLM-dependent dissolution of homologous recombination intermediates. Proc Natl Acad Sci U S A *103*, 4068-4073. 10.1073/pnas.0508295103.
66. Wu, L., and Hickson, I.D. (2003). The Bloom's syndrome helicase suppresses crossing over during homologous recombination. Nature *426*, 870-874. 10.1038/nature02253.
67. Krokan, H.E., Standal, R., and Slupphaug, G. (1997). DNA glycosylases in the base excision repair of DNA. Biochem J *325 (Pt 1)*, 1-16. 10.1042/bj3250001.
68. Wallace, S.S. (2014). Base excision repair: a critical player in many games. DNA Repair (Amst) *19*, 14-26. 10.1016/j.dnarep.2014.03.030.
69. Demple, B., Herman, T., and Chen, D.S. (1991). Cloning and expression of APE, the cDNA encoding the major human apurinic endonuclease: definition of a family of DNA repair enzymes. Proc Natl Acad Sci U S A *88*, 11450-11454. 10.1073/pnas.88.24.11450.

70. Sobol, R.W., Horton, J.K., Kuhn, R., Gu, H., Singhal, R.K., Prasad, R., Rajewsky, K., and Wilson, S.H. (1996). Requirement of mammalian DNA polymerase-beta in base-excision repair. Nature *379*, 183-186. 10.1038/379183a0.
71. Caldecott, K.W., McKeown, C.K., Tucker, J.D., Ljungquist, S., and Thompson, L.H. (1994). An interaction between the mammalian DNA repair protein XRCC1 and DNA ligase III. Mol Cell Biol *14*, 68-76. 10.1128/mcb.14.1.68-76.1994.
72. Gary, R., Kim, K., Cornelius, H.L., Park, M.S., and Matsumoto, Y. (1999). Proliferating cell nuclear antigen facilitates excision in long-patch base excision repair. J Biol Chem *274*, 4354-4363. 10.1074/jbc.274.7.4354.
73. Parsons, J.L., Preston, B.D., O'Connor, T.R., and Dianov, G.L. (2007). DNA polymerase delta-dependent repair of DNA single strand breaks containing 3'-end proximal lesions. Nucleic Acids Res *35*, 1054-1063. 10.1093/nar/gkl1115.
74. Pascucci, B., Stucki, M., Jonsson, Z.O., Dogliotti, E., and Hubscher, U. (1999). Long patch base excision repair with purified human proteins. DNA ligase I as patch size mediator for DNA polymerases delta and epsilon. J Biol Chem *274*, 33696-33702. 10.1074/jbc.274.47.33696.
75. Sattler, U., Frit, P., Salles, B., and Calsou, P. (2003). Long-patch DNA repair synthesis during base excision repair in mammalian cells. EMBO Rep *4*, 363-367. 10.1038/sj.embor.embor796.
76. Scharer, O.D. (2013). Nucleotide excision repair in eukaryotes. Cold Spring Harb Perspect Biol *5*, a012609. 10.1101/cshperspect.a012609.
77. Marteijn, J.A., Lans, H., Vermeulen, W., and Hoeijmakers, J.H. (2014). Understanding nucleotide excision repair and its roles in cancer and ageing. Nat Rev Mol Cell Biol *15*, 465-481. 10.1038/nrm3822.
78. Sugasawa, K., Ng, J.M., Masutani, C., Iwai, S., van der Spek, P.J., Eker, A.P., Hanaoka, F., Bootsma, D., and Hoeijmakers, J.H. (1998). Xeroderma pigmentosum group C protein complex is the initiator of global genome nucleotide excision repair. Mol Cell *2*, 223-232. 10.1016/s1097-2765(00)80132-x.
79. Hanawalt, P.C. (2002). Subpathways of nucleotide excision repair and their regulation. Oncogene *21*, 8949-8956. 10.1038/sj.onc.1206096.
80. Sugitani, N., Sivley, R.M., Perry, K.E., Capra, J.A., and Chazin, W.J. (2016). XPA: A key scaffold for human nucleotide excision repair. DNA Repair (Amst) *44*, 123-135. 10.1016/j.dnarep.2016.05.018.
81. Coin, F., Marinoni, J.C., Rodolfo, C., Fribourg, S., Pedrini, A.M., and Egly, J.M. (1998). Mutations in the XPD helicase gene result in XP and TTD phenotypes, preventing interaction between XPD and the p44 subunit of TFIIH. Nat Genet *20*, 184-188. 10.1038/2491.
82. de Laat, W.L., Appeldoorn, E., Jaspers, N.G., and Hoeijmakers, J.H. (1998). DNA structural elements required for ERCC1-XPF endonuclease activity. J Biol Chem *273*, 7835-7842. 10.1074/jbc.273.14.7835.
83. Sijbers, A.M., de Laat, W.L., Ariza, R.R., Biggerstaff, M., Wei, Y.F., Moggs, J.G., Carter, K.C., Shell, B.K., Evans, E., de Jong, M.C., et al. (1996). Xeroderma pigmentosum group F caused by a defect in a structure-specific DNA repair endonuclease. Cell *86*, 811-822. 10.1016/s0092-8674(00)80155-5.

84. O'Donovan, A., Davies, A.A., Moggs, J.G., West, S.C., and Wood, R.D. (1994). XPG endonuclease makes the 3' incision in human DNA nucleotide excision repair. Nature *371*, 432-435. 10.1038/371432a0.
85. Staresincic, L., Fagbemi, A.F., Enzlin, J.H., Gourdin, A.M., Wijgers, N., Dunand-Sauthier, I., Giglia-Mari, G., Clarkson, S.G., Vermeulen, W., and Scharer, O.D. (2009). Coordination of dual incision and repair synthesis in human nucleotide excision repair. EMBO J *28*, 1111-1120. 10.1038/emboj.2009.49.
86. Ogi, T., Limsirichaikul, S., Overmeer, R.M., Volker, M., Takenaka, K., Cloney, R., Nakazawa, Y., Niimi, A., Miki, Y., Jaspers, N.G., et al. (2010). Three DNA polymerases, recruited by different mechanisms, carry out NER repair synthesis in human cells. Mol Cell *37*, 714-727. 10.1016/j.molcel.2010.02.009.
87. Jiricny, J. (2013). Postreplicative mismatch repair. Cold Spring Harb Perspect Biol *5*, a012633. 10.1101/cshperspect.a012633.
88. Palombo, F., Gallinari, P., Iaccarino, I., Lettieri, T., Hughes, M., D'Arrigo, A., Truong, O., Hsuan, J.J., and Jiricny, J. (1995). GTBP, a 160-kilodalton protein essential for mismatch-binding activity in human cells. Science *268*, 1912-1914. 10.1126/science.7604265.
89. Drummond, J.T., Genschel, J., Wolf, E., and Modrich, P. (1997). DHFR/MSH3 amplification in methotrexate-resistant cells alters the hMutSalpha/hMutSbeta ratio and reduces the efficiency of base-base mismatch repair. Proc Natl Acad Sci U S A *94*, 10144-10149. 10.1073/pnas.94.19.10144.
90. Genschel, J., Littman, S.J., Drummond, J.T., and Modrich, P. (1998). Isolation of MutSbeta from human cells and comparison of the mismatch repair specificities of MutSbeta and MutSalpha. J Biol Chem *273*, 19895-19901. 10.1074/jbc.273.31.19895.
91. Prolla, T.A., Pang, Q., Alani, E., Kolodner, R.D., and Liskay, R.M. (1994). MLH1, PMS1, and MSH2 interactions during the initiation of DNA mismatch repair in yeast. Science *265*, 1091-1093. 10.1126/science.8066446.
92. Tishkoff, D.X., Boerger, A.L., Bertrand, P., Filosi, N., Gaida, G.M., Kane, M.F., and Kolodner, R.D. (1997). Identification and characterization of Saccharomyces cerevisiae EXO1, a gene encoding an exonuclease that interacts with MSH2. Proc Natl Acad Sci U S A *94*, 7487-7492. 10.1073/pnas.94.14.7487.
93. el-Deiry, W.S., Tokino, T., Velculescu, V.E., Levy, D.B., Parsons, R., Trent, J.M., Lin, D., Mercer, W.E., Kinzler, K.W., and Vogelstein, B. (1993). WAF1, a potential mediator of p53 tumor suppression. Cell *75*, 817-825. 10.1016/0092-8674(93)90500-p.
94. Harper, J.W., Adami, G.R., Wei, N., Keyomarsi, K., and Elledge, S.J. (1993). The p21 Cdk-interacting protein Cip1 is a potent inhibitor of G1 cyclin-dependent kinases. Cell *75*, 805-816. 10.1016/0092-8674(93)90499-g.
95. Xiong, Y., Hannon, G.J., Zhang, H., Casso, D., Kobayashi, R., and Beach, D. (1993). p21 is a universal inhibitor of cyclin kinases. Nature *366*, 701-704. 10.1038/366701a0.
96. Chellappan, S.P., Hiebert, S., Mudryj, M., Horowitz, J.M., and Nevins, J.R. (1991). The E2F transcription factor is a cellular target for the RB protein. Cell *65*, 1053-1061. 10.1016/0092-8674(91)90557-f.
97. Classon, M., and Harlow, E. (2002). The retinoblastoma tumour suppressor in development and cancer. Nat Rev Cancer *2*, 910-917. 10.1038/nrc950.

98. Serrano, M., Lin, A.W., McCurrach, M.E., Beach, D., and Lowe, S.W. (1997). Oncogenic ras provokes premature cell senescence associated with accumulation of p53 and p16INK4a. Cell *88*, 593-602. 10.1016/s0092-8674(00)81902-9.
99. Kumari, R., and Jat, P. (2021). Mechanisms of Cellular Senescence: Cell Cycle Arrest and Senescence Associated Secretory Phenotype. Front Cell Dev Biol *9*, 645593. 10.3389/fcell.2021.645593.
100. Miyashita, T., and Reed, J.C. (1995). Tumor suppressor p53 is a direct transcriptional activator of the human bax gene. Cell *80*, 293-299. 10.1016/0092-8674(95)90412-3.
101. Nakano, K., and Vousden, K.H. (2001). PUMA, a novel proapoptotic gene, is induced by p53. Mol Cell *7*, 683-694. 10.1016/s1097-2765(01)00214-3.
102. Kluck, R.M., Bossy-Wetzel, E., Green, D.R., and Newmeyer, D.D. (1997). The release of cytochrome c from mitochondria: a primary site for Bcl-2 regulation of apoptosis. Science *275*, 1132-1136. 10.1126/science.275.5303.1132.
103. Liu, X., Kim, C.N., Yang, J., Jemmerson, R., and Wang, X. (1996). Induction of apoptotic program in cell-free extracts: requirement for dATP and cytochrome c. Cell *86*, 147-157. 10.1016/s0092-8674(00)80085-9.
104. Oda, E., Ohki, R., Murasawa, H., Nemoto, J., Shibue, T., Yamashita, T., Tokino, T., Taniguchi, T., and Tanaka, N. (2000). Noxa, a BH3-only member of the Bcl-2 family and candidate mediator of p53-induced apoptosis. Science *288*, 1053-1058. 10.1126/science.288.5468.1053.
105. Youle, R.J., and Strasser, A. (2008). The BCL-2 protein family: opposing activities that mediate cell death. Nat Rev Mol Cell Biol *9*, 47-59. 10.1038/nrm2308.
106. Campisi, J., and d'Adda di Fagagna, F. (2007). Cellular senescence: when bad things happen to good cells. Nat Rev Mol Cell Biol *8*, 729-740. 10.1038/nrm2233.
107. Roos, W.P., and Kaina, B. (2013). DNA damage-induced cell death: from specific DNA lesions to the DNA damage response and apoptosis. Cancer Lett *332*, 237-248. 10.1016/j.canlet.2012.01.007.
108. Shiloh, Y. (2003). ATM and related protein kinases: safeguarding genome integrity. Nat Rev Cancer *3*, 155-168. 10.1038/nrc1011.
109. Hopfner, K.P., Craig, L., Moncalian, G., Zinkel, R.A., Usui, T., Owen, B.A., Karcher, A., Henderson, B., Bodmer, J.L., McMurray, C.T., et al. (2002). The Rad50 zinc-hook is a structure joining Mre11 complexes in DNA recombination and repair. Nature *418*, 562-566. 10.1038/nature00922.
110. Lammens, K., Bemeleit, D.J., Mockel, C., Clausing, E., Schele, A., Hartung, S., Schiller, C.B., Lucas, M., Angermuller, C., Soding, J., et al. (2011). The Mre11:Rad50 structure shows an ATP-dependent molecular clamp in DNA double-strand break repair. Cell *145*, 54-66. 10.1016/j.cell.2011.02.038.
111. You, Z., Chahwan, C., Bailis, J., Hunter, T., and Russell, P. (2005). ATM activation and its recruitment to damaged DNA require binding to the C terminus of Nbs1. Mol Cell Biol *25*, 5363-5379. 10.1128/MCB.25.13.5363-5379.2005.
112. Bakkenist, C.J., and Kastan, M.B. (2003). DNA damage activates ATM through intermolecular autophosphorylation and dimer dissociation. Nature *421*, 499-506. 10.1038/nature01368.

113. Sun, Y., Xu, Y., Roy, K., and Price, B.D. (2007). DNA damage-induced acetylation of lysine 3016 of ATM activates ATM kinase activity. Mol Cell Biol *27*, 8502-8509. 10.1128/MCB.01382-07.
114. Sun, Y., Jiang, X., Chen, S., Fernandes, N., and Price, B.D. (2005). A role for the Tip60 histone acetyltransferase in the acetylation and activation of ATM. Proc Natl Acad Sci U S A *102*, 13182-13187. 10.1073/pnas.0504211102.
115. Jungmichel, S., Clapperton, J.A., Lloyd, J., Hari, F.J., Spycher, C., Pavic, L., Li, J., Haire, L.F., Bonalli, M., Larsen, D.H., et al. (2012). The molecular basis of ATM-dependent dimerization of the Mdc1 DNA damage checkpoint mediator. Nucleic Acids Res *40*, 3913-3928. 10.1093/nar/gkr1300.
116. Goodarzi, A.A., Noon, A.T., Deckbar, D., Ziv, Y., Shiloh, Y., Lobrich, M., and Jeggo, P.A. (2008). ATM signaling facilitates repair of DNA double-strand breaks associated with heterochromatin. Mol Cell *31*, 167-177. 10.1016/j.molcel.2008.05.017.
117. Ziv, Y., Bielopolski, D., Galanty, Y., Lukas, C., Taya, Y., Schultz, D.C., Lukas, J., Bekker-Jensen, S., Bartek, J., and Shiloh, Y. (2006). Chromatin relaxation in response to DNA double-strand breaks is modulated by a novel ATM- and KAP-1 dependent pathway. Nat Cell Biol *8*, 870-876. 10.1038/ncb1446.
118. Matsuoka, S., Huang, M., and Elledge, S.J. (1998). Linkage of ATM to cell cycle regulation by the Chk2 protein kinase. Science *282*, 1893-1897. 10.1126/science.282.5395.1893.
119. Rappold, I., Iwabuchi, K., Date, T., and Chen, J. (2001). Tumor suppressor p53 binding protein 1 (53BP1) is involved in DNA damage-signaling pathways. J Cell Biol *153*, 613-620. 10.1083/jcb.153.3.613.
120. Cortez, D., Wang, Y., Qin, J., and Elledge, S.J. (1999). Requirement of ATM-dependent phosphorylation of brca1 in the DNA damage response to double-strand breaks. Science *286*, 1162-1166. 10.1126/science.286.5442.1162.
121. Banin, S., Moyal, L., Shieh, S., Taya, Y., Anderson, C.W., Chessa, L., Smorodinsky, N.I., Prives, C., Reiss, Y., Shiloh, Y., and Ziv, Y. (1998). Enhanced phosphorylation of p53 by ATM in response to DNA damage. Science *281*, 1674-1677. 10.1126/science.281.5383.1674.
122. Dumaz, N., and Meek, D.W. (1999). Serine15 phosphorylation stimulates p53 transactivation but does not directly influence interaction with HDM2. EMBO J *18*, 7002-7010. 10.1093/emboj/18.24.7002.
123. Khosravi, R., Maya, R., Gottlieb, T., Oren, M., Shiloh, Y., and Shkedy, D. (1999). Rapid ATM-dependent phosphorylation of MDM2 precedes p53 accumulation in response to DNA damage. Proc Natl Acad Sci U S A *96*, 14973-14977. 10.1073/pnas.96.26.14973.
124. Maya, R., Balass, M., Kim, S.T., Shkedy, D., Leal, J.F., Shifman, O., Moas, M., Buschmann, T., Ronai, Z., Shiloh, Y., et al. (2001). ATM-dependent phosphorylation of Mdm2 on serine 395: role in p53 activation by DNA damage. Genes Dev *15*, 1067-1077. 10.1101/gad.886901.
125. Guo, Z., Kozlov, S., Lavin, M.F., Person, M.D., and Paull, T.T. (2010). ATM activation by oxidative stress. Science *330*, 517-521. 10.1126/science.1192912.

126. Tripathi, D.N., Chowdhury, R., Trudel, L.J., Tee, A.R., Slack, R.S., Walker, C.L., and Wogan, G.N. (2013). Reactive nitrogen species regulate autophagy through ATM-AMPK-TSC2-mediated suppression of mTORC1. Proc Natl Acad Sci U S A *110*, E2950-2957. 10.1073/pnas.1307736110.
127. Alexander, A., Cai, S.L., Kim, J., Nanez, A., Sahin, M., MacLean, K.H., Inoki, K., Guan, K.L., Shen, J., Person, M.D., et al. (2010). ATM signals to TSC2 in the cytoplasm to regulate mTORC1 in response to ROS. Proc Natl Acad Sci U S A *107*, 4153-4158. 10.1073/pnas.0913860107.
128. Zhang, J., Tripathi, D.N., Jing, J., Alexander, A., Kim, J., Powell, R.T., Dere, R., Tait-Mulder, J., Lee, J.H., Paull, T.T., et al. (2015). ATM functions at the peroxisome to induce pexophagy in response to ROS. Nat Cell Biol *17*, 1259-1269. 10.1038/ncb3230.
129. Valentin-Vega, Y.A., Maclean, K.H., Tait-Mulder, J., Milasta, S., Steeves, M., Dorsey, F.C., Cleveland, J.L., Green, D.R., and Kastan, M.B. (2012). Mitochondrial dysfunction in ataxia-telangiectasia. Blood *119*, 1490-1500. 10.1182/blood-2011-08-373639.
130. Yang, D.Q., and Kastan, M.B. (2000). Participation of ATM in insulin signalling through phosphorylation of eIF-4E-binding protein 1. Nat Cell Biol *2*, 893-898. 10.1038/35046542.
131. Ching, J.K., Luebbert Sh Fau - Collins, R.L.t., Collins Rl 4th Fau - Zhang, Z., Zhang Z Fau - Marupudi, N., Marupudi N Fau - Banerjee, S., Banerjee S Fau - Hurd, R.D., Hurd Rd Fau - Ralston, L., Ralston L Fau - Fisher, J.S., and Fisher, J.S. Ataxia telangiectasia mutated impacts insulin-like growth factor 1 signalling in skeletal muscle.
132. Halaby, M.J., Hibma, J.C., He, J., and Yang, D.Q. (2008). ATM protein kinase mediates full activation of Akt and regulates glucose transporter 4 translocation by insulin in muscle cells. Cell Signal *20*, 1555-1563. 10.1016/j.cellsig.2008.04.011.
133. Viniegra, J.G., Martinez, N., Modirassari, P., Hernandez Losa, J., Parada Cobo, C., Sanchez-Arevalo Lobo, V.J., Aceves Luquero, C.I., Alvarez-Vallina, L., Ramon y Cajal, S., Rojas, J.M., and Sanchez-Prieto, R. (2005). Full activation of PKB/Akt in response to insulin or ionizing radiation is mediated through ATM. J Biol Chem *280*, 4029-4036. 10.1074/jbc.M410344200.
134. Schneider, J.G., Finck, B.N., Ren, J., Standley, K.N., Takagi, M., Maclean, K.H., Bernal-Mizrachi, C., Muslin, A.J., Kastan, M.B., and Semenkovich, C.F. (2006). ATM-dependent suppression of stress signaling reduces vascular disease in metabolic syndrome. Cell Metab *4*, 377-389. 10.1016/j.cmet.2006.10.002.
135. Fernandes, S.A., and Demetriades, C. (2021). The Multifaceted Role of Nutrient Sensing and mTORC1 Signaling in Physiology and Aging. Front Aging *2*, 707372. 10.3389/fragi.2021.707372.
136. Gonzalez, A., and Hall, M.N. (2017). Nutrient sensing and TOR signaling in yeast and mammals. EMBO J *36*, 397-408. 10.15252/embj.201696010.
137. He, L., Cho, S., and Blenis, J. (2025). mTORC1, the maestro of cell metabolism and growth. Genes Dev *39*, 109-131. 10.1101/gad.352084.124.
138. Liu, G.Y., and Sabatini, D.M. (2020). mTOR at the nexus of nutrition, growth, ageing and disease. Nat Rev Mol Cell Biol *21*, 183-203. 10.1038/s41580-019-0199-y.

139. Garcia-Martinez, J.M., and Alessi, D.R. (2008). mTOR complex 2 (mTORC2) controls hydrophobic motif phosphorylation and activation of serum- and glucocorticoid-induced protein kinase 1 (SGK1). Biochem J *416*, 375-385. 10.1042/BJ20081668.
140. Hagiwara, A., Cornu, M., Cybulski, N., Polak, P., Betz, C., Trapani, F., Terracciano, L., Heim, M.H., Ruegg, M.A., and Hall, M.N. (2012). Hepatic mTORC2 activates glycolysis and lipogenesis through Akt, glucokinase, and SREBP1c. Cell Metab *15*, 725-738. 10.1016/j.cmet.2012.03.015.
141. Ikenoue, T., Inoki, K., Yang, Q., Zhou, X., and Guan, K.L. (2008). Essential function of TORC2 in PKC and Akt turn motif phosphorylation, maturation and signalling. EMBO J *27*, 1919-1931. 10.1038/emboj.2008.119.
142. Jacinto, E., Loewith, R., Schmidt, A., Lin, S., Ruegg, M.A., Hall, A., and Hall, M.N. (2004). Mammalian TOR complex 2 controls the actin cytoskeleton and is rapamycin insensitive. Nat Cell Biol *6*, 1122-1128. 10.1038/ncb1183.
143. Kumar, A., Lawrence, J.C., Jr., Jung, D.Y., Ko, H.J., Keller, S.R., Kim, J.K., Magnuson, M.A., and Harris, T.E. (2010). Fat cell-specific ablation of rictor in mice impairs insulin-regulated fat cell and whole-body glucose and lipid metabolism. Diabetes *59*, 1397-1406. 10.2337/db09-1061.
144. Li, X., and Gao, T. (2014). mTORC2 phosphorylates protein kinase Czeta to regulate its stability and activity. EMBO Rep *15*, 191-198. 10.1002/embr.201338119.
145. Sarbassov, D.D., Ali, S.M., Kim, D.H., Guertin, D.A., Latek, R.R., Erdjument-Bromage, H., Tempst, P., and Sabatini, D.M. (2004). Rictor, a novel binding partner of mTOR, defines a rapamycin-insensitive and raptor-independent pathway that regulates the cytoskeleton. Curr Biol *14*, 1296-1302. 10.1016/j.cub.2004.06.054.
146. Sarbassov, D.D., Guertin, D.A., Ali, S.M., and Sabatini, D.M. (2005). Phosphorylation and regulation of Akt/PKB by the rictor-mTOR complex. Science *307*, 1098-1101. 10.1126/science.1106148.
147. Inoki, K., Li, Y., Zhu, T., Wu, J., and Guan, K.L. (2002). TSC2 is phosphorylated and inhibited by Akt and suppresses mTOR signalling. Nat Cell Biol *4*, 648-657. 10.1038/ncb839.
148. Hara, K., Maruki, Y., Long, X., Yoshino, K., Oshiro, N., Hidayat, S., Tokunaga, C., Avruch, J., and Yonezawa, K. (2002). Raptor, a binding partner of target of rapamycin (TOR), mediates TOR action. Cell *110*, 177-189. 10.1016/s0092-8674(02)00833-4.
149. Kim, D.H., Sarbassov, D.D., Ali, S.M., Latek, R.R., Guntur, K.V., Erdjument-Bromage, H., Tempst, P., and Sabatini, D.M. (2003). GbetaL, a positive regulator of the rapamycin-sensitive pathway required for the nutrient-sensitive interaction between raptor and mTOR. Mol Cell *11*, 895-904. 10.1016/s1097-2765(03)00114-x.
150. Peterson, T.R., Laplante, M., Thoreen, C.C., Sancak, Y., Kang, S.A., Kuehl, W.M., Gray, N.S., and Sabatini, D.M. (2009). DEPTOR is an mTOR inhibitor frequently overexpressed in multiple myeloma cells and required for their survival. Cell *137*, 873-886. 10.1016/j.cell.2009.03.046.
151. Sancak, Y., Thoreen, C.C., Peterson, T.R., Lindquist, R.A., Kang, S.A., Spooner, E., Carr, S.A., and Sabatini, D.M. (2007). PRAS40 is an insulin-regulated inhibitor of the mTORC1 protein kinase. Mol Cell *25*, 903-915. 10.1016/j.molcel.2007.03.003.

152. Vander Haar, E., Lee, S.I., Bandhakavi, S., Griffin, T.J., and Kim, D.H. (2007). Insulin signalling to mTOR mediated by the Akt/PKB substrate PRAS40. Nat Cell Biol *9*, 316-323. 10.1038/ncb1547.
153. Nojima, H., Tokunaga, C., Eguchi, S., Oshiro, N., Hidayat, S., Yoshino, K., Hara, K., Tanaka, N., Avruch, J., and Yonezawa, K. (2003). The mammalian target of rapamycin (mTOR) partner, raptor, binds the mTOR substrates p70 S6 kinase and 4E-BP1 through their TOR signaling (TOS) motif. J Biol Chem *278*, 15461-15464. 10.1074/jbc.C200665200.
154. Saxton, R.A., and Sabatini, D.M. (2017). mTOR Signaling in Growth, Metabolism, and Disease. Cell *169*, 361-371. 10.1016/j.cell.2017.03.035.
155. Ma, X.M., and Blenis, J. (2009). Molecular mechanisms of mTOR-mediated translational control. Nat Rev Mol Cell Biol *10*, 307-318. 10.1038/nrm2672.
156. Gingras, A.C., Gygi, S.P., Raught, B., Polakiewicz, R.D., Abraham, R.T., Hoekstra, M.F., Aebersold, R., and Sonenberg, N. (1999). Regulation of 4E-BP1 phosphorylation: a novel two-step mechanism. Genes Dev *13*, 1422-1437. 10.1101/gad.13.11.1422.
157. Pause, A., Belsham, G.J., Gingras, A.C., Donze, O., Lin, T.A., Lawrence, J.C., Jr., and Sonenberg, N. (1994). Insulin-dependent stimulation of protein synthesis by phosphorylation of a regulator of 5'-cap function. Nature *371*, 762-767. 10.1038/371762a0.
158. Gingras, A.C., Raught, B., and Sonenberg, N. (2001). Regulation of translation initiation by FRAP/mTOR. Genes Dev *15*, 807-826. 10.1101/gad.887201.
159. Burnett, P.E., Barrow, R.K., Cohen, N.A., Snyder, S.H., and Sabatini, D.M. (1998). RAFT1 phosphorylation of the translational regulators p70 S6 kinase and 4E-BP1. Proc Natl Acad Sci U S A *95*, 1432-1437. 10.1073/pnas.95.4.1432.
160. Price, D.J., Grove, J.R., Calvo, V., Avruch, J., and Bierer, B.E. (1992). Rapamycin-induced inhibition of the 70-kilodalton S6 protein kinase. Science *257*, 973-977. 10.1126/science.1380182.
161. Pullen, N., Dennis, P.B., Andjelkovic, M., Dufner, A., Kozma, S.C., Hemmings, B.A., and Thomas, G. (1998). Phosphorylation and activation of p70s6k by PDK1. Science *279*, 707-710. 10.1126/science.279.5351.707.
162. Chauvin, C., Koka, V., Nouschi, A., Mieulet, V., Hoareau-Aveilla, C., Dreazen, A., Cagnard, N., Carpentier, W., Kiss, T., Meyuhas, O., and Pende, M. (2014). Ribosomal protein S6 kinase activity controls the ribosome biogenesis transcriptional program. Oncogene *33*, 474-483. 10.1038/onc.2012.606.
163. Ruvinsky, I., Sharon, N., Lerer, T., Cohen, H., Stolovich-Rain, M., Nir, T., Dor, Y., Zisman, P., and Meyuhas, O. (2005). Ribosomal protein S6 phosphorylation is a determinant of cell size and glucose homeostasis. Genes Dev *19*, 2199-2211. 10.1101/gad.351605.
164. Holz, M.K., Ballif, B.A., Gygi, S.P., and Blenis, J. (2005). mTOR and S6K1 mediate assembly of the translation preinitiation complex through dynamic protein interchange and ordered phosphorylation events. Cell *123*, 569-580. 10.1016/j.cell.2005.10.024.

165. Dorrello, N.V., Peschiaroli, A., Guardavaccaro, D., Colburn, N.H., Sherman, N.E., and Pagano, M. (2006). S6K1- and betaTRCP-mediated degradation of PDCD4 promotes protein translation and cell growth. Science *314*, 467-471. 10.1126/science.1130276.
166. Ma, X.M., Yoon, S.O., Richardson, C.J., Julich, K., and Blenis, J. (2008). SKAR links pre-mRNA splicing to mTOR/S6K1-mediated enhanced translation efficiency of spliced mRNAs. Cell *133*, 303-313. 10.1016/j.cell.2008.02.031.
167. Wang, X., Li, W., Williams, M., Terada, N., Alessi, D.R., and Proud, C.G. (2001). Regulation of elongation factor 2 kinase by p90(RSK1) and p70 S6 kinase. EMBO J *20*, 4370-4379. 10.1093/emboj/20.16.4370.
168. Hannan, K.M., Brandenburger, Y., Jenkins, A., Sharkey, K., Cavanaugh, A., Rothblum, L., Moss, T., Poortinga, G., McArthur, G.A., Pearson, R.B., and Hannan, R.D. (2003). mTOR-dependent regulation of ribosomal gene transcription requires S6K1 and is mediated by phosphorylation of the carboxy-terminal activation domain of the nucleolar transcription factor UBF. Mol Cell Biol *23*, 8862-8877. 10.1128/MCB.23.23.8862-8877.2003.
169. Mayer, C., Zhao, J., Yuan, X., and Grummt, I. (2004). mTOR-dependent activation of the transcription factor TIF-IA links rRNA synthesis to nutrient availability. Genes Dev *18*, 423-434. 10.1101/gad.285504.
170. Shor, B., Wu, J., Shakey, Q., Toral-Barza, L., Shi, C., Follettie, M., and Yu, K. (2010). Requirement of the mTOR kinase for the regulation of Maf1 phosphorylation and control of RNA polymerase III-dependent transcription in cancer cells. J Biol Chem *285*, 15380-15392. 10.1074/jbc.M109.071639.
171. Michels, A.A., Robitaille, A.M., Buczynski-Ruchonnet, D., Hodroj, W., Reina, J.H., Hall, M.N., and Hernandez, N. (2010). mTORC1 directly phosphorylates and regulates human MAF1. Mol Cell Biol *30*, 3749-3757. 10.1128/MCB.00319-10.
172. Hsieh, A.C., Liu, Y., Edlind, M.P., Ingolia, N.T., Janes, M.R., Sher, A., Shi, E.Y., Stumpf, C.R., Christensen, C., Bonham, M.J., et al. (2012). The translational landscape of mTOR signalling steers cancer initiation and metastasis. Nature *485*, 55-61. 10.1038/nature10912.
173. Thoreen, C.C., Chantranupong, L., Keys, H.R., Wang, T., Gray, N.S., and Sabatini, D.M. (2012). A unifying model for mTORC1-mediated regulation of mRNA translation. Nature *485*, 109-113. 10.1038/nature11083.
174. Settembre, C., Di Malta, C., Polito, V.A., Garcia Arencibia, M., Vetrini, F., Erdin, S., Erdin, S.U., Huynh, T., Medina, D., Colella, P., et al. (2011). TFEB links autophagy to lysosomal biogenesis. Science *332*, 1429-1433. 10.1126/science.1204592.
175. Sardiello, M., Palmieri, M., di Ronza, A., Medina, D.L., Valenza, M., Gennarino, V.A., Di Malta, C., Donaudy, F., Embrione, V., Polishchuk, R.S., et al. (2009). A gene network regulating lysosomal biogenesis and function. Science *325*, 473-477. 10.1126/science.1174447.
176. Roczniak-Ferguson, A., Petit, C.S., Froehlich, F., Qian, S., Ky, J., Angarola, B., Walther, T.C., and Ferguson, S.M. (2012). The transcription factor TFEB links mTORC1 signaling to transcriptional control of lysosome homeostasis. Sci Signal *5*, ra42. 10.1126/scisignal.2002790.

177. Martina, J.A., Diab, H.I., Lishu, L., Jeong, A.L., Patange, S., Raben, N., and Puertollano, R. (2014). The nutrient-responsive transcription factor TFE3 promotes autophagy, lysosomal biogenesis, and clearance of cellular debris. Sci Signal *7*, ra9. 10.1126/scisignal.2004754.
178. Li, K., Wada, S., Gosis, B.S., Thorsheim, C., Loose, P., and Arany, Z. (2022). Folliculin promotes substrate-selective mTORC1 activity by activating RagC to recruit TFE3. PLoS Biol *20*, e3001594. 10.1371/journal.pbio.3001594.
179. Martina, J.A., and Puertollano, R. (2018). Protein phosphatase 2A stimulates activation of TFEB and TFE3 transcription factors in response to oxidative stress. J Biol Chem *293*, 12525-12534. 10.1074/jbc.RA118.003471.
180. Medina, D.L., Fraldi, A., Bouche, V., Annunziata, F., Mansueto, G., Spampanato, C., Puri, C., Pignata, A., Martina, J.A., Sardiello, M., et al. (2011). Transcriptional activation of lysosomal exocytosis promotes cellular clearance. Dev Cell *21*, 421-430. 10.1016/j.devcel.2011.07.016.
181. Settembre, C., Zoncu, R., Medina, D.L., Vetrini, F., Erdin, S., Erdin, S., Huynh, T., Ferron, M., Karsenty, G., Vellard, M.C., et al. (2012). A lysosome-to-nucleus signalling mechanism senses and regulates the lysosome via mTOR and TFEB. EMBO J *31*, 1095-1108. 10.1038/emboj.2012.32.
182. Zhang, X., Cheng, X., Yu, L., Yang, J., Calvo, R., Patnaik, S., Hu, X., Gao, Q., Yang, M., Lawas, M., et al. (2016). MCOLN1 is a ROS sensor in lysosomes that regulates autophagy. Nat Commun *7*, 12109. 10.1038/ncomms12109.
183. Napolitano, G., Esposito, A., Choi, H., Matarese, M., Benedetti, V., Di Malta, C., Monfregola, J., Medina, D.L., Lippincott-Schwartz, J., and Ballabio, A. (2018). mTOR-dependent phosphorylation controls TFEB nuclear export. Nat Commun *9*, 3312. 10.1038/s41467-018-05862-6.
184. Palmieri, M., Impey, S., Kang, H., di Ronza, A., Pelz, C., Sardiello, M., and Ballabio, A. (2011). Characterization of the CLEAR network reveals an integrated control of cellular clearance pathways. Hum Mol Genet *20*, 3852-3866. 10.1093/hmg/ddr306.
185. Kim, J., Kundu, M., Viollet, B., and Guan, K.L. (2011). AMPK and mTOR regulate autophagy through direct phosphorylation of Ulk1. Nat Cell Biol *13*, 132-141. 10.1038/ncb2152.
186. Ganley, I.G., Lam du, H., Wang, J., Ding, X., Chen, S., and Jiang, X. (2009). ULK1.ATG13.FIP200 complex mediates mTOR signaling and is essential for autophagy. J Biol Chem *284*, 12297-12305. 10.1074/jbc.M900573200.
187. Hosokawa, N., Hara, T., Kaizuka, T., Kishi, C., Takamura, A., Miura, Y., Iemura, S., Natsume, T., Takehana, K., Yamada, N., et al. (2009). Nutrient-dependent mTORC1 association with the ULK1-Atg13-FIP200 complex required for autophagy. Mol Biol Cell *20*, 1981-1991. 10.1091/mbc.e08-12-1248.
188. Nazio, F., Strappazzon, F., Antonioli, M., Bielli, P., Cianfanelli, V., Bordi, M., Gretzmeier, C., Dengjel, J., Piacentini, M., Fimia, G.M., and Cecconi, F. (2013). mTOR inhibits autophagy by controlling ULK1 ubiquitylation, self-association and function through AMBRA1 and TRAF6. Nat Cell Biol *15*, 406-416. 10.1038/ncb2708.

189. Yuan, H.X., Russell, R.C., and Guan, K.L. (2013). Regulation of PIK3C3/VPS34 complexes by MTOR in nutrient stress-induced autophagy. Autophagy *9*, 1983-1995. 10.4161/auto.26058.
190. Kim, Y.M., Jung, C.H., Seo, M., Kim, E.K., Park, J.M., Bae, S.S., and Kim, D.H. (2015). mTORC1 phosphorylates UVRAG to negatively regulate autophagosome and endosome maturation. Mol Cell *57*, 207-218. 10.1016/j.molcel.2014.11.013.
191. Deng, L., Chen, L., Zhao, L., Xu, Y., Peng, X., Wang, X., Ding, L., Jin, J., Teng, H., Wang, Y., et al. (2019). Ubiquitination of Rheb governs growth factor-induced mTORC1 activation. Cell Res *29*, 136-150. 10.1038/s41422-018-0120-9.
192. Kim, S.T., Lim, D.S., Canman, C.E., and Kastan, M.B. (1999). Substrate specificities and identification of putative substrates of ATM kinase family members. J Biol Chem *274*, 37538-37543. 10.1074/jbc.274.53.37538.
193. Yao, Y., Hong, S., Ikeda, T., Mori, H., MacDougald, O.A., Nada, S., Okada, M., and Inoki, K. (2020). Amino Acids Enhance Polyubiquitination of Rheb and Its Binding to mTORC1 by Blocking Lysosomal ATXN3 Deubiquitinase Activity. Mol Cell *80*, 437-451 e436. 10.1016/j.molcel.2020.10.004.
194. Zheng, M., Wang, Y.H., Wu, X.N., Wu, S.Q., Lu, B.J., Dong, M.Q., Zhang, H., Sun, P., Lin, S.C., Guan, K.L., and Han, J. (2011). Inactivation of Rheb by PRAK-mediated phosphorylation is essential for energy-depletion-induced suppression of mTORC1. Nat Cell Biol *13*, 263-272. 10.1038/ncb2168.
195. Inoki, K., Li, Y., Xu, T., and Guan, K.L. (2003). Rheb GTPase is a direct target of TSC2 GAP activity and regulates mTOR signaling. Genes Dev *17*, 1829-1834. 10.1101/gad.1110003.
196. Long, X., Lin, Y., Ortiz-Vega, S., Yonezawa, K., and Avruch, J. (2005). Rheb binds and regulates the mTOR kinase. Curr Biol *15*, 702-713. 10.1016/j.cub.2005.02.053.
197. Manning, B.D., Tee, A.R., Logsdon, M.N., Blenis, J., and Cantley, L.C. (2002). Identification of the tuberous sclerosis complex-2 tumor suppressor gene product tuberin as a target of the phosphoinositide 3-kinase/akt pathway. Mol Cell *10*, 151-162. 10.1016/s1097-2765(02)00568-3.
198. Ma, L., Chen, Z., Erdjument-Bromage, H., Tempst, P., and Pandolfi, P.P. (2005). Phosphorylation and functional inactivation of TSC2 by Erk implications for tuberous sclerosis and cancer pathogenesis. Cell *121*, 179-193. 10.1016/j.cell.2005.02.031.
199. Roux, P.P., Ballif, B.A., Anjum, R., Gygi, S.P., and Blenis, J. (2004). Tumor-promoting phorbol esters and activated Ras inactivate the tuberous sclerosis tumor suppressor complex via p90 ribosomal S6 kinase. Proc Natl Acad Sci U S A *101*, 13489-13494. 10.1073/pnas.0405659101.
200. Ma, L., Teruya-Feldstein, J., Bonner, P., Bernardi, R., Franz, D.N., Witte, D., Cordon-Cardo, C., and Pandolfi, P.P. (2007). Identification of S664 TSC2 phosphorylation as a marker for extracellular signal-regulated kinase mediated mTOR activation in tuberous sclerosis and human cancer. Cancer Res *67*, 7106-7112. 10.1158/0008-5472.CAN-06-4798.
201. Corradetti, M.N., Inoki, K., Bardeesy, N., DePinho, R.A., and Guan, K.L. (2004). Regulation of the TSC pathway by LKB1: evidence of a molecular link between

tuberous sclerosis complex and Peutz-Jeghers syndrome. Genes Dev *18*, 1533-1538. 10.1101/gad.1199104.

202. Inoki, K., Zhu, T., and Guan, K.L. (2003). TSC2 mediates cellular energy response to control cell growth and survival. Cell *115*, 577-590. 10.1016/s0092-8674(03)00929-2.
203. Shaw, R.J., Kosmatka, M., Bardeesy, N., Hurley, R.L., Witters, L.A., DePinho, R.A., and Cantley, L.C. (2004). The tumor suppressor LKB1 kinase directly activates AMP-activated kinase and regulates apoptosis in response to energy stress. Proc Natl Acad Sci U S A *101*, 3329-3335. 10.1073/pnas.0308061100.
204. Gwinn, D.M., Shackelford, D.B., Egan, D.F., Mihaylova, M.M., Mery, A., Vasquez, D.S., Turk, B.E., and Shaw, R.J. (2008). AMPK phosphorylation of raptor mediates a metabolic checkpoint. Mol Cell *30*, 214-226. 10.1016/j.molcel.2008.03.003.
205. Brugarolas, J., Lei, K., Hurley, R.L., Manning, B.D., Reiling, J.H., Hafen, E., Witters, L.A., Ellisen, L.W., and Kaelin, W.G., Jr. (2004). Regulation of mTOR function in response to hypoxia by REDD1 and the TSC1/TSC2 tumor suppressor complex. Genes Dev *18*, 2893-2904. 10.1101/gad.1256804.
206. Demetriades, C., Doumpas, N., and Teleman, A.A. (2014). Regulation of TORC1 in response to amino acid starvation via lysosomal recruitment of TSC2. Cell *156*, 786-799. 10.1016/j.cell.2014.01.024.
207. Menon, S., Dibble, C.C., Talbott, G., Hoxhaj, G., Valvezan, A.J., Takahashi, H., Cantley, L.C., and Manning, B.D. (2014). Spatial control of the TSC complex integrates insulin and nutrient regulation of mTORC1 at the lysosome. Cell *156*, 771-785. 10.1016/j.cell.2013.11.049.
208. Hanker, A.B., Mitin, N., Wilder, R.S., Henske, E.P., Tamanoi, F., Cox, A.D., and Der, C.J. (2010). Differential requirement of CAAX-mediated posttranslational processing for Rheb localization and signaling. Oncogene *29*, 380-391. 10.1038/onc.2009.336.
209. Angarola, B., and Ferguson, S.M. (2019). Weak membrane interactions allow Rheb to activate mTORC1 signaling without major lysosome enrichment. Mol Biol Cell *30*, 2750-2760. 10.1091/mbc.E19-03-0146.
210. Buerger, C., DeVries, B., and Stambolic, V. (2006). Localization of Rheb to the endomembrane is critical for its signaling function. Biochem Biophys Res Commun *344*, 869-880. 10.1016/j.bbrc.2006.03.220.
211. Zhang, F., Xiong, X., Li, Z., Wang, H., Wang, W., Zhao, Y., and Sun, Y. (2025). RHEB neddylation by the UBE2F-SAG axis enhances mTORC1 activity and aggravates liver tumorigenesis. EMBO J *44*, 1185-1219. 10.1038/s44318-024-00353-5.
212. Kim, E., Goraksha-Hicks, P., Li, L., Neufeld, T.P., and Guan, K.L. (2008). Regulation of TORC1 by Rag GTPases in nutrient response. Nat Cell Biol *10*, 935-945. 10.1038/ncb1753.
213. Sancak, Y., Peterson, T.R., Shaul, Y.D., Lindquist, R.A., Thoreen, C.C., Bar-Peled, L., and Sabatini, D.M. (2008). The Rag GTPases bind raptor and mediate amino acid signaling to mTORC1. Science *320*, 1496-1501. 10.1126/science.1157535.
214. Bar-Peled, L., Schweitzer, L.D., Zoncu, R., and Sabatini, D.M. (2012). Ragulator is a GEF for the rag GTPases that signal amino acid levels to mTORC1. Cell *150*, 1196-1208. 10.1016/j.cell.2012.07.032.

215. Bar-Peled, L., Chantranupong, L., Cherniack, A.D., Chen, W.W., Ottina, K.A., Grabiner, B.C., Spear, E.D., Carter, S.L., Meyerson, M., and Sabatini, D.M. (2013). A Tumor suppressor complex with GAP activity for the Rag GTPases that signal amino acid sufficiency to mTORC1. Science *340*, 1100-1106. 10.1126/science.1232044.
216. Wolfson, R.L., Chantranupong, L., Wyant, G.A., Gu, X., Orozco, J.M., Shen, K., Condon, K.J., Petri, S., Kedir, J., Scaria, S.M., et al. (2017). KICSTOR recruits GATOR1 to the lysosome and is necessary for nutrients to regulate mTORC1. Nature *543*, 438-442. 10.1038/nature21423.
217. Tsun, Z.Y., Bar-Peled, L., Chantranupong, L., Zoncu, R., Wang, T., Kim, C., Spooner, E., and Sabatini, D.M. (2013). The folliculin tumor suppressor is a GAP for the RagC/D GTPases that signal amino acid levels to mTORC1. Mol Cell *52*, 495-505. 10.1016/j.molcel.2013.09.016.
218. Zoncu, R., Bar-Peled, L., Efeyan, A., Wang, S., Sancak, Y., and Sabatini, D.M. (2011). mTORC1 senses lysosomal amino acids through an inside-out mechanism that requires the vacuolar H(+)-ATPase. Science *334*, 678-683. 10.1126/science.1207056.
219. Rebsamen, M., Pochini, L., Stasyk, T., de Araujo, M.E., Galluccio, M., Kandasamy, R.K., Snijder, B., Fauster, A., Rudashevskaya, E.L., Bruckner, M., et al. (2015). SLC38A9 is a component of the lysosomal amino acid sensing machinery that controls mTORC1. Nature *519*, 477-481. 10.1038/nature14107.
220. Wang, S., Tsun, Z.Y., Wolfson, R.L., Shen, K., Wyant, G.A., Plovanich, M.E., Yuan, E.D., Jones, T.D., Chantranupong, L., Comb, W., et al. (2015). Metabolism. Lysosomal amino acid transporter SLC38A9 signals arginine sufficiency to mTORC1. Science *347*, 188-194. 10.1126/science.1257132.
221. Abu-Remaileh, M., Wyant, G.A., Kim, C., Laqtom, N.N., Abbasi, M., Chan, S.H., Freinkman, E., and Sabatini, D.M. (2017). Lysosomal metabolomics reveals V-ATPase- and mTOR-dependent regulation of amino acid efflux from lysosomes. Science *358*, 807-813. 10.1126/science.aan6298.
222. Castellano, B.M., Thelen, A.M., Moldavski, O., Feltes, M., van der Welle, R.E., Mydock-McGrane, L., Jiang, X., van Eijkeren, R.J., Davis, O.B., Louie, S.M., et al. (2017). Lysosomal cholesterol activates mTORC1 via an SLC38A9-Niemann-Pick C1 signaling complex. Science *355*, 1306-1311. 10.1126/science.aag1417.
223. Pu, J., Schindler, C., Jia, R., Jarnik, M., Backlund, P., and Bonifacino, J.S. (2015). BORC, a multisubunit complex that regulates lysosome positioning. Dev Cell *33*, 176-188. 10.1016/j.devcel.2015.02.011.
224. Korolchuk, V.I., Saiki, S., Lichtenberg, M., Siddiqi, F.H., Roberts, E.A., Imarisio, S., Jahreiss, L., Sarkar, S., Futter, M., Menzies, F.M., et al. (2011). Lysosomal positioning coordinates cellular nutrient responses. Nat Cell Biol *13*, 453-460. 10.1038/ncb2204.
225. Wolfson, R.L., Chantranupong, L., Saxton, R.A., Shen, K., Scaria, S.M., Cantor, J.R., and Sabatini, D.M. (2016). Sestrin2 is a leucine sensor for the mTORC1 pathway. Science *351*, 43-48. 10.1126/science.aab2674.
226. Chantranupong, L., Scaria, S.M., Saxton, R.A., Gygi, M.P., Shen, K., Wyant, G.A., Wang, T., Harper, J.W., Gygi, S.P., and Sabatini, D.M. (2016). The CASTOR Proteins Are Arginine Sensors for the mTORC1 Pathway. Cell *165*, 153-164. 10.1016/j.cell.2016.02.035.

227. Gu, X., Orozco, J.M., Saxton, R.A., Condon, K.J., Liu, G.Y., Krawczyk, P.A., Scaria, S.M., Harper, J.W., Gygi, S.P., and Sabatini, D.M. (2017). SAMTOR is an S-adenosylmethionine sensor for the mTORC1 pathway. Science *358*, 813-818. 10.1126/science.aao3265.
228. Han, J.M., Jeong, S.J., Park, M.C., Kim, G., Kwon, N.H., Kim, H.K., Ha, S.H., Ryu, S.H., and Kim, S. (2012). Leucyl-tRNA synthetase is an intracellular leucine sensor for the mTORC1-signaling pathway. Cell *149*, 410-424. 10.1016/j.cell.2012.02.044.
229. Jewell, J.L., Kim, Y.C., Russell, R.C., Yu, F.X., Park, H.W., Plouffe, S.W., Tagliabracci, V.S., and Guan, K.L. (2015). Metabolism. Differential regulation of mTORC1 by leucine and glutamine. Science *347*, 194-198. 10.1126/science.1259472.
230. Efeyan, A., Zoncu, R., Chang, S., Gumper, I., Snitkin, H., Wolfson, R.L., Kirak, O., Sabatini, D.D., and Sabatini, D.M. (2013). Regulation of mTORC1 by the Rag GTPases is necessary for neonatal autophagy and survival. Nature *493*, 679-683. 10.1038/nature11745.
231. Li, M., Zhang, C.S., Feng, J.W., Wei, X., Zhang, C., Xie, C., Wu, Y., Hawley, S.A., Atrih, A., Lamont, D.J., et al. (2021). Aldolase is a sensor for both low and high glucose, linking to AMPK and mTORC1. Cell Res *31*, 478-481. 10.1038/s41422-020-00456-8.
232. Orozco, J.M., Krawczyk, P.A., Scaria, S.M., Cangelosi, A.L., Chan, S.H., Kunchok, T., Lewis, C.A., and Sabatini, D.M. (2020). Dihydroxyacetone phosphate signals glucose availability to mTORC1. Nat Metab *2*, 893-901. 10.1038/s42255-020-0250-5.
233. Zhang, C.S., Jiang, B., Li, M., Zhu, M., Peng, Y., Zhang, Y.L., Wu, Y.Q., Li, T.Y., Liang, Y., Lu, Z., et al. (2014). The lysosomal v-ATPase-Ragulator complex is a common activator for AMPK and mTORC1, acting as a switch between catabolism and anabolism. Cell Metab *20*, 526-540. 10.1016/j.cmet.2014.06.014.
234. Martina, J.A., and Puertollano, R. (2013). Rag GTPases mediate amino acid-dependent recruitment of TFEB and MITF to lysosomes. J Cell Biol *200*, 475-491. 10.1083/jcb.201209135.
235. Nüchel, J., Tauber, M., Nolte, J.L., Mörgelin, M., Türk, C., Eckes, B., Demetriades, C., and Plomann, M. (2021). An mTORC1-GRASP55 signaling axis controls unconventional secretion to reshape the extracellular proteome upon stress. Mol Cell *81*, 3275-3293.e3212. 10.1016/j.molcel.2021.06.017.
236. Fernandes, S.A., Angelidaki, D.D., Nuchel, J., Pan, J., Gollwitzer, P., Elkis, Y., Artoni, F., Wilhelm, S., Kovacevic-Sarmiento, M., and Demetriades, C. (2024). Spatial and functional separation of mTORC1 signalling in response to different amino acid sources. Nat Cell Biol *26*, 1918-1933. 10.1038/s41556-024-01523-7.
237. Zhong, Y., Zhou, X., Guan, K.L., and Zhang, J. (2022). Rheb regulates nuclear mTORC1 activity independent of farnesylation. Cell Chem Biol *29*, 1037-1045 e1034. 10.1016/j.chembiol.2022.02.006.
238. Zhou, X., Clister, T.L., Lowry, P.R., Seldin, M.M., Wong, G.W., and Zhang, J. (2015). Dynamic Visualization of mTORC1 Activity in Living Cells. Cell Rep *10*, 1767-1777. 10.1016/j.celrep.2015.02.031.
239. Zhou, X., Zhong, Y., Molinar-Inglis, O., Kunkel, M.T., Chen, M., Sun, T., Zhang, J., Shyy, J.Y., Trejo, J., Newton, A.C., and Zhang, J. (2020). Location-specific inhibition of Akt

reveals regulation of mTORC1 activity in the nucleus. Nat Commun *11*, 6088. 10.1038/s41467-020-19937-w.

240. Tangudu, N.K., Grumet, A.N., Fang, R., Buj, R., Cole, A.R., Uboveja, A., Amalric, A., Yang, B., Huang, Z., Happe, C., et al. (2025). ATR promotes mTORC1 activity via de novo cholesterol synthesis. EMBO Rep *26*, 3574-3593. 10.1038/s44319-025-00451-3.
241. Jang, S.K., Hong, S.E., Lee, D.H., Kim, J.Y., Kim, J.Y., Ye, S.K., Hong, J., Park, I.C., and Jin, H.O. (2021). Inhibition of mTORC1 through ATF4-induced REDD1 and Sestrin2 expression by Metformin. BMC Cancer *21*, 803. 10.1186/s12885-021-08346-x.
242. Katiyar, S., Liu, E., Knutzen, C.A., Lang, E.S., Lombardo, C.R., Sankar, S., Toth, J.I., Petroski, M.D., Ronai, Z., and Chiang, G.G. (2009). REDD1, an inhibitor of mTOR signalling, is regulated by the CUL4A-DDB1 ubiquitin ligase. EMBO Rep *10*, 866-872. 10.1038/embor.2009.93.
243. Kim, J.S., Ro, S.H., Kim, M., Park, H.W., Semple, I.A., Park, H., Cho, U.S., Wang, W., Guan, K.L., Karin, M., and Lee, J.H. (2015). Sestrin2 inhibits mTORC1 through modulation of GATOR complexes. Sci Rep *5*, 9502. 10.1038/srep09502.
244. Parmigiani, A., Nourbakhsh, A., Ding, B., Wang, W., Kim, Y.C., Akopiants, K., Guan, K.L., Karin, M., and Budanov, A.V. (2014). Sestrins inhibit mTORC1 kinase activation through the GATOR complex. Cell Rep *9*, 1281-1291. 10.1016/j.celrep.2014.10.019.
245. Xu, D., Dai, W., Kutzler, L., Lacko, H.A., Jefferson, L.S., Dennis, M.D., and Kimball, S.R. (2020). ATF4-Mediated Upregulation of REDD1 and Sestrin2 Suppresses mTORC1 Activity during Prolonged Leucine Deprivation. J Nutr *150*, 1022-1030. 10.1093/jn/nxz309.
246. Budanov, A.V., and Karin, M. (2008). p53 target genes sestrin1 and sestrin2 connect genotoxic stress and mTOR signaling. Cell *134*, 451-460. 10.1016/j.cell.2008.06.028.
247. Corradetti, M.N., Inoki, K., and Guan, K.L. (2005). The stress-inducted proteins RTP801 and RTP801L are negative regulators of the mammalian target of rapamycin pathway. J Biol Chem *280*, 9769-9772. 10.1074/jbc.C400557200.
248. Feng, Z., Hu, W., de Stanchina, E., Teresky, A.K., Jin, S., Lowe, S., and Levine, A.J. (2007). The regulation of AMPK beta1, TSC2, and PTEN expression by p53: stress, cell and tissue specificity, and the role of these gene products in modulating the IGF-1-AKT-mTOR pathways. Cancer Res *67*, 3043-3053. 10.1158/0008-5472.CAN-06-4149.
249. Tu, Y., Ji, C., Yang, B., Yang, Z., Gu, H., Lu, C.C., Wang, R., Su, Z.L., Chen, B., Sun, W.L., et al. (2013). DNA-dependent protein kinase catalytic subunit (DNA-PKcs)-SIN1 association mediates ultraviolet B (UVB)-induced Akt Ser-473 phosphorylation and skin cell survival. Mol Cancer *12*, 172. 10.1186/1476-4598-12-172.
250. Liu, L., Dai, X., Yin, S., Liu, P., Hill, E.G., Wei, W., and Gan, W. (2022). DNA-PK promotes activation of the survival kinase AKT in response to DNA damage through an mTORC2-ECT2 pathway. Sci Signal *15*, eabh2290. 10.1126/scisignal.abh2290.
251. Xie, X., Hu, H., Tong, X., Li, L., Liu, X., Chen, M., Yuan, H., Xie, X., Li, Q., Zhang, Y., et al. (2018). The mTOR-S6K pathway links growth signalling to DNA damage response by targeting RNF168. Nat Cell Biol *20*, 320-331. 10.1038/s41556-017-0033-8.
252. Amar-Schwartz, A., Ben Hur, V., Jbara, A., Cohen, Y., Barnabas, G.D., Arbib, E., Siegfried, Z., Mashahreh, B., Hassouna, F., Shilo, A., et al. (2022). S6K1

phosphorylates Cdk1 and MSH6 to regulate DNA repair. Elife *11*. 10.7554/eLife.79128.

253. Koppenhafer, S.L., Goss, K.L., Terry, W.W., and Gordon, D.J. (2018). mTORC1/2 and Protein Translation Regulate Levels of CHK1 and the Sensitivity to CHK1 Inhibitors in Ewing Sarcoma Cells. Mol Cancer Ther *17*, 2676-2688. 10.1158/1535-7163.MCT-18-0260.
254. Yu, Z.J., Luo, H.H., Shang, Z.F., Guan, H., Xiao, B.B., Liu, X.D., Wang, Y., Huang, B., and Zhou, P.K. (2017). Stabilization of 4E-BP1 by PI3K kinase and its involvement in CHK2 phosphorylation in the cellular response to radiation. Int J Med Sci *14*, 452-461. 10.7150/ijms.18329.
255. Brady, O.A., Jeong, E., Martina, J.A., Pirooznia, M., Tunc, I., and Puertollano, R. (2018). The transcription factors TFE3 and TFEB amplify p53 dependent transcriptional programs in response to DNA damage. Elife *7*. 10.7554/eLife.40856.
256. Slade, L., Biswas, D., Ihionu, F., El Hiani, Y., Kienesberger, P.C., and Pulinilkunnil, T. (2020). A lysosome independent role for TFEB in activating DNA repair and inhibiting apoptosis in breast cancer cells. Biochem J *477*, 137-160. 10.1042/BCJ20190596.
257. Saucedo, L.J., Gao, X., Chiarelli, D.A., Li, L., Pan, D., and Edgar, B.A. (2003). Rheb promotes cell growth as a component of the insulin/TOR signalling network. Nat Cell Biol *5*, 566-571. 10.1038/ncb996.
258. Stocker, H., Radimerski, T., Schindelholz, B., Wittwer, F., Belawat, P., Daram, P., Breuer, S., Thomas, G., and Hafen, E. (2003). Rheb is an essential regulator of S6K in controlling cell growth in Drosophila. Nat Cell Biol *5*, 559-565. 10.1038/ncb995.
259. Zhang, Y., Gao, X., Saucedo, L.J., Ru, B., Edgar, B.A., and Pan, D. (2003). Rheb is a direct target of the tuberous sclerosis tumour suppressor proteins. Nat Cell Biol *5*, 578-581. 10.1038/ncb999.
260. Hornbeck, P.V., Zhang, B., Murray, B., Kornhauser, J.M., Latham, V., and Skrzypek, E. (2015). PhosphoSitePlus, 2014: mutations, PTMs and recalibrations. Nucleic Acids Res *43*, D512-520. 10.1093/nar/gku1267.
261. Hande, K.R. (1998). Etoposide: four decades of development of a topoisomerase II inhibitor. Eur J Cancer *34*, 1514-1521. 10.1016/s0959-8049(98)00228-7.
262. Gewirtz, D.A. (1999). A critical evaluation of the mechanisms of action proposed for the antitumor effects of the anthracycline antibiotics adriamycin and daunorubicin. Biochem Pharmacol *57*, 727-741. 10.1016/s0006-2952(98)00307-4.
263. Elford, H.L. (1968). Effect of hydroxyurea on ribonucleotide reductase. Biochem Biophys Res Commun *33*, 129-135. 10.1016/0006-291x(68)90266-0.
264. Young, C.W., and Hodas, S. (1964). HYDROXYUREA: INHIBITORY EFFECT ON DNA METABOLISM. Science *146*, 1172-1174. 10.1126/science.146.3648.1172.
265. Acharya, A., and Demetriades, C. (2024). mTORC1 activity licenses its own release from the lysosomal surface. Mol Cell *84*, 4385-4400 e4387. 10.1016/j.molcel.2024.10.008.
266. Alesi, N., Akl, E.W., Khabibullin, D., Liu, H.J., Nidhiry, A.S., Garner, E.R., Filippakis, H., Lam, H.C., Shi, W., Viswanathan, S.R., et al. (2021). TSC2 regulates lysosome biogenesis via a non-canonical RAGC and TFEB-dependent mechanism. Nat Commun *12*, 4245. 10.1038/s41467-021-24499-6.

267. Alesi, N., Khabibullin, D., Rosenthal, D.M., Akl, E.W., Cory, P.M., Alchoueiry, M., Salem, S., Daou, M., Gibbons, W.F., Chen, J.A., et al. (2024). TFEB drives mTORC1 hyperactivation and kidney disease in Tuberous Sclerosis Complex. Nat Commun *15*, 406. 10.1038/s41467-023-44229-4.
268. Gollwitzer, P., Grutzmacher, N., Wilhelm, S., Kummel, D., and Demetriades, C. (2022). A Rag GTPase dimer code defines the regulation of mTORC1 by amino acids. Nat Cell Biol *24*, 1394-1406. 10.1038/s41556-022-00976-y.
269. Nüchel, J., Omidi, M., Fernandes, S.A., Tauber, M., Pohl, S., Plomann, M., and Demetriades, C. (2024). GRASP55 Safeguards Proper Lysosome Function by Controlling Sorting of Lysosomal Enzymes at the Golgi. bioRxiv, 2024.2012.2010.627846. 10.1101/2024.12.10.627846.
270. Asrani, K., Woo, J., Mendes, A.A., Schaffer, E., Vidotto, T., Villanueva, C.R., Feng, K., Oliveira, L., Murali, S., Liu, H.B., et al. (2022). An mTORC1-mediated negative feedback loop constrains amino acid-induced FLCN-Rag activation in renal cells with TSC2 loss. Nat Commun *13*, 6808. 10.1038/s41467-022-34617-7.
271. Napolitano, G., Di Malta, C., Esposito, A., de Araujo, M.E.G., Pece, S., Bertalot, G., Matarese, M., Benedetti, V., Zampelli, A., Stasyk, T., et al. (2020). A substrate-specific mTORC1 pathway underlies Birt-Hogg-Dube syndrome. Nature *585*, 597-602. 10.1038/s41586-020-2444-0.
272. Puertollano, R., Ferguson, S.M., Brugarolas, J., and Ballabio, A. (2018). The complex relationship between TFEB transcription factor phosphorylation and subcellular localization. EMBO J *37*. 10.15252/embj.201798804.
273. Linding, R., Jensen, L.J., Ostheimer, G.J., van Vugt, M.A., Jorgensen, C., Miron, I.M., Diella, F., Colwill, K., Taylor, L., Elder, K., et al. (2007). Systematic discovery of in vivo phosphorylation networks. Cell *129*, 1415-1426. 10.1016/j.cell.2007.05.052.
274. Linding, R., Jensen, L.J., Pasculescu, A., Olhovsky, M., Colwill, K., Bork, P., Yaffe, M.B., and Pawson, T. (2008). NetworKIN: a resource for exploring cellular phosphorylation networks. Nucleic Acids Res *36*, D695-699. 10.1093/nar/gkm902.
275. Pisonero-Vaquero, S., Soldati, C., Cesana, M., Ballabio, A., and Medina, D.L. (2020). TFEB Modulates p21/WAF1/CIP1 during the DNA Damage Response. Cells *9*. 10.3390/cells9051186.
276. Slade, L., Biswas, D., Kienesberger, P.C., and Pulinilkunnil, T. (2022). Loss of transcription factor EB dysregulates the G1/S transition and DNA replication in mammary epithelial cells. J Biol Chem *298*, 102692. 10.1016/j.jbc.2022.102692.
277. Lawrence, R.E., Fromm, S.A., Fu, Y., Yokom, A.L., Kim, D.J., Thelen, A.M., Young, L.N., Lim, C.Y., Samelson, A.J., Hurley, J.H., and Zoncu, R. (2019). Structural mechanism of a Rag GTPase activation checkpoint by the lysosomal folliculin complex. Science *366*, 971-977. 10.1126/science.aax0364.
278. Li, J., Wada, S., Weaver, L.K., Biswas, C., Behrens, E.M., and Arany, Z. (2019). Myeloid Folliculin balances mTOR activation to maintain innate immunity homeostasis. JCI Insight *5*. 10.1172/jci.insight.126939.
279. Wada, S., Neinast, M., Jang, C., Ibrahim, Y.H., Lee, G., Babu, A., Li, J., Hoshino, A., Rowe, G.C., Rhee, J., et al. (2016). The tumor suppressor FLCN mediates an alternate

mTOR pathway to regulate browning of adipose tissue. Genes Dev *30*, 2551-2564. 10.1101/gad.287953.116.

280. Paglin, S., Lee, N.Y., Nakar, C., Fitzgerald, M., Plotkin, J., Deuel, B., Hackett, N., McMahill, M., Sphicas, E., Lampen, N., and Yahalom, J. (2005). Rapamycin-sensitive pathway regulates mitochondrial membrane potential, autophagy, and survival in irradiated MCF-7 cells. Cancer Res *65*, 11061-11070. 10.1158/0008-5472.CAN-05-1083.
281. Lai, K.P., Leong, W.F., Chau, J.F., Jia, D., Zeng, L., Liu, H., He, L., Hao, A., Zhang, H., Meek, D., et al. (2010). S6K1 is a multifaceted regulator of Mdm2 that connects nutrient status and DNA damage response. EMBO J *29*, 2994-3006. 10.1038/emboj.2010.166.
282. Braun, F., Mandel, A.M., Blomberg, L., Wong, M.N., Chatzinikolaou, G., Meyer, D.H., Reinelt, A., Nair, V., Akbar-Haase, R., McCown, P.J., et al. (2025). Loss of genome maintenance is linked to mTOR complex 1 signaling and accelerates podocyte damage. JCI Insight *10*. 10.1172/jci.insight.172370.
283. Gomes, L.R., Menck, C.F.M., and Leandro, G.S. (2017). Autophagy Roles in the Modulation of DNA Repair Pathways. Int J Mol Sci *18*. 10.3390/ijms18112351.
284. Kim, J., Lee, S., Kim, H., Lee, H., Seong, K.M., Youn, H., and Youn, B. (2021). Autophagic Organelles in DNA Damage Response. Front Cell Dev Biol *9*, 668735. 10.3389/fcell.2021.668735.
285. Lascaux, P., Hoslett, G., Tribble, S., Trugenberger, C., Anticevic, I., Otten, C., Torrecilla, I., Koukouravas, S., Zhao, Y., Yang, H., et al. (2024). TEX264 drives selective autophagy of DNA lesions to promote DNA repair and cell survival. Cell *187*, 5698-5718 e5626. 10.1016/j.cell.2024.08.020.
286. Liu, E.Y., Xu, N., O'Prey, J., Lao, L.Y., Joshi, S., Long, J.S., O'Prey, M., Croft, D.R., Beaumatin, F., Baudot, A.D., et al. (2015). Loss of autophagy causes a synthetic lethal deficiency in DNA repair. Proc Natl Acad Sci U S A *112*, 773-778. 10.1073/pnas.1409563112.
287. Wang, Y., Zhang, N., Zhang, L., Li, R., Fu, W., Ma, K., Li, X., Wang, L., Wang, J., Zhang, H., et al. (2016). Autophagy Regulates Chromatin Ubiquitination in DNA Damage Response through Elimination of SQSTM1/p62. Mol Cell *63*, 34-48. 10.1016/j.molcel.2016.05.027.
288. Zhang, Z., Yue, P., Lu, T., Wang, Y., Wei, Y., and Wei, X. (2021). Role of lysosomes in physiological activities, diseases, and therapy. J Hematol Oncol *14*, 79. 10.1186/s13045-021-01087-1.
289. Settembre, C., De Cegli, R., Mansueto, G., Saha, P.K., Vetrini, F., Visvikis, O., Huynh, T., Carissimo, A., Palmer, D., Klisch, T.J., et al. (2013). TFEB controls cellular lipid metabolism through a starvation-induced autoregulatory loop. Nat Cell Biol *15*, 647-658. 10.1038/ncb2718.
290. Nicastro, R., Brohee, L., Alba, J., Nuchel, J., Figlia, G., Kipschull, S., Gollwitzer, P., Romero-Pozuelo, J., Fernandes, S.A., Lamprakis, A., et al. (2023). Malonyl-CoA is a conserved endogenous ATP-competitive mTORC1 inhibitor. Nat Cell Biol *25*, 1303-1318. 10.1038/s41556-023-01198-6.

291. Ran, F.A., Hsu, P.D., Wright, J., Agarwala, V., Scott, D.A., and Zhang, F. (2013). Genome engineering using the CRISPR-Cas9 system. Nat Protoc *8*, 2281-2308. 10.1038/nprot.2013.143.
292. Kowarz, E., Löscher, D., and Marschalek, R. (2015). Optimized Sleeping Beauty transposons rapidly generate stable transgenic cell lines. Biotechnol J *10*, 647-653. 10.1002/biot.201400821.
293. Plescher, M., Teleman, A.A., and Demetriades, C. (2015). TSC2 mediates hyperosmotic stress-induced inactivation of mTORC1. Sci Rep *5*, 13828. 10.1038/srep13828.
294. Canman, C.E., Lim, D.S., Cimprich, K.A., Taya, Y., Tamai, K., Sakaguchi, K., Appella, E., Kastan, M.B., and Siliciano, J.D. (1998). Activation of the ATM kinase by ionizing radiation and phosphorylation of p53. Science *281*, 1677-1679. 10.1126/science.281.5383.1677.
295. Schindelin, J., Arganda-Carreras, I., Frise, E., Kaynig, V., Longair, M., Pietzsch, T., Preibisch, S., Rueden, C., Saalfeld, S., Schmid, B., et al. (2012). Fiji: an open-source platform for biological-image analysis. Nat Methods *9*, 676-682. 10.1038/nmeth.2019.

Appendix I. Contributions

Beyond my main PhD project presented in this thesis, I contributed to several other research projects led by colleagues in the Demetriades laboratory.

1. *The tumor suppressor CYLD acts as a deubiquitinase for mTOR to constrain its activity*.
*Fernandes, S. A., **Pan, J.**, Terziyska, D. S., Koyuncu, S., Ding, X., Németh, I. B., Wilhelm, S., Nüchel, J., Al-Gburi, S., Gonidas, C., Pasparakis, M., Mosialos, G., Széll, M., Teleman, A. A., Eming, S. A., Vilchez, D., & Demetriades, C*.

bioRxiv (2025). https://doi.org/10.1101/2025.09.01.673523

I contributed to this study through experimental work and provided scientific input during the development of the project.

2. *Spatial and functional separation of mTORC1 signalling in response to different amino acid sources. Nat Cell Biol 26, 1918–1933*
*Fernandes, SA, Angelidaki, DD, Nuechel J, **Pan, J**, Gollwitzer, P, Elkis, Y, Artoni, F, Wilhelm, S, KovacevicSarmiento, M, Demetriades, C*.

Nature Cell Biology 26, 1918-1933 (2024). https://doi.org/10.1038/s41556-024-01523-7

I contributed to this publication by performing experiments and by providing scientific input during project development.